

Dissertation

**Precise Predictions**

for

**Neutralino and Chargino Pair Production**

in

**Supersymmetry**

ausgeführt zum Zwecke der Erlangung des akademischen Grades eines  
Doktors der technischen Wissenschaften unter der Leitung von

Univ. Prof. Walter Majerotto

E 136

Institut für Theoretische Physik

und

Institut für Hochenergiephysik der ÖAW

eingereicht an der Technischen Universität Wien  
Technisch–naturwissenschaftliche Fakultät

von

**Dipl. Ing. Wilhelm Öller**

9625709

Odoakergasse 10-18/6/17, 1160 Wien

[oeller@hephy.oeaw.ac.at](mailto:oeller@hephy.oeaw.ac.at)

Wien, im Oktober 2005



# Kurzfassung

Supersymmetrische Theorien wie das Minimale Supersymmetrische Standardmodell (MSSM) sagen die Existenz von Partnerteilchen zu den bereits bekannten Elementarteilchen voraus. Zu diesen zählen unter anderem die sogenannten Neutralinos und Charginos, die Superpartner der Eich- und Higgs-Bosonen.

Sollte nun Supersymmetrie (SUSY) in der Natur realisiert sein, können diese SUSY-Teilchen bei zukünftigen Beschleunigerexperimenten entdeckt und deren Eigenschaften insbesondere an einem Elektron-Positron Linearbeschleuniger mit hoher Präzision bestimmt werden.

Die vorliegende Arbeit beschäftigt sich daher in ausführlicher Weise mit der Berechnung von Observablen zur Neutralino- und Chargino-Produktion in Elektron-Positron Annihilationen im Rahmen des MSSM. Der Schwerpunkt wird hierbei auf die Ermittlung der zugehörigen Einschleifen-Strahlungskorrekturen gelegt, deren Berücksichtigung unerlässlich ist, um die geforderte Präzision zu erhalten. Die dafür notwendige Berechnung von hunderten von Feynman-Diagrammen wird unter Anwendung spezieller algebraischer Software durchgeführt. Dabei stößt man jedoch auf drei Probleme: Durch Integration der (quadratischen) Feynman-Amplituden über die freien Teilchen-Impulse kommt es zu den sogenannten ultraviolett- (UV), den infrarot- (IR) und den kollinearen Divergenzen. Diese müssen mittels spezieller Verfahren behandelt werden, um physikalisch sinnvolle Ergebnisse zu erhalten. Die UV-Divergenzen können im Rahmen der Regularisierung und anschließender Renormierung entfernt werden. Das dafür verwendete on-shell Renormierungsschema wird in konsistenter und detaillierter Weise hergeleitet. Besonderer Wert wird dabei auf eine eindeutige Definition der “weichen” SUSY Brechungsparameter gelegt. IR-Divergenzen entstehen durch Austausch virtueller Photonen. Sinnvolle Observable können daher nur dann erhalten werden wenn zusätzlich zu den Schleifen-Beiträgen auch reelle Photonabstrahlung berücksichtigt wird. Hierbei treten nun die erwähnten kollinearen Divergenzen auf, da Photonen auch kollinear zu den einlaufenden Elektron- und Positron- Strahlen abgestrahlt werden. Diese werden durch die endliche Elektronmasse regularisiert. Da die Masse aber im Vergleich zur Strahlenergie um Größenordnungen kleiner ist, liefern kollineare Photonen sehr hohe Beiträge zu den Strahlungskorrekturen.

Dies führt zu zwei weiteren Schwierigkeiten. Einerseits müssen die numerischen Probleme gelöst werden, indem die Beiträge der kollinearen Photonen von der numerischen Integration über den Phasenraum separiert und analytisch behandelt werden. Andererseits ist es notwendig höhere Ordnungen dieser großen kollinearen Korrekturen mitzuberechnen, um ein hinreichend genaues Ergebnis zu erzielen.

Auch wenn nur die Summe aller Teilbeiträge vernünftige Observable liefert, hat dennoch eine möglichst physikalisch motivierte Aufspaltung der gesamten berücksichtigten Strahlungskorrekturen Vorteile und wird daher ebenfalls diskutiert.



# Abstract

Supersymmetric theories like the Minimal Supersymmetric Standard Model (MSSM) predict the existence of partner particles to the well-established elementary particles. Among others are the so-called neutralinos and charginos, the superpartners of the gauge and Higgs bosons.

If Supersymmetry (SUSY) is realized in nature, the SUSY-particles can be discovered at future collider experiments. In particular on a linear collider their properties can be determined at high precision.

Therefore this thesis deals in an extensive way with the calculation of observables in neutralino and chargino production in electron-positron annihilations within the MSSM. Emphasis is put on the determination of the corresponding one-loop radiative corrections, whose consideration is essential to obtain the required precision. The necessary calculation of hundreds of Feynman diagrams is performed by application of special algebraic software.

However, one meets three problems: By integration of the (squared) Feynman-amplitudes over the free particle momenta, the so-called ultraviolet (UV), infrared (IR), and collinear divergences are introduced. These have to be treated by special techniques to obtain physically meaningful results. The UV-divergences can be removed within the scope of regularization and subsequent renormalization. The applied on-shell renormalization scheme is deduced in a consistent and detailed way. Particular importance is given to a unique definition of the “soft” SUSY-breaking parameters. IR-divergences originate from the exchange of virtual photons. Meaningful observables are only obtained, if in addition to the loop-contributions also real photon emission is considered. In this connection, the mentioned collinear divergences arise, since photons are also radiated off collinearly to the incoming electron-positron beams. These are regularized by the finite electron mass. But due to the fact, that the mass is by many orders of magnitude smaller than the beam energy, the collinear photons yield large contributions to the radiative corrections.

This leads to two difficulties: At one hand, the numerical problems need to be solved. Therefore, the contributions of collinear photons are separated from the numerical phase-space integration and further treated in an analytical way. On the other hand, it is necessary to take higher orders of these large collinear corrections into account, in order to obtain a result of adequate accuracy.

Even if only the sum of all these components yields a reasonable observable, a physically motivated separation of the complete considered radiative corrections has its advantages and is therefore also discussed.



# Contents

<b>Kurzfassung</b>	<b>iii</b>
<b>Abstract</b>	<b>v</b>
<b>1 Introduction</b>	<b>1</b>
<b>2 The Minimal Supersymmetric Standard Model</b>	<b>4</b>
2.1 Higgs sector . . . . .	5
2.2 Sfermion sector . . . . .	7
2.3 Chargino sector . . . . .	8
2.4 Neutralino sector . . . . .	9
<b>3 Renormalization of the MSSM</b>	<b>10</b>
3.1 Divergences and regularization . . . . .	10
3.1.1 Dimensional regularization . . . . .	10
3.1.2 Dimensional reduction . . . . .	12
3.1.3 Constrained differential renormalization . . . . .	13
3.2 Gauge boson and SM fermion sector . . . . .	14
3.3 Charge Renormalization . . . . .	16
3.3.1 Thomson limit . . . . .	16
3.3.2 Effective electric charge at high energies . . . . .	18
3.3.3 Effective renormalization schemes for $\alpha$ at $\mathbf{Q} = m_Z$ . . . . .	19
3.3.4 The fine-structure constant in the $G_F$ scheme . . . . .	20
3.4 Higgs sector . . . . .	21
3.5 Neutralinos and charginos . . . . .	22
3.6 Sfermion sector . . . . .	28
<b>4 Structure function formalism in QED</b>	<b>31</b>
4.1 Mass singularities . . . . .	31
4.2 Mass factorization theorem . . . . .	31
4.3 Evolution equations . . . . .	34
4.4 Soft photon resummation . . . . .	37
4.5 Leading-Log result . . . . .	39

<b>5</b>	<b>Pair Production of Charginos and Neutralinos in <math>e^+e^-</math> collisions</b>	<b>41</b>
5.1	Tree-Level . . . . .	41
5.2	Virtual Corrections . . . . .	44
5.3	QED corrections . . . . .	45
5.3.1	Soft-photon region . . . . .	48
5.3.2	Collinear region . . . . .	50
5.3.3	Finite region . . . . .	51
5.3.4	The structure function approach . . . . .	54
5.4	Definition of weak and QED corrections . . . . .	55
<b>6</b>	<b>Numerical Results</b>	<b>57</b>
6.1	Chargino Production . . . . .	58
6.2	Neutralino Production . . . . .	64
<b>A</b>	<b>Feynman-rules</b>	<b>69</b>
A.1	Definitions . . . . .	69
A.2	Counter-term Lagrangian . . . . .	70
<b>B</b>	<b>Reference Point SPS1a'</b>	<b>75</b>
	<b>Bibliography</b>	<b>78</b>
	<b>Curriculum Vitae</b>	<b>82</b>
	<b>List of Publications</b>	<b>83</b>

# Chapter 1

## Introduction

At present state, the Standard Model (SM) of electroweak and strong interactions [1, 2] of elementary particle physics describes almost all currently available experimental data with high precision. Despite its great success, it is a common belief that it can only be an effective theory describing physics at energies that are available at current collider experiments, and has to be extended to gain a full picture of fundamental interactions realized in nature. The reason for that: The SM leaves too many questions unanswered.

- It does not incorporate gravity, the fourth fundamental force.
- There is no explanation for the experimentally found mass spectrum of the matter particles, the fermions. The masses of the quarks and leptons are free input parameters of the SM and only accessible by measurement.
- Why are there three generations of fermions?
- How does the mechanism of electroweak symmetry breaking (EWSB) work exactly? In the SM an additional fundamental  $SU(2)_L$  doublet field  $\phi$  of spin 0 and a corresponding potential  $V(\phi)$  are introduced just by hand, but until today the experimental evidence, the expected discovery of the Higgs particle, is missing.
- The SM is based on the  $U(1)_Y \otimes SU(2)_L \otimes SU(3)_C$  gauge symmetry, a direct product of three groups each with an own coupling constant. Hence, it cannot be considered as a true unification of the electroweak and strong interactions. Therefore, it is assumed that at a higher scale a more fundamental theory, the Grand Unified Theory (GUT), exists where the three forces are unified in one gauge group described by only one single gauge coupling. If a model is an effective low-energy limit of such a GUT, the extrapolation of the three coupling constants up to the GUT scale using renormalization group techniques should meet in one point. Unfortunately this is not exactly realized in the SM [3].
- Observations in astro-physics yield that a large contribution of non-baryonic, non-luminous matter to the critical density of the universe is needed, which is also likely to be non-relativistic [4]. The WMAP satellite measurements [5] of the cosmic microwave background have shown that this cold dark matter amounts about a fourth of the

present energy of the universe. Therefore, a fairly massive and electrically neutral particle that is stable and has only weak interactions is required, but the SM fails to offer a candidate for the dark matter problem.

- The evaluation of the radiative corrections to the squared Higgs mass reveals the so-called naturalness or hierarchy problem. Using a cut-off regularization, it turns out that the divergent expression is quadratic in the cut-off scale  $\Lambda$ . This scale can be interpreted as the point where an effective theory is no longer valid and new physics enters. In the case of the SM, this scale should be the GUT scale which is of  $O(10^{16} \text{ GeV})$ . Phenomenological aspects demand that the mass of the Higgs boson is in the range of the electroweak scale  $O(100 \text{ GeV})$ , although the mass corrections show that it is sensitive to the GUT scale. Therefore an unnatural fine-tuning is necessary, so that the Higgs particle remains to be light.

Even if we deny a physical interpretation of the cut-off scale and use dimensional regularization, the naturalness problem remains evident. While physics at very high energies should decouple in the calculation of observables at the electroweak scale, the Higgs mass persists to be sensitive to possible contributions from heavy particles in the corresponding loop diagrams.

The corrections to the masses of the gauge bosons and the fermions are protected by gauge and chiral symmetry against this sensitivity and depend only logarithmically on the cut-off scale. So it seems that a lack of symmetry is responsible for the naturalness problem in the Higgs sector.

Several of these mentioned problems can be solved by introducing Supersymmetry (SUSY) [6, 7, 8, 9], which makes supersymmetric theories to be widely considered as the most attractive extensions of the SM.

Supersymmetry is a symmetry that connects bosons and fermions, mediated by the SUSY generators  $\mathcal{Q}$ , which transform fermionic into bosonic states and vice-versa

$$\mathcal{Q}|\text{Fermion}\rangle = |\text{Boson}\rangle, \quad \mathcal{Q}|\text{Boson}\rangle = |\text{Fermion}\rangle. \quad (1.1)$$

In the beginning SUSY was introduced for less phenomenological but more aesthetical and purely theoretical reasons. For example it is the most general symmetry that a non-trivial quantum field theory can possess [10]. If SUSY is made local it is possible to incorporate gravity and maybe this will help to find a theory where all four fundamental forces are considered. Supersymmetry is the correct symmetry that helps to solve the hierarchy problem. Exact SUSY predicts that each known particle has a mirror-particle with the same mass and quantum numbers, except the spin which differs by  $1/2$ . So the fermionic contributions to the Higgs mass are supplemented by loop diagrams with their bosonic superpartners, which cancel the complete cut-off dependence.

Unfortunately no such superpartners to the known particles have been found yet and therefore SUSY must be broken. Even then, the hierarchy problem can be solved if the masses of the superpartners are not too heavy ( $\leq \text{few TeV}$ ). This is the main reason for low-energy supersymmetry.

Furthermore the additional particles modify the slopes of the renormalization group evolved gauge couplings and gauge unification is possible. In supersymmetric theories with R-parity

conservation, the lightest supersymmetric particle (LSP) is stable. If this particle is electrically neutral it can serve as a dark matter candidate. There are several possible candidates like the superpartners of the neutral gauge bosons and Higgses, the neutralinos.

SUSY can also help to get a better understanding of the EWSB mechanism. In SUSY theories it is possible to assume a positive squared Higgs mass parameter at the GUT scale. Due to the heavy mass of the top quark and its superpartners, the evolution downwards yields a negative value at the electroweak scale. So the typical “mexican hat” shape of the Higgs potential and as a consequence EWSB itself appear as output of such a calculation and do not need to be adjusted by hand.

If SUSY is realized in nature, it is expected to be found at the next generation of colliders, the LHC and a future linear collider (LC). Therefore supersymmetric theories are part of the most active fields in present elementary particle phenomenology.

### **This thesis is organized as follows:**

Since all calculations are done within the framework of the MSSM, chapter 2 gives a short introduction to this model and additionally specifies the used conventions.

Chapter 3 considers in detail the regularization and renormalization schemes used in this thesis. An on-shell scheme for the masses and fields of all SUSY-partners is applied, that is applicable independent of the corresponding particle mixing characters. Effective renormalization schemes for the fine-structure constant are reviewed.

Afterwards chapter 4 gives a short survey to the structure function formalism in QED. Starting from the mass factorization theorem, all necessary formulas for the calculation of universal photonic corrections are presented.

The main topic of this thesis is discussed in chapter 5, the pair production of neutralinos and charginos in electron-positron annihilation. The calculation of virtual and real corrections are explicitly discussed. The QED corrections are treated using the phase-space slicing method. Furthermore a physically motivated separation of weak and QED corrections is presented.

Chapter 6 gives numerical results for several observables: The total cross-section, the forward-backward and the left-right asymmetry. Further, distributions in the photon energy and the scattering angle for chargino production with an additional photon in the final-state are presented.

In appendix A an analytic expression for the necessary counter-term Lagrangian is given.

At last, appendix B defines the MSSM scenario that is used in the numerics. The SPS1a' scenario serves as benchmark point to perform high precision calculations. The importance of the translation from  $\overline{\text{DR}}$  to on-shell parameters is emphasized.

# Chapter 2

## The Minimal Supersymmetric Standard Model

The minimal supersymmetric extension of the SM contains only those fields and couplings that are necessary for consistency. It is constructed from the following ingredients:

- **Minimal particle content:**

The MSSM is based on the same gauge group as the SM. SUSY implies, that in addition to the gauge bosons fermionic superpartners are introduced. These spin  $\frac{1}{2}$  “gauginos” are the bino  $\tilde{B}$ , the three winos  $\tilde{W}_i$  and the eight gluinos  $\tilde{g}_a$  for the gauge groups  $U(1)_Y$ ,  $SU(2)_L$  and  $SU(3)_C$ , respectively. The gauge bosons and the gauginos are combined to vector supermultiplets.

According to the SM, the MSSM contains three generations of leptons and quarks. The right- and left-handed components are arranged in different chiral superfields together with their spin 0 SUSY partners, the sleptons and squarks.

In contrast to the SM, two chiral superfields  $\hat{H}_1$  and  $\hat{H}_2$  with opposite hypercharge are needed to cancel chiral anomalies. The scalar components are two Higgs doublets, which give separately masses to the up- and down-type fermions, by their non-vanishing vacuum expectation values. The fermionic parts are the “higgsinos”, which mix with the gauginos to form the mass eigenstates of the so-called charginos and neutralinos. An overview about the particle content in the MSSM is given in Tab. 2.1

- **R-Parity conservation:**

The most general gauge-invariant and renormalizable Lagrangian would contain terms of lepton and baryon number violating interactions. To cope with the severe experimental constraints on lepton or baryon number violating processes, whereas the non-observation of the proton-decay is the most obvious one, a multiplicative symmetry called R-parity is imposed. It is defined by

$$R_p = (-1)^{3B+L+2s}, \quad (2.1)$$

where  $L$  and  $B$  are the lepton and baryon number, respectively, and  $s$  is the spin quantum number. Hence, ordinary particles have R-parity  $R_p = +1$  and their SUSY-partners  $R_p = -1$ . This has important phenomenological consequences: In collider

Superfield	$SU(3)_C$	$SU(2)_L$	$U(1)_Y$	Particle	Spin	Superpartner	Spin
$\hat{B}$	1	1	0	$B^\mu$	1	$\tilde{B}$	$\frac{1}{2}$
$\hat{W}_i$	1	3	0	$W_i^\mu$	1	$\tilde{W}_i$	$\frac{1}{2}$
$\hat{g}_a$	8	1	0	$g_a^\mu$	1	$\tilde{g}_a$	$\frac{1}{2}$
$\hat{Q}$	3	2	$\frac{1}{3}$	$(u_L, d_L)$	$\frac{1}{2}$	$(\tilde{u}_L, \tilde{d}_L)$	0
$\hat{U}^c$	$\bar{3}$	1	$-\frac{4}{3}$	$\bar{u}_R$	$\frac{1}{2}$	$\tilde{u}_R^*$	0
$\hat{D}^c$	$\bar{3}$	1	$\frac{2}{3}$	$\bar{d}_R$	$\frac{1}{2}$	$\tilde{d}_R^*$	0
$\hat{L}$	1	2	-1	$(\nu_L, e_L)$	$\frac{1}{2}$	$(\tilde{\nu}_L, \tilde{e}_L)$	0
$\hat{E}^c$	1	1	2	$\bar{e}_R$	$\frac{1}{2}$	$\tilde{e}_R^*$	0
$\hat{H}_1$	1	2	-1	$\mathcal{H}_1$	0	$\tilde{\mathcal{H}}_1$	$\frac{1}{2}$
$\hat{H}_2$	1	2	1	$\mathcal{H}_2$	0	$\tilde{\mathcal{H}}_2$	$\frac{1}{2}$

Table 2.1: Superfield and particle content of the MSSM

experiments, SUSY-particles can only be produced in even numbers. The corresponding decay products contain always an odd number of SUSY-partners. Thus, the lightest supersymmetric particle (LSP) is absolutely stable.

- **Soft SUSY-breaking:**

Realistic models must contain SUSY-breaking, although there is no hint how the SUSY-breaking mechanism works. To be as general as possible, terms are just added to the Lagrangian that break SUSY explicitly. In order to sustain the solution of the hierarchy problem, only “soft” terms are considered, who do not reintroduce quadratic divergences [11].

## 2.1 Higgs sector

Both complex  $SU(2)_L$  Higgs doublets that are required in the MSSM acquire a non-vanishing vacuum expectation value (VEV)

$$\langle \mathcal{H}_1 \rangle = \begin{pmatrix} v_1/\sqrt{2} \\ 0 \end{pmatrix} \quad \text{and} \quad \langle \mathcal{H}_2 \rangle = \begin{pmatrix} 0 \\ v_2/\sqrt{2} \end{pmatrix}. \quad (2.2)$$

Thus, the two doublets with opposite hypercharge can be parameterized in the following way

$$\mathcal{H}_1 \equiv \begin{pmatrix} H_1^0 \\ H_1^- \end{pmatrix} = \begin{pmatrix} (v_1 + \phi_1^0 + i\chi_1^0)/\sqrt{2} \\ \phi_1^- \end{pmatrix}, \quad Y_{\mathcal{H}_1} = -1, \quad (2.3)$$

$$\mathcal{H}_2 \equiv \begin{pmatrix} H_2^+ \\ H_2^0 \end{pmatrix} = \begin{pmatrix} \phi_2^+ \\ (v_2 + \phi_2^0 + i\chi_2^0)/\sqrt{2} \end{pmatrix}, \quad Y_{\mathcal{H}_2} = +1. \quad (2.4)$$

The tree-level Higgs potential in the MSSM can be written as

$$V_H = (M_{H_1}^2 + |\mu|^2) |\mathcal{H}_1|^2 + (M_{H_2}^2 + |\mu|^2) |\mathcal{H}_2|^2 - (B\mu \varepsilon_{ab} \mathcal{H}_1^a \mathcal{H}_2^b + \text{h.c.}) + \frac{g^2 + g'^2}{8} (|\mathcal{H}_1|^2 - |\mathcal{H}_2|^2)^2 + \frac{g^2}{2} |\mathcal{H}_1^\dagger \mathcal{H}_2|^2, \quad (2.5)$$

whereas  $M_{H_1}^2$ ,  $M_{H_2}^2$ , and  $B$  are soft SUSY-breaking parameters and  $\mu$  the MSSM analogue to the SM Higgs mass parameter. The Higgs self-interaction is determined by the  $U(1)_Y$  and  $SU(2)_L$  gauge couplings  $g'$  and  $g$ , in contrast to the SM where it is introduced by hand. The anti-symmetric  $\varepsilon$  tensor is fixed by  $\varepsilon_{12} = -1$ . A phase-convention for the two Higgs-doublets can be chosen in such a way that the two vacuum expectation values and the product  $B\mu$  are real.

As a consequence of electroweak symmetry breaking, the gauge bosons receive the masses

$$m_Z^2 = \frac{g^2 + g'^2}{4} (v_1^2 + v_2^2), \quad m_W^2 = \frac{g^2}{4} (v_1^2 + v_2^2). \quad (2.6)$$

Hence, the sum of the squared vacuum expectation values can be related to the experimentally known  $Z$ -mass

$$v^2 \equiv v_1^2 + v_2^2 = \frac{4m_Z^2}{g'^2 + g^2} \approx (246 \text{ GeV})^2. \quad (2.7)$$

The mixing angle  $\beta$  is defined through the ratio of the VEV's

$$\tan \beta \equiv \frac{v_2}{v_1} \geq 0, \quad 0 \leq \beta \leq \frac{\pi}{2} \quad (2.8)$$

and remains as a free parameter of the theory. By the requirement, that the two ground states  $\langle \mathcal{H}_1 \rangle, \langle \mathcal{H}_2 \rangle$  describe indeed a local minimum of the Higgs-potential,

$$\left. \frac{\partial V_H}{\partial H_1^0} \right|_{\langle H_n^0 \rangle = v_n} = \left. \frac{\partial V_H}{\partial H_2^0} \right|_{\langle H_n^0 \rangle = v_n} = 0, \quad (2.9)$$

the following two restricting conditions are obtained

$$M_{H_1}^2 + |\mu|^2 = -B\mu \tan \beta - \frac{1}{2} m_Z^2 \cos 2\beta, \quad (2.10)$$

$$M_{H_2}^2 + |\mu|^2 = -B\mu \cot \beta + \frac{1}{2} m_Z^2 \cos 2\beta. \quad (2.11)$$

The Higgs mass matrix has the form

$$\mathcal{M}_{ij}^{2,\text{Higgs}} = \frac{1}{2} \left. \frac{\partial^2 V_H}{\partial \mathcal{H}_i \partial \mathcal{H}_j} \right|_{\langle H_n^0 \rangle = v_n}. \quad (2.12)$$

At tree-level and in CP-invariant theories even at higher order,  $\mathcal{M}_{ij}^{2,\text{Higgs}}$  can be decomposed into four independent  $2 \times 2$  blocks. A subsequent diagonalization yields the following mass

eigenstates

$$\begin{pmatrix} G^\pm \\ H^\pm \end{pmatrix} = \begin{pmatrix} -\cos\beta & \sin\beta \\ \sin\beta & \cos\beta \end{pmatrix} \begin{pmatrix} \phi_1^\pm \\ \phi_2^\pm \end{pmatrix}, \quad (2.13)$$

$$\begin{pmatrix} H^0 \\ h^0 \end{pmatrix} = \begin{pmatrix} \cos\alpha & \sin\alpha \\ -\sin\alpha & \cos\alpha \end{pmatrix} \begin{pmatrix} \phi_1^0 \\ \phi_2^0 \end{pmatrix}, \quad (2.14)$$

$$\begin{pmatrix} G^0 \\ A^0 \end{pmatrix} = \begin{pmatrix} -\cos\beta & \sin\beta \\ \sin\beta & \cos\beta \end{pmatrix} \begin{pmatrix} \chi_1^0 \\ \chi_2^0 \end{pmatrix}. \quad (2.15)$$

The three unphysical Goldstone modes  $G^0$  and  $G^\pm$  with zero mass are absorbed by the longitudinal components of the massive vector bosons. The spectrum of physical states consists of three neutral bosons, two CP-even eigenstates ( $h^0$ ,  $H^0$ ), a CP-odd one ( $A^0$ ), and two charged ( $H^\pm$ ) Higgs particles. The original six degrees of freedom in the Higgs potential, the four soft SUSY-breaking parameters and the two VEV's are reduced due to the eqs. (2.7, 2.10, 2.11). For the remaining three we choose the common input

$$m_{A^0}, \quad \tan\beta, \quad \text{and} \quad \mu.$$

The tree-level values of the charged and the CP-even Higgs masses and the Higgs mixing angle  $\alpha$ , expressed in terms of these input parameters and the gauge boson masses are

$$m_{H^\pm}^2 = m_{A^0}^2 + m_W^2, \quad (2.16)$$

$$m_{h^0, H^0}^2 = \frac{1}{2} \left[ m_{A^0}^2 + m_Z^2 \mp \sqrt{(m_{A^0}^2 + m_Z^2)^2 - 4m_{A^0}^2 m_Z^2 \cos^2 2\beta} \right]. \quad (2.17)$$

$$\tan 2\alpha = \tan 2\beta \frac{m_{A^0}^2 + m_Z^2}{m_{A^0}^2 - m_Z^2}, \quad -\frac{\pi}{2} \leq \alpha \leq 0. \quad (2.18)$$

## 2.2 Sfermion sector

We assume no generation mixing for fermions and sfermions. The mass matrix for each generation of squarks or sleptons can therefore be written as

$$\mathcal{M}_{\tilde{f}}^2 = \begin{pmatrix} (M_{\tilde{f}}^{LL})^2 + m_f^2 & (M_{\tilde{f}}^{LR})^* m_f \\ M_{\tilde{f}}^{LR} m_f & (M_{\tilde{f}}^{RR})^2 + m_f^2 \end{pmatrix}, \quad (2.19)$$

with

$$(M_{\tilde{f}}^{LL})^2 = m_Z^2 \cos 2\beta (I_f^{3L} - e_f \sin^2 \theta_W) + \begin{cases} M_{\tilde{Q}}^2 & \text{for left-handed squarks,} \\ M_{\tilde{L}}^2 & \text{for left-handed sleptons,} \end{cases} \quad (2.20)$$

$$M_{\tilde{f}}^{LR} = A_f - \mu^* (\tan\beta)^{-2} I_f^{3L} \quad (2.21)$$

$$(M_{\tilde{f}}^{RR})^2 = m_Z^2 \cos 2\beta e_f \sin^2 \theta_W + \begin{cases} M_{\tilde{U}}^2 & \text{for right-handed u-type squarks,} \\ M_{\tilde{D}}^2 & \text{for right-handed d-type squarks,} \\ M_{\tilde{E}}^2 & \text{for right-handed sleptons.} \end{cases} \quad (2.22)$$

$M_{\tilde{Q},\tilde{L}}$  and  $M_{\tilde{U},\tilde{D},\tilde{E}}$  are soft SUSY-breaking masses and  $A_f$  are trilinear breaking parameters.  $I_f^{3L}$  is the third component of the weak isospin,  $e_f$  the electric charge in terms of the elementary charge and  $m_f$  the mass of the corresponding fermionic SUSY-partner.

The mass matrix can be rotated by introducing the unitary matrix  $\mathbf{R}^{\tilde{f}}$

$$\mathcal{M}_{\tilde{f}}^2 = \mathbf{R}^{\tilde{f}\dagger} \begin{pmatrix} m_{\tilde{f}_1}^2 & 0 \\ 0 & m_{\tilde{f}_2}^2 \end{pmatrix} \mathbf{R}^{\tilde{f}}, \quad (2.23)$$

which results in the sfermion masses

$$m_{\tilde{f}_{1,2}}^2 = m_f^2 + \frac{1}{2} \left( (M_{\tilde{f}}^{LL})^2 + (M_{\tilde{f}}^{RR})^2 \mp \sqrt{\left( (M_{\tilde{f}}^{LL})^2 - (M_{\tilde{f}}^{RR})^2 \right)^2 + 4m_f^2 |M_{\tilde{f}}^{LR}|^2} \right). \quad (2.24)$$

## 2.3 Chargino sector

The fermionic superpartners of the  $W$ -boson and charged Higgs boson, called charginos, are given in the Weyl representation as [12]

$$\psi^+ = (-i\lambda^+, \psi_{H_2}^1), \quad \psi^- = (-i\lambda^-, \psi_{H_1}^2). \quad (2.25)$$

The mass term of the Lagrangian in this basis reads

$$\mathcal{L} = -\frac{1}{2} (\psi^+, \psi^-) \cdot \begin{pmatrix} 0 & X^T \\ X & 0 \end{pmatrix} \cdot \begin{pmatrix} \psi^+ \\ \psi^- \end{pmatrix} + \text{h.c.} \quad (2.26)$$

with the chargino mass matrix

$$X = \begin{pmatrix} M & \sqrt{2}m_W \sin \beta \\ \sqrt{2}m_W \cos \beta & \mu \end{pmatrix}. \quad (2.27)$$

Without loss of generality the  $SU(2)_L$  mass parameter  $M$  can be chosen to be real. The mass matrix is rotated using two unitary matrices  $U$  and  $V$

$$U^* X V^\dagger = \text{diag}(m_{\tilde{\chi}_1^\pm}, m_{\tilde{\chi}_2^\pm}), \quad 0 \leq m_{\tilde{\chi}_1^\pm} \leq m_{\tilde{\chi}_2^\pm}. \quad (2.28)$$

The Dirac mass eigenstates can be constructed in two ways. As negatively or positively charged ones

$$\tilde{\chi}_i^- \equiv \begin{pmatrix} \chi_i^- \\ \bar{\chi}_i^+ \end{pmatrix} = \begin{pmatrix} U_{ij} \psi_j^- \\ V_{ij}^* \bar{\psi}_j^+ \end{pmatrix}, \quad \text{or} \quad \tilde{\chi}_i^+ \equiv \begin{pmatrix} \chi_i^+ \\ \bar{\chi}_i^- \end{pmatrix} = \begin{pmatrix} V_{ij} \psi_j^+ \\ U_{ij}^* \bar{\psi}_j^- \end{pmatrix}. \quad (2.29)$$

The mass eigenvalues are given by

$$m_{\tilde{\chi}_{1,2}^\pm}^2 = \frac{1}{2} \left[ M^2 + |\mu|^2 + 2m_W^2 \mp \sqrt{(M^2 + |\mu|^2 + 2m_W^2)^2 - 4|m_W^2 \sin 2\beta - \mu M|^2} \right]. \quad (2.30)$$

## 2.4 Neutralino sector

The neutralinos are the fermionic superpartners of the  $U(1)_Y$  and  $SU(2)_L$  gauge fields  $B^\mu$  and  $W^{3\mu}$  and of the neutral components of the two Higgs doublets,  $H_1^0$  and  $H_2^0$ . In the original interaction base, they can be combined to a vector of four Weyl states

$$\psi_j^0 = (-i\lambda', -i\lambda^3, \psi_{H_1}^1, \psi_{H_2}^2). \quad (2.31)$$

The corresponding bilinear Lagrangian has the form

$$\mathcal{L} = -\frac{1}{2} (\psi^0)^T Y \psi^0 + \text{h.c.}, \quad (2.32)$$

where we have introduced the neutralino mass matrix

$$Y = \begin{pmatrix} M' & 0 & -m_Z \sin \theta_W \cos \beta & m_Z \sin \theta_W \sin \beta \\ 0 & M & m_Z \cos \theta_W \cos \beta & -m_Z \cos \theta_W \sin \beta \\ -m_Z \sin \theta_W \cos \beta & m_Z \cos \theta_W \cos \beta & 0 & -\mu \\ m_Z \sin \theta_W \sin \beta & -m_Z \cos \theta_W \sin \beta & -\mu & 0 \end{pmatrix}. \quad (2.33)$$

Due to the Majorana nature, the mass matrix can be diagonalized by using only one rotation matrix

$$N^* Y N^\dagger = \text{diag}(m_{\tilde{\chi}_1^0}, m_{\tilde{\chi}_2^0}, m_{\tilde{\chi}_3^0}, m_{\tilde{\chi}_4^0}), \quad (2.34)$$

with  $0 \leq m_{\tilde{\chi}_1^0} \leq m_{\tilde{\chi}_2^0} \leq m_{\tilde{\chi}_3^0} \leq m_{\tilde{\chi}_4^0}$  by definition. The neutralino fields can be expressed as the Majorana spinors

$$\tilde{\chi}_i^0 \equiv \begin{pmatrix} \chi_i^0 \\ \bar{\chi}_i^0 \end{pmatrix} = \begin{pmatrix} N_{ij} \psi_j^0 \\ N_{ij}^* \bar{\psi}_j^0 \end{pmatrix}. \quad (2.35)$$

# Chapter 3

## Renormalization of the MSSM

### 3.1 Divergences and regularization

The inclusion of higher order corrections in the calculation of Green functions and S-Matrix elements beyond the tree-level approximation has two main complications. First, tree-level relations between the Lagrangian parameters and physical observables are no longer valid. So the Lagrangian parameters cannot be considered as “physical” quantities, but depend on a certain definition. Second, the calculation of higher order Feynman diagrams (in momentum space) leads to the integration over indefinite momenta. Such integrals can diverge for large momenta (or equivalently in the Fourier-transformed position space, for small distances), e.g.

$$\int \frac{d^4q}{q^2 - m^2 + i\epsilon}. \quad (3.1)$$

These so-called UV-divergences have to be treated in a proper way. The first step is to give such integrals an intermediate well-defined meaning, the so-called regularization. Several regularization schemes are known. The physically best motivated one is perhaps to introduce a cut  $\Lambda$  on the energy. The integral is now  $\Lambda$  dependent and diverges in the limit  $\Lambda \rightarrow \infty$ . However this cut-off scheme is very inconvenient in practical calculations and furthermore breaks Lorentz invariance. Therefore, we use the schemes discussed in the next sections, which do not spoil gauge and Lorentz invariance. In a second step, the renormalization procedure, renormalization constants (RC's) of the Lagrangian parameters and the fields have to be introduced. These RC's absorb the UV-divergences and it is possible to obtain UV-finite results for Green functions and S-Matrix elements. A theory in which this is possible in all orders of perturbation theory is called renormalizable. Calculations in finite orders of perturbation theory are naturally renormalization scheme dependent, but differ only by higher order contributions.

#### 3.1.1 Dimensional regularization

The definition of regularized expressions in dimensional regularization (DREG) [13] is done in the following way. An analytical continuation of four-vectors, like momenta and vector fields, from 4 to D dimensions has to be performed. We introduce the difference between

four and  $D$  dimensions by the parameter  $\varepsilon = 4 - D$ . In general, the integrals of one-loop Feynman diagrams can be defined by

$$T_{\mu_1, \dots, \mu_M}^N(p_1, \dots, p_{N-1}, m_0, \dots, m_{N-1}) = \frac{(2\pi\mu)^{4-D}}{i\pi^2} \times \int d^D q \frac{q_{\mu_1} \cdots q_{\mu_M}}{(q^2 - m_0^2 + i\varepsilon)[(q + p_1)^2 - m_1^2 + i\varepsilon] \cdots [(q + p_{N-1})^2 - m_{N-1}^2 + i\varepsilon]} \quad (3.2)$$

and can be expanded in a Laurent series around the pole  $\varepsilon = 0$ . Due the change in the dimension of the integrals, it necessary to introduce an arbitrary mass parameter  $\mu$ , which vanishes in the limit  $\varepsilon \rightarrow 0$ . All UV-divergent integrals have the same pole structure  $\propto \frac{1}{\varepsilon}$ . The methods for calculating such integrals are based on the work of t'Hooft and Veltman [14], and Passarino and Veltman [15]. Therefore these integrals are known in the literature as *Passarino-Veltman integrals*. The scalar integrals up to four propagators in the convention

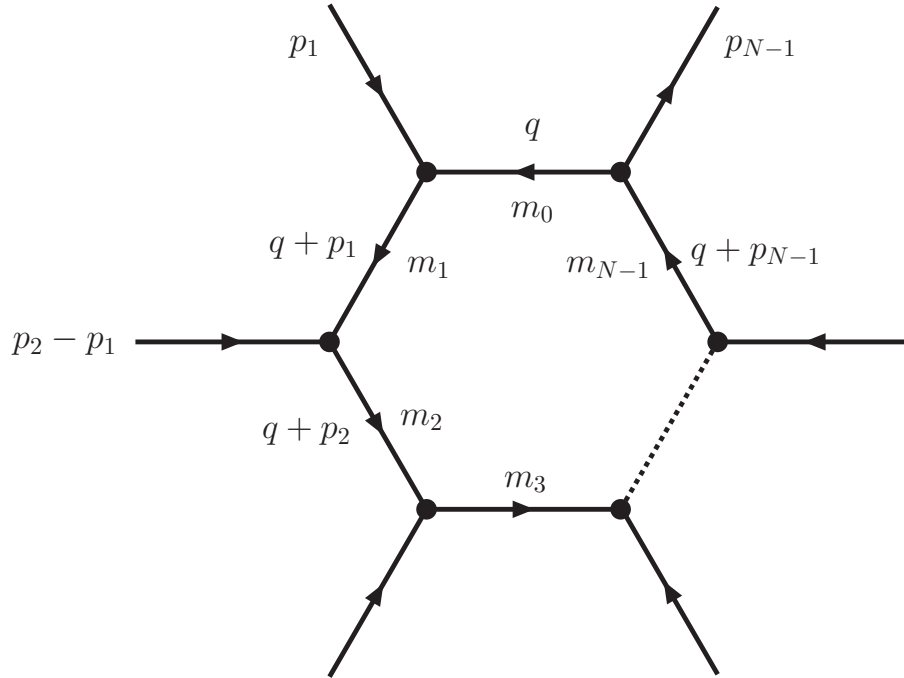


Figure 3.1: Conventions for the Passarino-Veltman integrals.

of A. Denner [16] are

$$T^1 \equiv A_0(m_0^2), \quad (3.3)$$

$$T^2 \equiv B_0(p_1^2, m_0^2, m_1^2), \quad (3.4)$$

$$T^3 \equiv C_0(p_1^2, (p_1 - p_2)^2, p_2^2, m_0^2, m_1^2, m_2^2), \quad (3.5)$$

$$T^4 \equiv D_0(p_1^2, (p_1 - p_2)^2, (p_2 - p_3)^2, p_3^2, p_2^2, (p_1 - p_3)^2, m_0^2, m_1^2, m_2^2, m_3^2). \quad (3.6)$$

The advantage of such a definition compared with eq. (3.2), is quite simple. All arguments are scalars and no explicit 4-momenta occur, so they are well defined for a later numerical

evaluation.

As an example, we give the analytical results for two of the basic scalar integrals

$$A_0(m^2) = m^2 \left[ \Delta + 1 + \log \frac{\mu^2}{m^2} \right], \quad (3.7)$$

$$B_0(m^2, 0, m^2) = \Delta + 2 + \log \frac{\mu^2}{m^2}. \quad (3.8)$$

We have defined the divergence parameter

$$\Delta = \frac{2}{\varepsilon} - \gamma_E + \log 4\pi, \quad (3.9)$$

whereas  $\gamma_E = 0.57721\dots$  is the Euler constant. For further analytical solutions of Passarino-Veltman integrals, we refer e.g. to [17].

Since dimensional regularization retains Lorentz invariance and the tensor integrals  $T_{\mu_1, \dots, \mu_M}^N$  are symmetric under interchange of the Lorentz indices  $\mu_i$ , they can be decomposed in terms of symmetric Lorentz tensors. The decomposition for some of the tensor integrals in the convention of [16] is given by:

$$B^\mu = p_1^\mu B_1 \quad (3.10)$$

$$B^{\mu\nu} = g^{\mu\nu} B_{00} + p_1^\mu p_1^\nu B_{11} \quad (3.11)$$

$$C^\mu = p_1^\mu C_1 + p_2^\mu C_2 \quad (3.12)$$

$$C^{\mu\nu} = g^{\mu\nu} C_{00} + p_1^\mu p_1^\nu C_{11} + (p_1^\mu p_2^\nu + p_2^\mu p_1^\nu) C_{12} + p_2^\mu p_2^\nu C_{22} \quad (3.13)$$

The momenta  $p_i^\mu$  are defined in Fig. 3.1.

In the minimal-subtraction scheme (MS), the terms proportional to  $\frac{1}{\varepsilon}$ , in the  $\overline{\text{MS}}$  scheme, the terms proportional to  $\Delta$  are subtracted to give finite results. These renormalization schemes lead to renormalized expressions. Other renormalization schemes, like the on-shell scheme as discussed in the next chapter, just differ by finite terms that are additionally subtracted. To calculate not only one-loop integrals, but a complete Feynman amplitude in DREG, an extension to  $D$  dimensions of the Lorentz covariants ( $\gamma_\mu, g_{\mu\nu}, \dots$ ) is necessary. For arbitrary  $D$  the metric tensor obeys the trace rule  $g_\mu^\mu = D$ . An extension of the Dirac algebra, can be defined in the following way:

$$\{\gamma^\mu, \gamma^\nu\} = 2g^{\mu\nu} \mathbb{1} \quad \rightarrow \quad \gamma^\mu \gamma_\mu = D \mathbb{1} \quad (3.14)$$

Problems arise if identities that depend on the 4-dimensional nature of objects are involved. In particular for the validity of Fierz identities, the definition of a  $D$ -dimensional  $\gamma^5$ , and relations that come along with the Levi-Civita  $\varepsilon$  tensor. For example, there is no consistent definition for the trace  $Tr(\gamma^5 \gamma_\mu \gamma_\nu \gamma_\rho \gamma_\sigma) = \varepsilon_{\mu\nu\rho\sigma} Tr \mathbb{1}$  in  $D$  dimensions. However, one can use the 4-dimensional definition for one-loop corrections in anomaly-free theories without inconsistencies.

### 3.1.2 Dimensional reduction

Unfortunately, DREG violates supersymmetry. In DREG vector-fields are reduced from 4 to  $D$  dimensions, which affects the corresponding degrees of freedom, respectively. Therefore, such vector-fields cannot be combined with its fermionic superpartners to a superfield. A modified version of DREG, dimensional reduction (DRED), was introduced by

W. Siegel [18]. The usual integration momenta are D-dimensional, equivalently to DREG, but all other tensors and spinors that are related to vector-fields are kept 4-dimensional. Working with 4- and D-dimensional objects, one has to introduce two different metric tensors: a 4-dimensional one  $g^{\mu\nu}$  with  $g^\mu{}_\mu = 4$  and a D-dimensional  $\hat{g}^{\mu\nu}$  with  $\hat{g}^\mu{}_\mu = D$ . To retain gauge invariance and field equations, one must demand that

$$g^{\alpha\beta}\hat{g}_{\beta\gamma} = \hat{g}_\gamma^\alpha. \quad (3.15)$$

The differences between DREG and DRED can be shown in a simple example, the product of self-contracted  $\gamma$  matrices and a Passarino-Veltman integral  $\gamma^\mu\gamma_\mu B_0(m^2, 0, m^2)$ :

DREG	DRED
$(4 - \varepsilon)(\Delta + 2 + \log \frac{\mu^2}{m^2}) + O(\varepsilon) = 4(\Delta + 2 + \log \frac{\mu^2}{m^2}) - 2 + O(\varepsilon)$	$4(\Delta + 2 + \log \frac{\mu^2}{m^2}) + O(\varepsilon)$

The additional  $\varepsilon$  in DREG produces, multiplied with the divergence factor  $\Delta$  in the  $B_0$  integral, a finite term 2. However, this example possibly gives the wrong impression that in DRED one only needs to consider the  $\varepsilon$  expansion for the basic integrals  $T_{\dots}^N$  and that the 4-dimensional expressions outside are irrelevant in this connection. This can be clarified in a simple second example

$$g_{\mu\nu}B^{\mu\nu} = g_{\mu\nu}(\hat{g}^{\mu\nu}B_{00} + p_1^\mu p_1^\nu B_{11}) = \hat{g}_\mu{}^\mu B_{00} + p_1^2 B_{11} = (4 - \varepsilon)B_{00} + p_1^2 B_{11}. \quad (3.16)$$

Eq. (3.15) “transforms” the 4-dimensional metric tensor outside the basic integral into a D-dimensional one. This yields the rule, that tensors with traces (e.g.  $g_{\mu\nu}B^{\mu\nu}$ ) and traceless objects (e.g.  $B^{\mu\nu}$ ) are regularized differently.

Equivalently to DREG, we can define a minimal subtraction renormalization that cancels only the divergent  $\frac{1}{\varepsilon} / \Delta$  terms. These schemes are called DR /  $\overline{\text{DR}}$ .

### 3.1.3 Constrained differential renormalization

Constrained differential renormalization (CDR) [19] was originally formulated in euclidean position space. The Feynman diagrams are rewritten in terms of a complete set of singular basic functions. The renormalization is done by replacing these divergent expressions with derivatives of well-behaved ones and no intermediate step of regularization is needed. The mass-less scalar propagator in euclidean x-space has the simple form

$$\Delta_0(x_E) = \frac{1}{4\pi^2 x_E^2}. \quad (3.17)$$

The UV-divergence for small distances in  $x_E$  is evident. Based on a set of rules and the CDR identity

$$\left[ \frac{1}{x_E^4} \right]^R = -\frac{1}{4} \square \frac{\log x_E^2 M^2}{x_E^2}, \quad (3.18)$$

where  $x_E$  is the euclidean coordinate and  $\square = \partial^\mu \partial_\mu$ , all other renormalized basic functions can be obtained. A main feature of these functions is, that they are different for trace

and traceless objects. It was shown in [20] that transforming these basic functions into Minkowski momentum-space, the renormalization is identical to the  $\overline{\text{DR}}$  renormalization at the one-loop level. The transformation of the CDR identity eq. (3.18) into the Minkowski momentum space yields

$$\left[ -i \int \frac{d^4 k}{(2\pi)^4} \frac{1}{k^2(k-p)^2} \right]^R = \frac{1}{16\pi^2} \log \frac{\bar{M}^2}{-p^2}, \quad (3.19)$$

with  $\bar{M} = 2Me^{\gamma_E}$ . In  $\overline{\text{DR}}$  this integral is renormalized in the following way

$$\left[ -i \int \frac{d^4 k}{(2\pi)^4} \frac{1}{k^2(k-p)^2} \right]^R = \frac{1}{16\pi^2} B_0(p^2, 0, 0)|_{\Delta \rightarrow 0} = \frac{1}{16\pi^2} (\log \frac{\mu^2}{-p^2} + 2) \quad (3.20)$$

Both schemes give the same result, if we impose for the arbitrary scales  $\bar{M}$  and  $\mu$  the relation

$$\bar{M}^2 = \mu^2 e^2. \quad (3.21)$$

The CDR rules define how the products of singular expressions and operators are properly renormalized. The combination of CDR rules and the CDR identity allows to construct regularized quantities for all possible divergent expressions at one loop. Inserting non-singular expressions, like the regularized D-dimensional integrals of DREG and DRED, the CDR rules are automatically fulfilled. Therefore the basic functions in CDR and DREG or DRED are identical if eq. (3.21) is valid. In CDR all Lorentz indices are contracted before the basic functions are identified. All other objects in a Feynman amplitude are naturally 4-dimensional. In DRED this is also true, if the contraction of Lorentz indices has been already performed. This is not valid for DREG, where even after the contraction D-dimensional objects (with  $\varepsilon$  terms) can occur. Hence, it can be said that the basic functions in CDR, DRED, and DREG are identical. For a complete Feynman amplitude CDR and DRED give the same result, differing from those in DREG.

The algorithmic approach of CDR, to express Feynman amplitudes in terms of basic functions, that are replaced by the corresponding renormalized ones, makes it attractive for automatized calculations in CDR or  $\overline{\text{DR}}$  at the one-loop level. Therefore the CDR scheme is implemented in Thomas Hahn's FormCalc package [21] for one-loop calculations in supersymmetric models.

## 3.2 Gauge boson and SM fermion sector

Since the minimal supersymmetric extension of the SM does not introduce further couplings between the SM particles, the renormalization used for the SM parameters can be taken from [16]. We use the common technique of multiplicative renormalization. The bare parameters are split into renormalized ones and their counter-terms

$$f_i \rightarrow (\delta_{ij} + \frac{1}{2}\delta Z_{ij}^L P_L + \frac{1}{2}\delta Z_{ij}^R P_R) f_j, \quad m_{f_i} \rightarrow m_{f_i} + \delta m_{f_i}, \quad (3.22)$$

$$m_W^2 \rightarrow m_W^2 + \delta m_W^2, \quad m_Z^2 \rightarrow m_Z^2 + \delta m_Z^2, \quad (3.23)$$

$$\begin{pmatrix} Z \\ A \end{pmatrix} \rightarrow \begin{pmatrix} 1 + \frac{1}{2}\delta Z_{ZZ} & \frac{1}{2}\delta Z_{ZA} \\ \frac{1}{2}\delta Z_{AZ} & 1 + \frac{1}{2}\delta Z_{AA} \end{pmatrix} \begin{pmatrix} Z \\ A \end{pmatrix}. \quad (3.24)$$

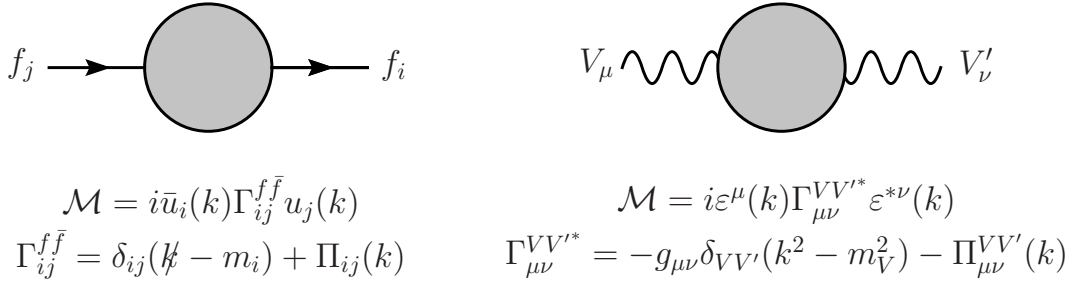


Figure 3.2: Two-point functions for mixing fermions and vector-particles.

The two point functions  $\Gamma_{ij}^{f\bar{f}}$  for fermions and  $\Gamma_{\mu\nu}^{VV'^*}$  for vector particles are generically given in Fig. 3.2. The self-energies  $\Pi(k)$  and accordingly the two point-functions  $\Gamma(k)$  can be decomposed in the following form

$$\Pi_{ij}(k) = \not{k}P_L\Pi_{ij}^L(k^2) + \not{k}P_R\Pi_{ij}^R(k^2) + P_L\Pi_{ij}^{SL}(k^2) + P_R\Pi_{ij}^{SR}(k^2), \quad (3.25)$$

$$\Pi_{\mu\nu}^{VV'}(k) = \left(g_{\mu\nu} - \frac{k_\mu k_\nu}{k^2}\right)\Pi_T^{VV'}(k^2) + \frac{k_\mu k_\nu}{k^2}\Pi_L^{VV'}(k^2). \quad (3.26)$$

These divergent expressions are renormalized by applying the usual on-shell conditions to the two-point functions. The renormalized mass parameters are defined to be the physical masses, i.e. the real parts of the poles of the corresponding propagators. We further demand, that close to its pole the propagators have tree-level form. As a consequence, an on-shell particle does not mix with others, and its propagator has residue one. This leads to conditions for the field renormalization constants.

$$\widetilde{\text{Re}}\hat{\Gamma}_{\mu\nu}^{VV'^*}(k)\varepsilon^\nu(k)\Big|_{k^2=m_V^2} = 0 \quad V, V' = A, Z, W, \quad (3.27)$$

$$\lim_{k^2 \rightarrow m_V^2} \frac{1}{k^2 - m_V^2} \widetilde{\text{Re}}\hat{\Gamma}_{\mu\nu}^{VV'^*}(k)\varepsilon^\nu(k) = -\varepsilon_\mu(k), \quad (3.28)$$

$$\widetilde{\text{Re}}\hat{\Gamma}_{ij}^{f\bar{f}}(k)u_j(k)\Big|_{k^2=m_{f_j}^2} = 0, \quad (3.29)$$

$$\lim_{k^2 \rightarrow m_{f_i}^2} \frac{\not{k} + m_{f_i}}{k^2 - m_{f_i}^2} \widetilde{\text{Re}}\hat{\Gamma}_{ii}^{f\bar{f}}(k)u_i(k) = u_i(k). \quad (3.30)$$

The condition  $\widetilde{\text{Re}}\hat{\Gamma}_T^{AA}(0) = 0$  is automatically fulfilled by a Lee identity. Please note that  $\widetilde{\text{Re}}$  only takes the real part of the loop integrals and does not affect the possibly complex couplings or gamma matrices. The vector boson renormalization constants are obtained as

$$\delta m_Z^2 = \widetilde{\text{Re}}\Pi_T^{ZZ}(m_Z^2), \quad \delta m_W^2 = \widetilde{\text{Re}}\Pi_T^{WW}(m_W^2), \quad (3.31)$$

$$\delta Z_{VV} = -\widetilde{\text{Re}}\dot{\Pi}_T^{VV}(m_V^2), \quad V = A, Z, W, \quad (3.32)$$

$$\delta Z_{AZ} = -\frac{2\widetilde{\text{Re}}\Pi_T^{AZ}(m_Z^2)}{m_Z^2}, \quad \delta Z_{ZA} = \frac{2\widetilde{\text{Re}}\Pi_T^{AZ}(0)}{m_Z^2}, \quad (3.33)$$

with  $\dot{\Pi}(m^2) = \left[ \frac{\partial}{\partial k^2} \Pi(k^2) \right]_{k^2=m^2}$ . The weak mixing angle  $\sin \theta_W \equiv s_W$  is fixed by the usual on-shell condition  $s_W^2 = 1 - c_W^2 = 1 - m_W^2/m_Z^2$

$$\frac{\delta c_W^2}{c_W^2} = \frac{\delta m_W^2}{m_W^2} - \frac{\delta m_Z^2}{m_Z^2}, \quad \frac{\delta s_W^2}{s_W^2} = -\frac{c_W^2}{s_W^2} \frac{\delta c_W^2}{c_W^2}. \quad (3.34)$$

The quark mixing matrix is assumed to be diagonal. Therefore no off-diagonal wave function counter-terms for the SM fermions have to be introduced. Thus we find the fermionic counter-terms (for simplicity the indices are omitted)

$$\delta m_f = \frac{1}{2} \widetilde{\text{Re}} [m_f (\Pi^L(m_f^2) + \Pi^R(m_f^2)) + \Pi^{SL}(m_f^2) + \Pi^{SR}(m_f^2)] \quad (3.35)$$

$$\delta Z^L = \widetilde{\text{Re}} \left[ -\Pi^L(m_f^2) - m_f^2 (\dot{\Pi}^L(m_f^2) + \dot{\Pi}^R(m_f^2)) + \frac{1}{2m_f} (\Pi^{SL}(m_f^2) - \Pi^{SR}(m_f^2)) - m_f (\dot{\Pi}^{SL}(m_f^2) + \dot{\Pi}^{SR}(m_f^2)) \right], \quad (3.36)$$

$$\delta Z^R = \delta Z^L (L \leftrightarrow R). \quad (3.37)$$

## 3.3 Charge Renormalization

### 3.3.1 Thomson limit

In the Thomson limit the electric charge is defined by the full electron-positron-photon vertex at vanishing photon momentum, i.e. for on-shell external particles, and the measured fine structure constant  $\alpha = e^2/(4\pi) = 1/137.036$ . (The renormalization can also be done for other external charged particles, due to charge universality. It gives the same charge definition.)

The counter-term  $\delta e$  is defined in such a way that it cancels the complete loop corrections, the vertex graphs and wave function corrections. In pure QED, the renormalized three-point function can be written at one-loop level in the form

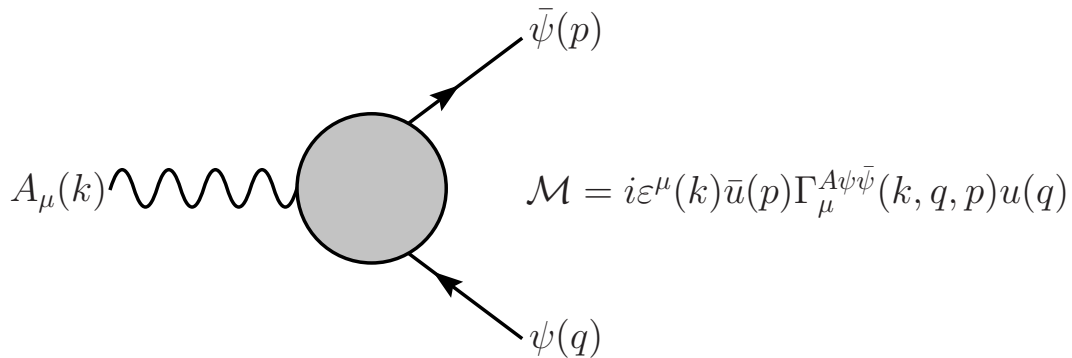


Figure 3.3: QED three-point function

$$\hat{\Gamma}_\mu^{A\psi\bar{\psi}} = e\gamma_\mu \left( 1 + \frac{\delta e}{e} + \frac{1}{2} \delta Z_{AA} + \delta Z_f \right) + e\Lambda_\mu^{A\psi\bar{\psi}} = e\gamma_\mu, \quad (3.38)$$

with the charge counter-term  $\delta e$ , the photon and electron/positron wave function corrections  $\delta Z_{AA}$  and  $\delta Z_f$ , and the vertex corrections  $\Lambda_\mu^{A\psi\bar{\psi}}$ . The QED Ward-Takahashi identity for the three-point vertex function  $\Gamma_\mu^{A\psi\bar{\psi}}(k, q, -q - k)$  and the two-point function  $\Gamma^{\psi\bar{\psi}}(q, -q) = -\Gamma^{\bar{\psi}\psi}(q, -q)$  with vanishing photon momentum is

$$\Gamma_\mu^{A\psi\bar{\psi}}(0, q, -q) = e \frac{\partial}{\partial q^\mu} \Gamma^{\psi\bar{\psi}}(q, -q). \quad (3.39)$$

So the vertex graphs cancel the electron/positron wave-function corrections and we obtain

$$\frac{\delta e}{e} = -\frac{1}{2} \delta Z_{AA} = \frac{1}{2} \frac{\Pi_T^{AA}(k^2)}{k^2} \Big|_{k^2=0} = \frac{1}{2} \frac{\partial \Pi_T^{AA}(k^2)}{\partial k^2} \Big|_{k^2=0}. \quad (3.40)$$

In the SM and in the MSSM, we have to consider additional loop corrections, including the  $\gamma - Z$  mixing. An identity similar to the QED Ward identity again relates the vertex graphs with wave function corrections and we get the counter-term [16]<sup>1</sup>

$$\frac{\delta e}{e} = -\frac{1}{2} \delta Z_{AA} + \frac{s_W}{2c_W} \delta Z_{ZA} = \frac{1}{2} \frac{\partial \Pi_T^{AA}(k^2)}{\partial k^2} \Big|_{k^2=0} + \frac{s_W}{c_W} \frac{\Pi_T^{AZ}(0)}{m_Z^2}. \quad (3.41)$$

The charge universality, the fact that the on-shell coupling constant of charged particles to the photon is independent of the species of the charged particles, holds in the SM as well as in the MSSM. Since the fermionic contributions to the transverse  $\gamma - Z$  mixing cancel at vanishing photon momentum  $\Pi_T^{AZ, \text{ferm}}(0) = 0$ , we have

$$\begin{aligned} \frac{\delta e^{\text{ferm}}}{e} &= -\frac{1}{2} \delta Z_{AA}^{\text{ferm}} = \sum_f \frac{N_C^f Q_f^2 e^2}{(4\pi)^2} \left( B_0(0, m_f^2, m_f^2) + 4\dot{B}_{00}(0, m_f^2, m_f^2) \right) \\ &= \frac{e^2}{(4\pi)^2} \frac{2}{3} \sum_f N_C^f Q_f^2 \left( \Delta + \log \frac{Q^2}{m_f^2} \right). \end{aligned} \quad (3.42)$$

The  $W$ -contribution to the counter-term is given by

$$\frac{\delta e^W}{e} = -\frac{e^2}{(4\pi)^2} \frac{1}{6} \left( 21 \left( \Delta + \log \frac{Q^2}{m_W^2} \right) + 2r \right), \quad (3.43)$$

with  $r=1/0$  in the  $\overline{\text{MS}}/\overline{\text{DR}}$  scheme. In the MSSM the additional SUSY contributions are

$$\begin{aligned} \frac{\delta e^{\text{SUSY}}}{e} &= \frac{e^2}{(4\pi)^2} \frac{1}{6} \left[ \sum_{\tilde{f}} \sum_{m=1}^2 N_C^f Q_f^2 \left( \Delta + \log \frac{Q^2}{m_{\tilde{f}_m}^2} \right) \right. \\ &\quad \left. + 4 \sum_{k=1}^2 \left( \Delta + \log \frac{Q^2}{m_{\tilde{\chi}_k^+}^2} \right) + \left( \Delta + \log \frac{Q^2}{m_{H^+}^2} \right) \right]. \end{aligned} \quad (3.44)$$

<sup>1</sup>The sign of the  $AZ$ -mixing term depends on the sign of the  $\text{SU}(2)$  covariant derivative  $D_\mu = \partial_\mu + \sigma i g_2 W_\mu$ , which we choose to be  $\sigma = +$ .

### 3.3.2 Effective electric charge at high energies

At lower energies, the vacuum polarization effects lead to a partial screening of the electric charge. Therefore the strength of the electromagnetic interaction grows logarithmically with the increasing energy scale. So the electric charge in the Thomson limit does not seem to be a proper input value for the calculation of processes in the GeV or TeV range.

At energies below the  $Z$ -pole an effective charge, or fine structure constant, can be defined by

$$\alpha_{\text{QED}}^{\text{eff}}(Q^2) = \frac{\alpha}{1 - \Delta\alpha(Q^2)}, \quad (3.45)$$

with the finite shift  $\Delta\alpha = \Delta\alpha_{\text{lep}} + \Delta\alpha_{\text{had}}^{(5)}$ , the so-called vacuum polarization

$$\Delta\alpha(Q^2) = 2 \left( \frac{\delta e}{e}(0) - \frac{\delta e}{e}(Q^2) \right)_{\text{QED}} = \Pi'(0) - \text{Re}\Pi'(Q^2), \quad (3.46)$$

and  $\Pi'(k^2) \equiv \frac{\Pi_T^{\text{AA}}(k^2)}{k^2}$ . Note, that  $Q^2$  denotes the squared momentum of the photon. The  $\mu^2$  scale dependence of  $\Pi'(k^2)$  cancels in  $\Delta\alpha(Q^2)$ .

In perturbation theory the leading light fermion ( $m_f \ll Q$ ) contribution is given by

$$\begin{aligned} \Delta\alpha(Q^2) &= \frac{\alpha}{3\pi} \sum_f Q_f^2 N_C^f \left[ -\frac{8}{3} + \beta_f^2 - \frac{1}{2}\beta_f(3 - \beta_f^2) \log\left(\frac{1 - \beta_f}{1 + \beta_f}\right) \right] \\ &= \frac{\alpha}{3\pi} \sum_f Q_f^2 N_C^f \left[ \log(Q^2/m_f^2) - \frac{5}{3} + O(m_f^2/Q^2) \right], \end{aligned} \quad (3.47)$$

where  $\beta_f = \sqrt{1 - 4m_f^2/Q^2}$ .

The leptonic contribution can be treated perturbatively. It is known up to three loops and takes at the  $Z$ -mass the value

$$\Delta\alpha_{\text{lep}}(m_Z^2) \simeq 0.031497687. \quad (3.48)$$

The corresponding quark loop contribution is substantially modified by low energy strong interaction effects and the result obtained in perturbation theory is not reliable. Fortunately, the hadronic contribution for the light quarks  $\Delta\alpha_{\text{had}}^{(5)}$  can be calculated from hadronic  $e^+e^-$ -annihilation data by using the dispersion relation

$$\text{Re}\Pi'(Q^2) - \Pi'(0) = \frac{Q^2}{\pi} \text{Re} \int_{s_0}^{\infty} ds \frac{\text{Im}\Pi'(s)}{s(s - Q^2 - i\varepsilon)} \quad (3.49)$$

and the optical theorem

$$\text{Im}\Pi'(s) = \frac{s}{e^2} \sigma_{\text{tot}}(e^+e^- \rightarrow \gamma^* \rightarrow \text{hadrons})(s). \quad (3.50)$$

Recent compilations yield the values  $\Delta\alpha_{\text{had}}^{(5)}(m_Z^2) = 0.02761 \pm 0.00036$  [22],  $\Delta\alpha_{\text{had}}^{(5)}(m_Z^2) = 0.02769 \pm 0.00035$  [23],  $\Delta\alpha_{\text{had}}^{(5)}(m_Z^2) = 0.02755 \pm 0.00023$  [24].

In an energy range near or above  $Q^2 = m_Z^2$  also the  $W$  contributes to the vacuum polarization. This leads to a gauge dependent result, since a single self-energy is not a measurable quantity. A more physical definition could be the complete electron form-factor, but far off-shell, i.e. at high energies, this is also not accessible by experiment. A measurable quantity is a cross-section, including all self-energy, vertex and box graphs. A more formal definition is the electric charge in the  $\overline{\text{MS}}$  (or  $\overline{\text{DR}}$ ) scheme. However this is not physical. For example, while contributions of heavy particles decouple from physics at low energies,  $\overline{\text{MS}}$  (or  $\overline{\text{DR}}$ ) parameters can get large contributions of the form  $\log(Q^2/M_{\text{heavy}})$  with  $Q^2 \ll M_{\text{heavy}}$ . However, it is possible to “define” a parameter, where only particles with masses below a certain scale  $M^2 \leq Q^2$  contribute. On the other hand, it is obvious that such a definition can lead again to problems in the context of gauge invariance, if only the light members of a gauge group multiplet are taken into account.

### 3.3.3 Effective renormalization schemes for $\alpha$ at $Q = m_Z$

The discussion in the last chapter shows that the pure on-shell renormalization eq.(3.41) gives two main problems. At first, the charge in the Thomson limit is far away from the scale of the corresponding process, which results in a large uncertainty due to higher order corrections. The second uncertainty comes from the large hadronic contributions, which cannot be reliably calculated in perturbation theory. So the definition of an effective charge seems to be necessary [25].

In the  $\alpha_{\text{QED}}^{\text{eff}}(m_Z^2)$  scheme, we use as input the effective QED charge at  $Q^2 = m_Z^2$

$$\alpha_{\text{QED}}^{\text{eff}}(m_Z^2) = \frac{\alpha}{1 - \Delta\alpha} = \frac{\alpha}{1 - \Delta\alpha_{\text{lep}} - \Delta\alpha_{\text{had}}^{(5)}} \simeq \frac{1}{128.9}. \quad (3.51)$$

The corresponding counter-term can be simply calculated:

$$\begin{aligned} \hat{\alpha}(Q^2) = \alpha + \delta\alpha_{\text{OS}}(Q^2) &= \alpha + \delta\alpha_{\text{OS}}(Q^2) + \alpha (\text{Re}\Pi'(m_Z^2) - \Pi'(0) + \Delta\alpha(m_Z^2)) \\ &= \frac{\alpha}{1 - \Delta\alpha(m_Z^2)} + \delta\alpha_{\text{OS}}(Q^2) + \alpha (\text{Re}\Pi'(m_Z^2) - \Pi'(0)) \end{aligned} \quad (3.52)$$

$\hat{\alpha}(Q^2)$  denotes the  $\overline{\text{DR}}$  parameter at the scale  $Q^2$  and  $\delta\alpha_{\text{OS}}(Q^2)$  is given by the UV finite part of eq.(3.41) in the  $\overline{\text{DR}}$  scheme, both at one-loop order.

Since  $\Delta\alpha$  and  $\Pi'(k^2)$  contain only the leptonic and the light quark contributions, the resummation in the last line takes higher orders correctly into account and does not spoil gauge invariance. The inclusion of  $\Delta\alpha$  in the tree-level definition leads to smaller one-loop corrections. The uncertainty in the hadronic contributions is cancelled in  $\delta\alpha_{\text{OS}}(Q^2) - \alpha\Pi'(0)$ .

In the  $\alpha_{\overline{\text{MS}}}(m_Z^2)$  scheme the value of the  $\overline{\text{MS}}$  parameter in the SM is used:  $\alpha_{\overline{\text{MS}}}(m_Z^2) \simeq 1/127.9$ . It is evaluated together with  $m_Z$ ,  $\Gamma_Z$  and  $\sin(\theta_W)_{\overline{\text{MS}}}(m_Z^2)$  from a global fit of  $e^+e^- \rightarrow f\bar{f}$  data at the  $Z$  pole. The counter-term is defined by

$$\begin{aligned} \hat{\alpha}(Q^2) = \alpha + \delta\alpha_{\text{OS}}(Q^2) &= \alpha + \delta\alpha_{\text{OS}}(Q^2) - \delta\alpha_{\overline{\text{MS}}}(m_Z^2) + \alpha\Delta\alpha_{\overline{\text{MS}}}(m_Z^2) \\ &= \frac{\alpha}{1 - \Delta\alpha_{\overline{\text{MS}}}(m_Z^2)} + \delta\alpha_{\text{OS}}(Q^2) - \delta\alpha_{\overline{\text{MS}}}(m_Z^2). \end{aligned} \quad (3.53)$$

In this definition, the counter-term  $\delta\alpha_{\overline{\text{MS}}}(m_Z^2)$  contains the full SM contributions in the  $\overline{\text{MS}}$  scheme, i.e. eqs. (3.42) to (3.44) at  $Q^2 = m_Z^2$  and  $r = 1$ . Please note, that  $\Delta\alpha(m_Z^2)$  and  $\Delta\alpha_{\overline{\text{MS}}}(m_Z^2)$  are not the same [26, 27], but

$$\Delta\alpha_{\overline{\text{MS}}}(m_Z^2) - \Delta\alpha(m_Z^2) = \frac{\alpha}{\pi} \left( \frac{5}{3} + \frac{55}{27} \left( 1 + \frac{\alpha_s}{\pi} \right) \right) - \frac{8\alpha}{9\pi} \log \frac{m_t}{m_Z} + \frac{\alpha}{2\pi} \left( \frac{7}{2} \log c_W^2 - \frac{1}{3} \right). \quad (3.54)$$

The first term are the leading fermionic contributions in  $O(\alpha)$  and  $O(\alpha\alpha_s)$  of the difference between the scale independent  $(\Pi'(0) - \text{Re}\Pi'(m_Z^2))$  and the self-energy  $\Pi'(0)$  at the scale  $Q^2 = m_Z^2$ . The  $O(\alpha)$  term can be easily seen from eqs.(3.42) and (3.47). The second and third term are the remaining SM top and  $W$  contributions. As discussed in the last chapter, also an effective parameter can be defined, where  $\delta\alpha_{\overline{\text{MS}}}^{\text{eff}}(m_Z^2)$  includes only the contributions of light fermions [28]. The effective fine structure constant  $\alpha_{\overline{\text{MS}}}^{\text{eff}}(m_Z^2)$  is then

$$\begin{aligned} \Delta\alpha_{\overline{\text{MS}}}^{\text{eff}}(m_Z^2) - \Delta\alpha(m_Z^2) &= \frac{\alpha}{\pi} \left( \frac{5}{3} + \frac{55}{27} \left( 1 + \frac{\alpha_s}{\pi} \right) \right), \\ \alpha_{\overline{\text{MS}}}^{\text{eff}}(m_Z^2) &= \frac{\alpha}{1 - \Delta\alpha_{\overline{\text{MS}}}^{\text{eff}}(m_Z^2)} \simeq \frac{1}{127.7}, \end{aligned} \quad (3.55)$$

and the corresponding counter-term is given by

$$\begin{aligned} \frac{\delta e}{e} &= \frac{1}{(4\pi)^2} \frac{e^2}{6} \left[ 4 \sum_f N_C^f e_f^2 \left( \Delta + \log \frac{Q^2}{x_f^2} \right) + \sum_{\tilde{f}} \sum_{m=1}^2 N_C^f e_f^2 \left( \Delta + \log \frac{Q^2}{m_{\tilde{f}m}^2} \right) \right. \\ &\quad \left. + 4 \sum_{k=1}^2 \left( \Delta + \log \frac{Q^2}{m_{\tilde{\chi}_k^+}^2} \right) + \left( \Delta + \log \frac{Q^2}{m_{H^+}^2} \right) - 21 \left( \Delta + \log \frac{Q^2}{m_W^2} \right) \right], \end{aligned} \quad (3.56)$$

with  $x_f = m_Z \forall m_f < m_Z$  and  $x_t = m_t$ .  $N_C^f$  is the colour factor,  $N_C^f = 1, 3$  for (s)leptons and (s)quarks, respectively.

### 3.3.4 The fine-structure constant in the $G_F$ scheme

In the so-called  $G_F$  scheme we use as input the Fermi constant  $G_F = 1.16637 * 10^{-5} \text{ GeV}^{-2}$ , which is defined by the muon life time

$$\frac{1}{\tau_\mu} = \frac{G_F^2 m_\mu^5}{192\pi^3} F \left( \frac{m_e^2}{m_\mu^2} \right) \left( 1 + \frac{3m_\mu^2}{5m_W^2} \right) (1 + \Delta_{\text{QED}}), \quad (3.57)$$

with  $F(x) = 1 - 8x - 12x^2 \log x + 8x^3 - x^4$ . By convention, the QED corrections within the Fermi Model  $\Delta_{\text{QED}}$  are included in this defining equation for  $G_F$ . Calculating the muon decay process in the SM (or its extensions) yields the following relation between the Fermi and the fine-structure constant

$$G_F = \frac{\pi\alpha}{\sqrt{2}s_W^2 m_W^2} (1 + \Delta r), \quad (3.58)$$

where  $\Delta r$  contains the remaining radiative corrections. At one-loop level the result for  $\Delta r$  can be decomposed in the form

$$\Delta r \equiv \Delta\alpha - \frac{c_W^2}{s_W^2} \Delta\rho + \Delta r_{\text{rem}}, \quad (3.59)$$

with the two dominant contributions  $\Delta\alpha$  and  $\Delta\rho$ .  $\Delta\alpha$  is again the vacuum polarization, and

$$\Delta\rho = \text{Re} \left( \frac{\Pi_T^{ZZ}(0)}{m_Z^2} - \frac{\Pi_T^{WW}(0)}{m_W^2} \right), \quad (3.60)$$

which is finite and sensitive to the  $m_Z - m_W$  mass relation. The remainder  $\Delta r_{\text{rem}}$  is typically of the order of  $\sim 0.01$ .

We can define an effective charge

$$\alpha_F = \frac{\sqrt{2}s_W^2 m_W^2}{\pi} G_F \simeq \frac{1}{132.5} \quad (3.61)$$

and include  $\Delta r$  in the corresponding counter-term of  $\alpha$

$$\hat{\alpha}(Q^2) = \alpha + \delta\alpha_{\text{OS}}(Q^2) = \alpha_F + \delta\alpha_{\text{OS}}(Q^2) - \alpha_F \Delta r. \quad (3.62)$$

Again the uncertainty  $\Delta\alpha$  in both terms,  $\Delta r$  and  $\delta\alpha_{\text{OS}}(Q^2)$ , cancel each other. Note, that we have used a resummation for  $\Delta r$  in the last equation. However, this does not correctly resum the leading contributions  $\Delta\alpha$  and  $\Delta\rho$  beyond  $O(\alpha)$ . A correct resummation up to  $O(\alpha^2)$ , see ref. [29], can be done by replacing  $\Delta r$  in eq. (3.62) with

$$\Delta r^{\text{res}} = 1 - \frac{1 - \Delta\alpha}{1 + \Delta r_{\text{rem}}} \frac{s_W^2 + c_W^2 \Delta\rho}{s_W^2}. \quad (3.63)$$

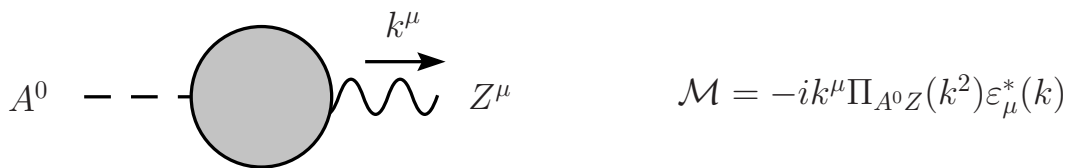
The counter-term for the electric charge in the  $G_F$  scheme has the form

$$\frac{\delta e}{e} = -\frac{1}{2} \delta Z_{AA} + \frac{s_W}{2c_W} \delta Z_{ZA} - \frac{1}{2} \Delta r. \quad (3.64)$$

### 3.4 Higgs sector

In the MSSM two complex Higgs doublets  $H_1$  and  $H_2$  are required, so the renormalization is more involved than in the SM. A detailed one-loop renormalization of the MSSM Higgs sector can be found e.g. in [30, 31]. In this thesis, we restrict the discussion to the case of  $\tan\beta$ . The renormalization of the ratio of the vacuum expectation values is by no means trivial [32]. In a definition by a specific physical process technical difficulties are introduced. A process independent renormalization on the other hand leads to gauge dependence and/or numerical instabilities. A convenient choice, is the condition, that the pseudo-scalar Higgs field  $A^0$  does not mix with the  $Z$  vector boson for on-shell momenta. Thus it appears that the renormalized  $A^0 Z$  mixing self-energy  $\Pi_{A^0 Z}$ , defined in Fig. 3.4, has to vanish for  $p^2 = m_{A^0}^2$ .

$$\text{Im} \left[ \widetilde{\text{Re}} \hat{\Pi}_{A^0 Z}(m_{A^0}^2) \right] = 0. \quad (3.65)$$

Figure 3.4:  $A^0 Z$  mixing self-energy

From this constraint a condition for the renormalization of  $\tan\beta$  can be obtained

$$\frac{\delta \tan\beta}{\tan\beta} = \frac{1}{m_Z \sin 2\beta} \operatorname{Im} \left[ \widetilde{\operatorname{Re}} \Pi_{A^0 Z}(m_{A^0}^2) \right]. \quad (3.66)$$

Unfortunately, the result is gauge dependent and can lead to big corrections for large  $\tan\beta$ . It can be improved by taking only the divergent part of the  $A^0 Z$  self energy, which makes it numerically more stable and in the class of  $R_\xi$  gauges  $\xi$  independent at one-loop level. We call the first scale independent definition “on-shell” in contrast to the second “ $\overline{\text{DR}}$  renormalization” at a certain scale  $Q$ . Both definitions and the translation between them are used in this thesis.

### 3.5 Neutralinos and charginos

The on-shell renormalization of the chargino, neutralino and sfermion sector is definitely more complicated than in the SM sector<sup>2</sup>. First of all, the mixing between the different particles has to be taken into account in contrast to the SM fermion sector, where the entries of the CKM matrix are such small, that they are negligible for our purposes. However, an on-shell renormalization for the CKM matrix is well-known [34] and a similar approach can be used for the  $\tilde{\chi}^\pm, \tilde{\chi}^0$  mixing matrices  $U$ ,  $V$ , and  $N$ .

The second problem is more subtle. In the (on-shell renormalized) SM, the masses of the particles are free and independent parameters of the theory. Contrary, in the SUSY sector of the MSSM the masses of the charginos, neutralino and sfermions depend on a limited set of SUSY-breaking parameters. As a consequence, the masses are not independent quantities, but relations between them occur (even at tree-level). In the neutralino-chargino system, there are only the free parameters  $M'$ ,  $M$ , and  $\mu$  that are not already fixed in the SM or Higgs sector of the model. One possible way of renormalization is to define on-shell conditions for only three of the six neutralino-chargino masses. As a consequence, the other four particles receive loop corrections to the on-shell masses, see e.g.[35]. However, such an approach seems to be problematic for our purpose, the calculation of observables to neutralino and chargino pair production. For example, choosing any three of the six masses is “undemocratic” and the numerical stability strongly depends on the gaugino-/higgsino-character of the three fixed on-shell masses.

The on-shell renormalization procedure used in this thesis, has been worked out in [36]. In addition, the formulas given here are also valid for the general MSSM with complex phases.

<sup>2</sup>For calculations of the one-loop corrections to the neutralino/chargino masses in the  $\overline{\text{DR}}$  scheme, we refer to [33]

After rotation from the interaction to the mass eigenstate basis, we nevertheless apply the on-shell conditions eq. (3.29, 3.30) for all six neutralinos/charginos, respectively. Hence, the introduced wave function and mass counter-terms are

$$\tilde{\chi}_i \rightarrow (\delta_{ij} + \frac{1}{2}\delta\tilde{Z}_{ij}^L P_L + \frac{1}{2}\delta\tilde{Z}_{ij}^R P_R)\tilde{\chi}_j, \quad m_{\tilde{\chi}_i} \rightarrow m_{\tilde{\chi}_i} + \delta m_{\tilde{\chi}_i}, \quad (3.67)$$

where  $\tilde{\chi}$  stands for both, charginos or neutralinos. These counter-terms are related to the corresponding self-energies by

$$\delta m_{\tilde{\chi}_i} = \frac{1}{2}\widetilde{\text{Re}} \left[ m_{\tilde{\chi}_i} (\Pi_{ii}^L(m_{\tilde{\chi}_i}^2) + \Pi_{ii}^R(m_{\tilde{\chi}_i}^2)) + \Pi_{ii}^{SL}(m_{\tilde{\chi}_i}^2) + \Pi_{ii}^{SR}(m_{\tilde{\chi}_i}^2) \right], \quad (3.68)$$

$$\delta\tilde{Z}_{ii}^L = \widetilde{\text{Re}} \left[ -\Pi_{ii}^L(m_{\tilde{\chi}_i}^2) - m_{\tilde{\chi}_i}^2 (\dot{\Pi}_{ii}^L(m_{\tilde{\chi}_i}^2) + \dot{\Pi}_{ii}^R(m_{\tilde{\chi}_i}^2)) + \frac{1}{2m_{\tilde{\chi}_i}} (\Pi_{ii}^{SL}(m_{\tilde{\chi}_i}^2) - \Pi_{ii}^{SR}(m_{\tilde{\chi}_i}^2)) - m_{\tilde{\chi}_i} (\dot{\Pi}_{ii}^{SL}(m_{\tilde{\chi}_i}^2) + \dot{\Pi}_{ii}^{SR}(m_{\tilde{\chi}_i}^2)) \right], \quad (3.69)$$

$$\delta\tilde{Z}_{ij}^L = c_{ij} \widetilde{\text{Re}} \left[ m_{\tilde{\chi}_j}^2 \Pi_{ij}^L(m_{\tilde{\chi}_j}^2) + m_{\tilde{\chi}_i} m_{\tilde{\chi}_j} \Pi_{ij}^R(m_{\tilde{\chi}_j}^2) + m_{\tilde{\chi}_i} \Pi_{ij}^{SL}(m_{\tilde{\chi}_j}^2) + m_{\tilde{\chi}_j} \Pi_{ij}^{SR}(m_{\tilde{\chi}_j}^2) \right], \quad (3.70)$$

$$\delta\tilde{Z}_{ii}^R = \delta\tilde{Z}_{ii}^L (L \leftrightarrow R), \quad \delta\tilde{Z}_{ij}^R = \delta\tilde{Z}_{ij}^L (L \leftrightarrow R), \quad c_{ij} = 2/(m_{\tilde{\chi}_i}^2 - m_{\tilde{\chi}_j}^2), \quad (3.71)$$

with  $\delta\tilde{Z} \equiv \delta\tilde{Z}^\pm/\delta\tilde{Z}^0$  and  $\Pi_{ii}(k^2)$  the chargino/neutralino self-energies, respectively. The renormalization constants have the same structure as for the SM fermions, besides the mixing counter-terms  $\delta\tilde{Z}_{ij}^{L/R}$  for  $i \neq j$  that have been neglected in the SM case. Special care has to be taken in the chargino sector. In principal, there are two possible ways to build the chargino Dirac states from the corresponding Weyl spinors and both are used in the literature. One in which the positively charged chargino is the ‘‘particle’’ and the negatively is the charge conjugated anti-particle ( $\tilde{\chi}^+$ ,  $\tilde{\chi}^{+,c}$ ) or vice versa ( $\tilde{\chi}^-$ ,  $\tilde{\chi}^{-,c}$ ). The renormalization is always done for the ‘‘particle’’, see for example eqs. (3.29, 3.30), and the counter-terms for the anti-particle are automatically delivered. So, the renormalization constants are oblique to this definition. To express the difference, we use  $\delta\tilde{Z}^+$  for the ( $\tilde{\chi}^+$ ,  $\tilde{\chi}^{+,c}$ ) case and  $\delta\tilde{Z}^-$  for ( $\tilde{\chi}^-$ ,  $\tilde{\chi}^{-,c}$ ). The translation from one to the other is just given by a charge conjugation

$$\delta\tilde{Z}_{ik}^{-,L} = (\delta\tilde{Z}_{ik}^{+,R})^*, \quad (\delta\tilde{Z}_{ik}^{-,R})^* = \delta\tilde{Z}_{ik}^{+,L}. \quad (3.72)$$

In a next step we have to define the neutralino and chargino rotation matrices at one-loop level. Unless experimental data is available, a process and scale independent fixing seems appropriate for an on-shell renormalization. We define the counter-terms in such a way that they cancel the rotation, induced by the anti-hermitian parts of the off-diagonal wave function corrections

$$\delta N_{ij} = \frac{1}{4} \sum_{k=1}^4 \left( \delta\tilde{Z}_{ik}^{0,L} - \delta\tilde{Z}_{ki}^{0,R} \right) N_{kj}, \quad (3.73)$$

$$\delta U_{ij} = \frac{1}{4} \sum_{k=1}^2 \left( (\delta\tilde{Z}_{ik}^{+,R})^* - \delta\tilde{Z}_{ki}^{+,R} \right) U_{kj}, \quad \delta V_{ij} = \frac{1}{4} \sum_{k=1}^2 \left( \delta\tilde{Z}_{ik}^{+,L} - (\delta\tilde{Z}_{ki}^{+,L})^* \right) V_{kj}. \quad (3.74)$$

These counter-terms have indeed the correct UV-divergence, which can be checked by comparing the renormalization before rotation in mass eigenstates (where no explicit renormalization constants for the rotation matrices are introduced) with our proposed renormalization after rotation [37]. As mentioned above, this fixing is similar to the one for the CKM matrix. Further, it is shown in [38] that this fixing eqs. (3.73) and (3.74), calculated within the Feynman-'t Hooft gauge, can be regarded as a gauge independent one.

The renormalization of the gauge eigenstate fields can be expressed in the following form:

$$\begin{pmatrix} \psi_j^+ \\ \bar{\psi}_j^- \end{pmatrix} \rightarrow \sum_{k=1}^2 \left[ (V_{ij}^* + \delta V_{ij}^* + \frac{1}{2} V_{kj}^* \delta \tilde{Z}_{ki}^{+,L}) P_L + (U_{ij} + \delta U_{ij} + \frac{1}{2} U_{kj} \delta \tilde{Z}_{ki}^{+,R}) P_R \right] \tilde{\chi}_i^+ \quad (3.75)$$

$$\begin{pmatrix} \psi_j^0 \\ \bar{\psi}_j^0 \end{pmatrix} \rightarrow \sum_{k=1}^4 \left[ (N_{ij}^* + \delta N_{ij}^* + \frac{1}{2} N_{kj}^* \delta \tilde{Z}_{ki}^{0,L}) P_L + (N_{ij} + \delta N_{ij} + \frac{1}{2} N_{kj} \delta \tilde{Z}_{ki}^{0,R}) P_R \right] \tilde{\chi}_i^0 \quad (3.76)$$

This shows, that in principle the counter-terms to the rotation matrices can be absorbed into redefined wave-function corrections. Inserting the fixing eqs. (3.73, 3.74) yields

$$\begin{pmatrix} \psi_j^+ \\ \bar{\psi}_j^- \end{pmatrix} \rightarrow \sum_{k=1}^2 \left[ \left( V_{ij}^* + \frac{1}{4} V_{kj}^* \left( \delta \tilde{Z}_{ki}^{+,L} + (\delta \tilde{Z}_{ik}^{+,L})^* \right) \right) P_L + \right. \quad (3.77) \\ \left. \left( U_{ij} + \frac{1}{4} U_{kj} \left( \delta \tilde{Z}_{ki}^{+,R} + (\delta \tilde{Z}_{ik}^{+,R})^* \right) \right) P_R \right] \tilde{\chi}_i^+,$$

$$\begin{pmatrix} \psi_j^0 \\ \bar{\psi}_j^0 \end{pmatrix} \rightarrow \sum_{k=1}^4 \left[ \left( N_{ij}^* + \frac{1}{4} N_{kj}^* \left( \delta \tilde{Z}_{ki}^{0,L} + (\delta \tilde{Z}_{ik}^{0,L})^* \right) \right) P_L + \right. \quad (3.78) \\ \left. \left( N_{ij} + \frac{1}{4} N_{kj} \left( \delta \tilde{Z}_{ki}^{0,R} + (\delta \tilde{Z}_{ik}^{0,R})^* \right) \right) P_R \right] \tilde{\chi}_i^0.$$

As one can see, the same result can be obtained by a redefinition of the wave-function corrections in a symmetric (hermitian) way

$$\delta \tilde{Z}_{ki}^{+,L/R} \rightarrow \frac{1}{2} \left( \delta \tilde{Z}_{ki}^{+,L/R} + (\delta \tilde{Z}_{ik}^{+,L/R})^* \right), \quad \delta \tilde{Z}_{ki}^{0,L/R} \rightarrow \frac{1}{2} \left( \delta \tilde{Z}_{ki}^{0,L/R} + (\delta \tilde{Z}_{ik}^{0,L/R})^* \right), \quad (3.79)$$

and setting  $\delta N_{ij} = \delta U_{ij} = \delta V_{ij} = 0$ .

From the counter-terms for the on-shell masses and the rotation matrices, the counter-terms for the mass matrix elements can be directly deduced

$$\delta Y_{ij} = \delta (N^T Y_D N)_{ij} = \delta N_{ni} (Y_D)_{nl} N_{lj} + N_{ni} \delta (Y_D)_{nl} N_{lj} + N_{ni} (Y_D)_{nl} \delta N_{lj}, \quad (3.80)$$

$$\delta X_{ij} = \delta (U^T X_D V)_{ij} = \delta U_{ni} (X_D)_{nl} V_{lj} + U_{ni} \delta (X_D)_{nl} V_{lj} + U_{ni} (X_D)_{nl} \delta V_{lj}. \quad (3.81)$$

The diagonalized mass matrices and its corresponding counter-terms are

$$(Y_D)_{nl} = \delta_{nl} m_{\tilde{\chi}_l^0}, \quad \delta (Y_D)_{nl} = \delta_{nl} \delta m_{\tilde{\chi}_l^0}, \quad (X_D)_{nl} = \delta_{nl} m_{\tilde{\chi}_l^\pm}, \quad \delta (X_D)_{nl} = \delta_{nl} \delta m_{\tilde{\chi}_l^\pm}. \quad (3.82)$$

Inserting the self-energies into the renormalization constants, we obtain

$$\delta Y_{ij} = \frac{1}{2} \sum_{l,n=1}^4 N_{ni} N_{lj} \widetilde{\text{Re}} \left[ m_{\tilde{\chi}_n^0} \Pi_{nl}^L(m_{\tilde{\chi}_n^0}^2) + m_{\tilde{\chi}_l^0} \Pi_{nl}^R(m_{\tilde{\chi}_l^0}^2) + \Pi_{nl}^{SL}(m_{\tilde{\chi}_l^0}^2) + \Pi_{nl}^{SL}(m_{\tilde{\chi}_n^0}^2) \right], \quad (3.83)$$

$$\delta X_{ij} = \frac{1}{2} \sum_{l,n=1}^2 U_{ni} V_{lj} \widetilde{\text{Re}} \left[ m_{\tilde{\chi}_n^\pm} \Pi_{nl}^L(m_{\tilde{\chi}_n^\pm}^2) + m_{\tilde{\chi}_l^\pm} \Pi_{nl}^R(m_{\tilde{\chi}_l^\pm}^2) + \Pi_{nl}^{SL}(m_{\tilde{\chi}_l^\pm}^2) + \Pi_{nl}^{SL}(m_{\tilde{\chi}_n^\pm}^2) \right]. \quad (3.84)$$

Due to the fact that we applied the on-shell conditions to all six neutralino/chargino masses, although they are not independent quantities, we have to include additional corrections. Let us consider the “bare” mass matrices  $X^0$ , and  $Y^0$  for the charginos and neutralinos, respectively. We can express them, on the one hand, by a tree-level mass matrix in terms of the on-shell parameters plus the corresponding counter-terms

$$Y^0 = Y_{\text{tree}} + \delta_c Y, \quad X^0 = X_{\text{tree}} + \delta_c X. \quad (3.85)$$

where  $\delta_c Y$  means the renormalization constants to the parameters in the tree-level mass matrix. On the other hand it can be expressed as the on-shell mass matrix, which gives the correct one-loop on-shell masses after diagonalization, plus the renormalization constants eqs. (3.83, 3.84)

$$Y^0 = Y + \delta Y, \quad X^0 = X + \delta X, \quad (3.86)$$

Eliminating the bare matrices we obtain

$$Y = Y_{\text{tree}} + (\delta_c Y - \delta Y) = Y_{\text{tree}} + \Delta Y, \quad X = X_{\text{tree}} + (\delta_c X - \delta X) = X_{\text{tree}} + \Delta X, \quad (3.87)$$

Since we have only a limited set of free parameters in the mass matrices, the on-shell masses cannot be expressed by tree-level relations between the input parameters. Therefore, the counter-terms cannot be defined in such a way that all entries in the UV-finite shifts  $\Delta Y$ ,  $\Delta X$  cancel.

In the on-shell scheme, one starts with the mass matrices  $Y_{\text{tree}}$ ,  $X_{\text{tree}}$ . So it is mandatory to include the UV-finite shifts already at tree-level if one wants to work out the one-loop contributions in a consistent way.

For a better understanding, we consider the case of the gaugino mass parameter  $M$ . The bare parameter  $M^0$  appears in the neutralino mass matrix as element  $Y_{22}$  and also in the chargino mass matrix in element  $X_{11}$ . The corresponding on-shell and bare parameters  $M$  and  $M^0$  are related by the counter-term  $\delta M$

$$M^0 = M + \delta M. \quad (3.88)$$

While the bare parameter is unique, the on-shell value depends on the UV-divergent part of the counter-term. So the fixing of the counter-term can be regarded as the definition of the on-shell Lagrangian parameter. Different renormalization schemes lead to different counter-terms to the Lagrangian parameters and thus to different “meanings” of this parameters. Therefore it is obvious that  $M$  cannot be defined by the counter-term  $\delta Y_{22}$  to the neutralino

mass matrix and simultaneously by the chargino mass matrix counter-term  $\delta X_{11}$ . The same holds for  $\mu$  and the parameters already fixed in the gauge and Higgs sector.

Therefore, we define  $M$  and  $\mu$  to be the parameters in the chargino mass matrix

$$M \equiv X_{11} \leftrightarrow \delta M \equiv \delta X_{11}, \quad \mu \equiv X_{22} \leftrightarrow \delta \mu \equiv \delta X_{22} \quad (3.89)$$

throughout the calculation. Within our approach, it is quite natural to define the  $U(1)_Y$  gaugino mass parameter  $M'$  according to

$$M' \equiv Y_{11} \leftrightarrow \delta M' \equiv \delta Y_{11}. \quad (3.90)$$

For all other mass matrix elements finite shifts have to be taken into account, e.g.:

$$M^0 = Y_{22} + \delta Y_{22} = X_{11} + \delta X_{11} \rightarrow Y_{22} = X_{11} + (\delta X_{11} - \delta Y_{11}) = M + \Delta M, \quad (3.91)$$

$$\mu^0 = -(Y_{34} + \delta Y_{34}) = X_{22} + \delta X_{22} \rightarrow Y_{34} = -X_{22} - (\delta X_{22} + \delta Y_{34}) = \mu + \Delta \mu. \quad (3.92)$$

For completeness, we give a list of all corrections to the neutralino/chargino mass matrix elements. The variation of the mass matrix in terms of the tree-level values is given by

$$\delta_c Y_{11} = \delta M' = \frac{\delta M'}{M'} Y_{11}, \quad (3.93)$$

$$\delta_c Y_{12} = \delta_c Y_{33} = \delta_c Y_{44} = 0, \quad (3.94)$$

$$\delta_c Y_{13} = -\delta(m_Z \sin \theta_W \cos \beta) = \left( \frac{\delta m_Z}{m_Z} + \frac{\delta \sin \theta_W}{\sin \theta_W} - \sin^2 \beta \frac{\delta \tan \beta}{\tan \beta} \right) Y_{13}, \quad (3.95)$$

$$\delta_c Y_{14} = \delta(m_Z \sin \theta_W \sin \beta) = \left( \frac{\delta m_Z}{m_Z} + \frac{\delta \sin \theta_W}{\sin \theta_W} + \cos^2 \beta \frac{\delta \tan \beta}{\tan \beta} \right) Y_{14}, \quad (3.96)$$

$$\delta_c Y_{22} = \delta M = \frac{\delta M}{M} Y_{22}, \quad (3.97)$$

$$\delta_c Y_{23} = \delta(m_Z \cos \theta_W \cos \beta) = \left( \frac{\delta m_Z}{m_Z} - \tan^2 \theta_W \frac{\delta \sin \theta_W}{\sin \theta_W} - \sin^2 \beta \frac{\delta \tan \beta}{\tan \beta} \right) Y_{23}, \quad (3.98)$$

$$\delta_c Y_{24} = -\delta(m_Z \cos \theta_W \sin \beta) = \left( \frac{\delta m_Z}{m_Z} - \tan^2 \theta_W \frac{\delta \sin \theta_W}{\sin \theta_W} + \cos^2 \beta \frac{\delta \tan \beta}{\tan \beta} \right) Y_{24}, \quad (3.99)$$

$$\delta_c Y_{34} = -\delta \mu = \frac{\delta \mu}{\mu} Y_{34}, \quad (3.100)$$

and

$$\delta_c X_{11} = \delta M = \frac{\delta M}{M} X_{11}, \quad (3.101)$$

$$\delta_c X_{12} = \sqrt{2}(\delta m_W \sin \beta + m_W \delta \sin \beta) = \left( \frac{\delta m_W}{m_W} + \cos^2 \beta \frac{\delta \tan \beta}{\tan \beta} \right) X_{12}, \quad (3.102)$$

$$\delta_c X_{21} = \sqrt{2}(\delta m_W \cos \beta + m_W \delta \cos \beta) = \left( \frac{\delta m_W}{m_W} - \sin^2 \beta \frac{\delta \tan \beta}{\tan \beta} \right) X_{21}, \quad (3.103)$$

$$\delta_c X_{22} = \delta \mu = \frac{\delta \mu}{\mu} X_{22}. \quad (3.104)$$

The UV-finite shifts are therefore

$$\Delta Y_{11} = 0, \quad (3.105)$$

$$\Delta Y_{12} = -\delta Y_{12}, \quad (3.106)$$

$$\Delta Y_{13} = \left( \frac{\delta m_Z}{m_Z} + \frac{\delta \sin \theta_W}{\sin \theta_W} - \sin^2 \beta \frac{\delta \tan \beta}{\tan \beta} \right) Y_{13} - \delta Y_{13}, \quad (3.107)$$

$$\Delta Y_{14} = \left( \frac{\delta m_Z}{m_Z} + \frac{\delta \sin \theta_W}{\sin \theta_W} + \cos^2 \beta \frac{\delta \tan \beta}{\tan \beta} \right) Y_{14} - \delta Y_{14}, \quad (3.108)$$

$$\Delta Y_{22} = \delta X_{11} - \delta Y_{22}, \quad (3.109)$$

$$\Delta Y_{23} = \left( \frac{\delta m_Z}{m_Z} - \tan^2 \theta_W \frac{\delta \sin \theta_W}{\sin \theta_W} - \sin^2 \beta \frac{\delta \tan \beta}{\tan \beta} \right) Y_{23} - \delta Y_{23}, \quad (3.110)$$

$$\Delta Y_{24} = \left( \frac{\delta m_Z}{m_Z} - \tan^2 \theta_W \frac{\delta \sin \theta_W}{\sin \theta_W} + \cos^2 \beta \frac{\delta \tan \beta}{\tan \beta} \right) Y_{24} - \delta Y_{24}, \quad (3.111)$$

$$\Delta Y_{33} = -\delta Y_{33}, \quad (3.112)$$

$$\Delta Y_{34} = -\delta X_{22} - \delta Y_{34}, \quad (3.113)$$

$$\Delta Y_{44} = -\delta Y_{44}, \quad (3.114)$$

and for the chargino mass matrix

$$\Delta X_{11} = 0, \quad (3.115)$$

$$\Delta X_{12} = \left( \frac{\delta m_W}{m_W} + \cos^2 \beta \frac{\delta \tan \beta}{\tan \beta} \right) X_{12} - \delta X_{12}, \quad (3.116)$$

$$\Delta X_{21} = \left( \frac{\delta m_W}{m_W} - \sin^2 \beta \frac{\delta \tan \beta}{\tan \beta} \right) X_{21} - \delta X_{21}, \quad (3.117)$$

$$\Delta X_{22} = 0. \quad (3.118)$$

If we assume a GUT relation of the form  $M' = c \tan^2 \theta_W M$  ( $c = \frac{5}{3}$  in SU(5) and  $c = 11$  in anomalously mediated SUSY-breaking models) for the  $\overline{\text{DR}}$  parameters, the shift  $\Delta Y_{11}$  is no longer zero, but

$$\Delta Y_{11} = \left( \frac{2}{\cos^2 \theta_W} \frac{\delta \sin \theta_W}{\sin \theta_W} + \frac{\delta M}{M} \right) Y_{11} - \delta Y_{11}. \quad (3.119)$$

Please note, that the UV finiteness of these shifts is a nontrivial check of this method. The so obtained one-loop corrected mass matrices give after diagonalization the one-loop on-shell neutralino and chargino masses. The corresponding rotation matrices have the appropriate values for the counter-terms eqs. (3.73) and (3.74). Note that in the presence of complex mass parameters this renormalization automatically includes the one-loop definition of CP violating phases.

For illustration Fig. 3.5 depicts numerical values for the corrections  $\Delta M$  and  $\Delta \mu$  given as a function of  $M$  and  $\mu$  and a fixed set for the other parameters. For  $\Delta M$  the corrections are in the range of  $\Delta M = -0.2$  GeV (white) and  $\Delta M = +0.6$  GeV (black). The corrections  $\Delta \mu$  are between  $\Delta \mu = -0.4$  GeV (white) and  $\Delta \mu = +0.5$  GeV (dark grey). The difference between two lines are 0.1 GeV.

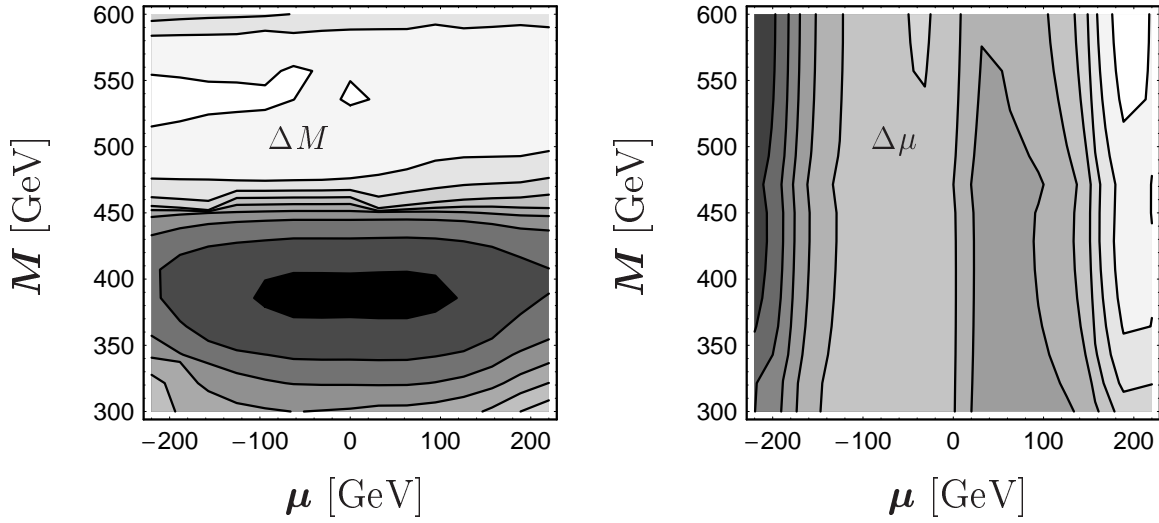


Figure 3.5: The corrections  $\Delta M$  and  $\Delta\mu$  as a function of  $M$  and  $\mu$  (fixed in the chargino sector) with the parameters  $\{m_{A^0}, \tan\beta, M_{\tilde{Q}_1}, M_{\tilde{Q}}, A\} = \{500, 7, 300, 300, -500\}$  GeV.  $M$  fulfills the SU(5) GUT relation.

### 3.6 Sfermion sector

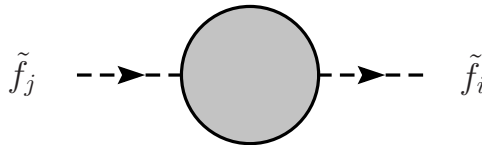
The on-shell renormalization applied to the fermionic SUSY particles can be naturally extended to the scalar sfermion sector. We consider the case, where the mixing between generations is neglected but the chiral L-R mixing is in general allowed. Therefore we introduce for the two superpartners of a fermion  $f$  the wave-function and mass counter-terms in the form

$$\tilde{f}_i \rightarrow (\delta_{ij} + \frac{1}{2}\delta Z_{ij}^{\tilde{f}})\tilde{f}_j, \quad m_{\tilde{f}_i}^2 \rightarrow m_{\tilde{f}_i}^2 + \delta m_{\tilde{f}_i}^2, \quad \text{for } \tilde{f} = \tilde{t}, \tilde{b}, \tilde{\tau}, \dots \quad (3.120)$$

The on-shell renormalization conditions for the scalar two-point functions are

$$\widetilde{\text{Re}}\hat{\Gamma}_{ij}(k^2)\Big|_{k^2=m_{\tilde{f}_j}^2} = 0, \quad \lim_{k^2 \rightarrow m_{\tilde{f}_i}^2} \frac{1}{k^2 - m_{\tilde{f}_i}^2} \widetilde{\text{Re}}\hat{\Gamma}_{ii}(k^2) = 1. \quad (3.121)$$

Then the counter-terms we receive are



$$\mathcal{M} = i\Gamma_{ij}^{\tilde{f}\tilde{f}}$$

$$\Gamma_{ij}^{\tilde{f}\tilde{f}} = \delta_{ij}(k^2 - m_{\tilde{f}_i}^2) + \Pi_{ij}^{\tilde{f}}(k^2)$$

Figure 3.6: Two-point functions for sfermions

$$\delta m_{\tilde{f}_i}^2 = \widetilde{\text{Re}}\Pi_{ii}^{\tilde{f}}(m_{\tilde{f}_i}^2), \quad (3.122)$$

$$\delta Z_{ij}^{\tilde{f}} = \frac{2}{m_{\tilde{f}_i}^2 - m_{\tilde{f}_j}^2} \widetilde{\text{Re}}\Pi_{ij}^{\tilde{f}}(m_{\tilde{f}_j}^2), \quad \delta Z_{ii}^{\tilde{f}} = -\widetilde{\text{Re}}\dot{\Pi}_{ii}^{\tilde{f}}(m_{\tilde{f}_i}^2). \quad (3.123)$$

The renormalization constant of the mixing matrix  $R^{\tilde{f}}$  is fixed analogously to the neutralino/chargino sector to cancel the anti-hermitian part of the wave-function corrections

$$\delta R_{ij}^{\tilde{f}} = \sum_{k=1}^2 \frac{1}{4} (\delta Z_{ik}^{\tilde{f}} - (\delta Z_{ki}^{\tilde{f}})^*) R_{kj}^{\tilde{f}} \quad \text{or} \quad \delta \mathbf{R}^{\tilde{f}} = \frac{1}{4} (\delta \mathbf{Z}^{\tilde{f}} - (\delta \mathbf{Z}^{\tilde{f}})^\dagger) \mathbf{R}^{\tilde{f}}. \quad (3.124)$$

In the next step, we consider the renormalization of the sfermion mass matrix. The counter-term  $\delta(\mathcal{M}_{\tilde{f}}^2)_{ij}$  to the on-shell sfermion mass matrix is obtained by

$$\delta(\mathcal{M}_{\tilde{f}}^2)_{ij} = \delta \mathbf{R}^{\tilde{f}\dagger} \begin{pmatrix} m_{\tilde{f}_1}^2 & 0 \\ 0 & m_{\tilde{f}_2}^2 \end{pmatrix} \mathbf{R}^{\tilde{f}} + \mathbf{R}^{\tilde{f}\dagger} \begin{pmatrix} \delta m_{\tilde{f}_1}^2 & 0 \\ 0 & \delta m_{\tilde{f}_2}^2 \end{pmatrix} \mathbf{R}^{\tilde{f}} + \mathbf{R}^{\tilde{f}\dagger} \begin{pmatrix} m_{\tilde{f}_1}^2 & 0 \\ 0 & m_{\tilde{f}_2}^2 \end{pmatrix} \delta \mathbf{R}^{\tilde{f}}. \quad (3.125)$$

Expressed in terms of sfermion self-energies it gives

$$\delta(\mathcal{M}_{\tilde{f}}^2)_{ij} = \frac{1}{2} \sum_{l,n=1}^2 (R_{ni}^{\tilde{f}})^* R_{lj}^{\tilde{f}} \widetilde{\text{Re}} \left[ \Pi_{nl}^{\tilde{f}}(m_{\tilde{f}_n}^2) + \Pi_{nl}^{\tilde{f}}(m_{\tilde{f}_l}^2) \right]. \quad (3.126)$$

We again introduce the variation to the parameters in the tree-level mass matrix

$$\delta_c(\mathcal{M}_{\tilde{f}}^2)_{11} = \delta M_{\tilde{Q},\tilde{L}}^2 + 2m_f \delta m_f + \delta m_Z^2 \cos 2\beta (I_f^{3L} - e_f \sin^2 \theta_W) + m_Z^2 (\delta \cos 2\beta (I_f^{3L} - e_f \sin^2 \theta_W) - \cos 2\beta e_f \delta \sin^2 \theta_W), \quad (3.127)$$

$$\delta_c(\mathcal{M}_{\tilde{f}}^2)_{12} = \delta(M_{\tilde{f}}^{LR})^* m_f + (M_{\tilde{f}}^{LR})^* \delta m_f, \quad (3.128)$$

$$\delta_c(\mathcal{M}_{\tilde{f}}^2)_{21} = \delta M_{\tilde{f}}^{LR} m_f + M_{\tilde{f}}^{LR} \delta m_f, \quad (3.129)$$

$$\delta_c(\mathcal{M}_{\tilde{f}}^2)_{22} = \delta M_{\tilde{U},\tilde{D},\tilde{E}}^2 + 2m_f \delta m_f + \delta m_Z^2 \cos 2\beta e_f \sin^2 \theta_W + m_Z^2 \delta \cos 2\beta e_f \sin^2 \theta_W + m_Z^2 \cos 2\beta e_f \delta \sin^2 \theta_W, \quad (3.130)$$

with

$$\delta M_{\tilde{f}}^{LR} = \begin{cases} \delta A_u - \delta \mu^* \cot \beta - \mu^* \delta \cot \beta & \text{for u-type sfermions} \\ \delta A_d - \delta \mu^* \tan \beta - \mu^* \delta \tan \beta & \text{for d-type sfermions} \end{cases} \quad (3.131)$$

The UV finite shifts between the tree-level and the on-shell mass-matrix have the form

$$\Delta(\mathcal{M}_{\tilde{f}}^2)_{ij} = \delta_c(\mathcal{M}_{\tilde{f}}^2)_{ij} - \delta(\mathcal{M}_{\tilde{f}}^2)_{ij}. \quad (3.132)$$

We fix the renormalization constants to the free parameters in the sfermion mass matrix in such a way, that they absorb all one-loop corrections stemming from other parameters in the same mass matrix entry. As a consequence the UV-finite shifts vanishes. Therefore we receive the following counter-terms for the trilinear coupling  $A_f$

$$m_f \delta A_f = \begin{cases} \delta(\mathcal{M}_{\tilde{u}}^2)_{21} - a_u \delta m_u + m_u \delta \mu^* \cot \beta + m_u \mu^* \delta \cot \beta & \text{for u-type sfermions} \\ \delta(\mathcal{M}_{\tilde{d}}^2)_{21} - a_d \delta m_d + m_d \delta \mu^* \tan \beta + m_d \mu^* \delta \tan \beta & \text{for d-type sfermions} \end{cases} \quad (3.133)$$

We fix  $A_f$  in the 21-element of the mass matrix but also the corrections in the 12-element vanish due to the hermiticity of  $\Delta \mathcal{M}_f^2$ .

The soft SUSY-breaking parameters  $M_{\tilde{U},\tilde{D},\tilde{E}}$  are independent for up and down-type sfermions and can therefore be renormalized independently

$$\begin{aligned} \delta M_{\tilde{U},\tilde{D},\tilde{E}}^2 &= \delta(\mathcal{M}_f^2)_{22} - 2m_f \delta m_f - \delta m_Z^2 \cos 2\beta e_f \sin^2 \theta_W \\ &\quad - m_Z^2 \delta \cos 2\beta e_f \sin^2 \theta_W - m_Z^2 \cos 2\beta e_f \delta \sin^2 \theta_W. \end{aligned} \quad (3.134)$$

Only in the 11-element a UV-finite shift has to be considered. In fact there is only one parameter  $M_{\tilde{Q},\tilde{L}}$  for up and down-type sfermions. We define the on-shell parameter in the down-type sfermion sector

$$\begin{aligned} \delta M_{\tilde{Q},\tilde{L}}^2 &= \delta(\mathcal{M}_b^2)_{11} - 2m_d \delta m_d - \delta m_Z^2 \cos 2\beta (I_d^{3L} - e_d \sin^2 \theta_W) \\ &\quad - m_Z^2 (\delta \cos 2\beta (I_d^{3L} - e_d \sin^2 \theta_W) - \cos 2\beta e_d \delta \sin^2 \theta_W) \end{aligned} \quad (3.135)$$

and obtain a shift in the 11-element of the up-type sfermion mass matrix

$$\Delta(\mathcal{M}_u^2)_{11} \equiv \Delta M_{\tilde{Q},\tilde{L}}^2 = (M_{\tilde{Q},\tilde{L}}^2)_i - (M_{\tilde{Q},\tilde{L}}^2)_{\bar{i}} \quad (3.136)$$

of the form

$$\begin{aligned} \Delta M_{\tilde{Q},\tilde{L}}^2 &= \delta M_{\tilde{Q},\tilde{L}}^2 + 2m_u \delta m_u + \delta m_Z^2 \cos 2\beta (I_u^{3L} - e_u \sin^2 \theta_W) \\ &\quad + m_Z^2 (\delta \cos 2\beta (I_u^{3L} - e_u \sin^2 \theta_W) - \cos 2\beta e_u \delta \sin^2 \theta_W) - \delta(\mathcal{M}_t^2)_{11}. \end{aligned} \quad (3.137)$$

In the most general case, the given formulas can be applied to the (third generation) squark renormalization. Two simplifications can be done in the slepton/sneutrino sector. First, there are no sneutrino parameters  $A_u$  and  $M_{\tilde{U}}$  and there is only one sneutrino per fermion generation. Fixing  $M_{\tilde{L}}$  in the down-type slepton mass matrix we only get mass corrections for the sneutrino. If we would fix  $M_{\tilde{L}}$  in the sneutrino sector, the sneutrino mass is unchanged, but both selectron masses and the rotation angle receive corrections. This is one reason why we fix  $M_{\tilde{Q},\tilde{L}}$  in the down-sfermion sector. Second, we can neglect the left-right mixing for the first generation sleptons, i.e.:  $\tilde{e}_L, \tilde{e}_R$  and no counter-terms for the mixing matrix is needed. In consistency with the general case, we fix  $M_{\tilde{L}_1}$  and  $M_{\tilde{E}_1}$  in such a way, that the selectron masses do not obtain one-loop corrections

$$\delta M_{\tilde{L}_1}^2 = \delta m_{\tilde{e}_L}^2 + \delta \left( m_Z^2 \cos 2\beta \left( \frac{1}{2} - \sin^2 \theta_W \right) \right), \quad (3.138)$$

$$\delta M_{\tilde{E}_1}^2 = \delta m_{\tilde{e}_R}^2 + \delta \left( m_Z^2 \cos 2\beta \sin^2 \theta_W \right). \quad (3.139)$$

Due to a finite shift in  $M_{\tilde{L}_1}$ , the sneutrino mass obtains the one-loop correction

$$\Delta m_{\tilde{\nu}_e}^2 = \Delta M_{\tilde{L}}^2 = \delta M_{\tilde{L}_1}^2 + \frac{1}{2} \delta \left( m_Z^2 \cos 2\beta \right) - \delta m_{\tilde{\nu}_e}^2. \quad (3.140)$$

# Chapter 4

## Structure function formalism in QED

### 4.1 Mass singularities

Besides the UV-divergences for infinite momenta, that are controlled by the renormalization procedure as discussed in the last chapter, also singularities for finite momenta appear in Feynman integrals. Two types of these so-called Landau singularities, the mass singularities, arise due to vanishing masses. The infrared divergences are connected with vanishing momenta, the collinear singularities with light-like collinear momenta. Such soft or collinear singularities appear not only in loop diagrams with virtual soft or collinear massless particles, but also for real emission of these particles, integrating the phase-space over the soft or collinear region. In properly defined observables the sum of virtual and real contributions cancel soft as well as collinear divergences and a physically meaningful result can be obtained.

For our purposes, we have to consider soft singularities in the case where soft virtual photons are attached to on-shell particles in the tree-level diagrams. In particular, photons attached to the incoming or outgoing particles, since we do not have to deal with resonances. These singularities can only be avoided by inclusion of at least the soft part of real photon radiation. The calculation of these corrections is further discussed in chapter 5.3.1.

In QED (or possible extensions, the SM or MSSM), where massless photons are radiated off from electrons, the masses of the particles act as natural cut-offs and no collinear singularities arise. Nevertheless, large logarithms of the form  $\log(Q^2/m_e^2)$  appear, reflecting the collinear singularity for  $m_e \rightarrow 0$ . This can lead to sizeable corrections proportional to  $\alpha^n \log^m(Q^2/m_e^2)$ , order by order in perturbation theory. For high precision experiments it is necessary to control these corrections beyond order  $\alpha$ . Methods were developed to improve (full one-loop) calculations with such contributions. The QED logarithms can be calculated in a process-independent way within the so-called structure-function formalism [39, 40]. This topic will be discussed in the following sections.

### 4.2 Mass factorization theorem

The structure-function formalism is based on the mass factorization theorem. In the following we concentrate on electron-positron collisions going into two “heavy” particles and

possibly additional undetected “light” particles, i.e. photons or/and electron-positron pairs.  $\bar{e}(p_1)e(p_2) \rightarrow X(q_1, M_1) + Y(q_2, M_2) (+Z)^1$ . We can define the following kinematical invariants (neglecting the electron mass):

$$s = (p_1 + p_2)^2 = 2p_1p_2, \quad t_{ij} = (p_i - q_j)^2 - M_j^2 = -2p_iq_j, \quad \text{with } i, j = \{1, 2\}. \quad (4.1)$$

The reduced kinematical variables, after an arbitrary number of undetected particles have been emitted by the incoming  $\bar{e}e$  beam, are:

$$\hat{s} = (\hat{p}_1 + \hat{p}_2)^2 = 2\hat{p}_1\hat{p}_2, \quad \hat{t}_{ij} = (\hat{p}_i - \hat{q}_j)^2 - M_j^2 = -2\hat{p}_i\hat{q}_j, \quad \text{with } i, j = \{1, 2\} \quad (4.2)$$

We define the fraction of energy carried away by collinear photons as  $(1 - x_i)$ . So, we get the simple relations:

$$\hat{p}_i = x_i p_i, \quad \hat{q}_i = q_i, \quad \hat{s} = x_1 x_2 s, \quad \hat{t}_{ij} = x_i t_{ij} \quad (4.3)$$

The mass factorization theorem links the mass finite hard scattering cross-section  $\hat{\sigma}_{ij \rightarrow XY}$

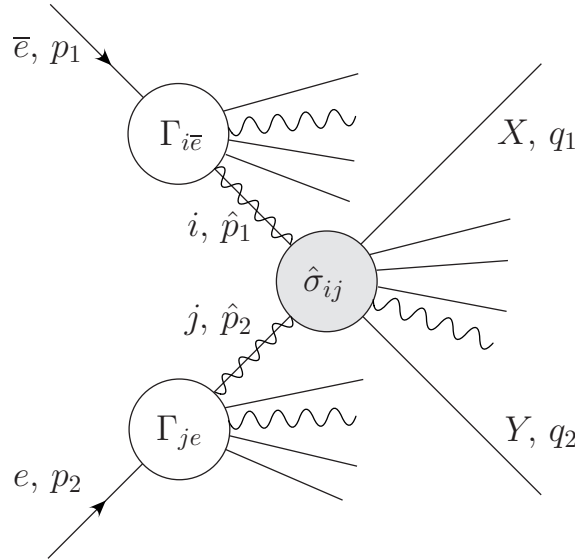


Figure 4.1: Mass Factorization Theorem

with the mass singular cross-section  $\sigma_{\bar{e}e \rightarrow XY+Z}$ , see Fig. (4.1):

$$s^4 \frac{d^4 \sigma_{\bar{e}e \rightarrow XY+Z}}{dt_{11} dt_{12} dt_{21} dt_{22}} = \int_0^1 \frac{dx_1}{x_1^2} \int_0^1 \frac{dx_2}{x_2^2} \Gamma_{i\bar{e}}(x_1, Q^2) \Gamma_{je}(x_2, Q^2) \hat{s}^4 \frac{d^4 \hat{\sigma}_{ij \rightarrow XY}}{d\hat{t}_{11} d\hat{t}_{12} d\hat{t}_{21} d\hat{t}_{22}}(Q^2) \quad (4.4)$$

Eq. (4.4) is the most general form and allows the implementation of cuts on the energies and angles of the produced particles. Other distributions, or also the total cross-section can be obtained using Jacobian-determinants. Inserting the relations eq. (4.3), we get the simple form:

$$d\sigma = \int_0^1 dx_1 \int_0^1 dx_2 \Gamma_{i\bar{e}}(x_1, Q^2) \Gamma_{je}(x_2, Q^2) d\hat{\sigma}_{ij}(Q^2) \quad (4.5)$$

<sup>1</sup>In this chapter we use for simplicity the writing  $e$  for electrons and  $\bar{e}$  for positrons.

All large logarithms on the right hand side are contained in the so-called splitting, or structure, functions  $\Gamma_{ij}$ . They state the probability to find in the particle  $j$  at the scale  $Q^2$  a parton  $i$  with fraction  $x$  of the longitudinal momentum. So  $(1-x)$  is the energy that is carried away by collinear radiation. This interpretation seems to be absurd, since electrons and photons are fundamental and not composite particles, but the formalism was taken over from QCD, where it is quite natural. Therefore, a “particle” electron can be defined as a cloud of real and virtual “partons”, electrons, positrons and photons.

For  $\bar{e}e$  collisions we have two possibilities: The incoming electron (positron) emits a photon and propagates further with reduced momentum into the shaded blob, with a probability defined by  $\Gamma_{ee}$  ( $\Gamma_{\bar{e}e}$ ). With the probability  $\Gamma_{\gamma e}$  ( $\Gamma_{\gamma\bar{e}}$ ) the electron (positron) can be scattered and a photon carrying the momentum fraction  $x$  arrives in the shaded region.

In general, both the splitting functions and the mass-finite cross-section  $\hat{\sigma}$  depend on the mass factorization scale  $Q^2$ . They can be expanded in ascending powers of  $\alpha$  and in the case of the structure functions in powers of  $L_e \equiv \log(Q^2/m_e^2)$  in the following form:

$$\Gamma_{ij}(x, Q^2) = \Gamma_{ij}^{\log}(x, Q^2) + \Gamma_{ij}^{\text{non-log}}(x, Q^2) \quad (4.6)$$

$$\Gamma_{ij}^{\log}(x, Q^2) = \delta_{ij}\delta(1-x) + \sum_{n=1}^{\infty} \left(\frac{\alpha}{\pi}\right)^n \sum_{m=1}^n a_{mn}^{ij}(x) L_e^m \quad (4.7)$$

$$\Gamma_{ij}^{\text{non-log}}(x, Q^2) = \sum_{n=1}^{\infty} \left(\frac{\alpha}{\pi}\right)^n b_n^{ij}(x) \quad (4.8)$$

$$d\hat{\sigma}_{ij}(Q^2) = d\sigma_{ij}^{\text{Born}} + \sum_{n=1}^{\infty} \left(\frac{\alpha}{\pi}\right)^n c_n^{ij}(x, Q^2) \quad (4.9)$$

The structure functions can be decomposed into a log and a non-log part. The scale dependence enters only via the logarithmic terms  $L_e^m$ . The coefficients  $a_{mn}^{ij}$  and  $b_n^{ij}$  can be obtained in a process-independent way, using renormalization group methods. The hard scattering cross-section also depends on  $x$  due to the reduced momenta  $\hat{p}_i$ . The coefficients  $c_n^{ij}$  include all other virtual and real corrections, which are model and process dependent. Inserting these formulas into eq. (4.4), we see that the process-dependent cross-section corrections mix with the process-independent terms of the structure functions and give terms proportional to  $\alpha^n L_e^m$  with  $n > m$ . The terms with  $\alpha^n L_e^n$  are only proportional to the Born cross-section and are therefore pure process-independent corrections. The so-called leading-log approximation (LL) considers only these terms.

According to the probabilistic interpretation, it is obvious that the splitting functions must respect the following relations, due to electron number and longitudinal momentum conservation:

$$\int_0^1 dx [\Gamma_{ee}(x, Q^2) - \Gamma_{\bar{e}e}(x, Q^2)] = 1 \quad (4.10)$$

$$\int_0^1 dx [\Gamma_{e\gamma}(x, Q^2) - \Gamma_{\bar{e}\gamma}(x, Q^2)] = 0 \quad (4.11)$$

$$\sum_{j=\bar{e},e,\gamma} \int_0^1 dx x \Gamma_{ji}(x, Q^2) = 1 \quad (4.12)$$

### 4.3 Evolution equations

For the electron-positron-photon system the so-called evolution equations can be adopted from the QCD case in the following form [41, 42]:

$$\frac{\partial \Gamma_{\bar{e}i}(x, Q^2)}{\partial (\log Q^2)} = \frac{\alpha(Q^2)}{2\pi} [P_{\bar{e}\bar{e}} \otimes \Gamma_{\bar{e}i} + P_{\bar{e}e} \otimes \Gamma_{ei} + P_{\bar{e}\gamma} \otimes \Gamma_{\gamma i}](x, Q^2) \quad (4.13)$$

$$\frac{\partial \Gamma_{ei}(x, Q^2)}{\partial (\log Q^2)} = \frac{\alpha(Q^2)}{2\pi} [P_{e\bar{e}} \otimes \Gamma_{\bar{e}i} + P_{ee} \otimes \Gamma_{ei} + P_{e\gamma} \otimes \Gamma_{\gamma i}](x, Q^2) \quad (4.14)$$

$$\frac{\partial \Gamma_{\gamma i}(x, Q^2)}{\partial (\log Q^2)} = \frac{\alpha(Q^2)}{2\pi} [P_{\gamma\bar{e}} \otimes \Gamma_{\bar{e}i} + P_{\gamma e} \otimes \Gamma_{ei} + P_{\gamma\gamma} \otimes \Gamma_{\gamma i}](x, Q^2) \quad (4.15)$$

For this set of integro-differential equations, we used the multiplicative convolution

$$\begin{aligned} [f \otimes g](x) &= \int_0^1 dy \int_0^1 dz \delta(x - yz) f(y) g(z) \\ &= \int_x^1 \frac{dz}{z} f\left(\frac{x}{z}\right) g(z). \end{aligned} \quad (4.16)$$

The kernel's  $P_{ij}(x)$  of these equations, the so-called Altarelli-Parisi functions [41, 40], have at order  $\alpha$  the form:

$$P_{ee}^0(x) = P_{\bar{e}\bar{e}}^0(x) = \left(\frac{1+x^2}{1-x}\right)_+ \quad (4.17)$$

$$P_{e\bar{e}}^0(x) = P_{\bar{e}e}^0(x) = 0 \quad (4.18)$$

$$P_{\gamma\bar{e}}^0(x) = P_{\gamma e}^0(x) = \frac{1+(1-x)^2}{x} \quad (4.19)$$

$$P_{\bar{e}\gamma}^0(x) = P_{e\gamma}^0(x) = x^2 + (1-x)^2 \quad (4.20)$$

$$P_{\gamma\gamma}^0(x) = -\frac{2}{3}\delta(1-x) \quad (4.21)$$

Here we have introduced the (+)-distribution, which is defined by

$$\int_0^1 dx f(x)(h(x))_+ = \int_0^1 (f(x) - f(1)) h(x), \quad (4.22)$$

or

$$(h(x))_+ = \lim_{\varepsilon \rightarrow 0} \left[ \theta(1-x-\varepsilon) h(x) - \delta(1-x-\varepsilon) \int_0^{1-\varepsilon} h(y) dy \right]. \quad (4.23)$$

Inserting these Kernel's in the evolution equations gives

$$\frac{\partial \Gamma_{\bar{e}i}(x, Q^2)}{\partial (\log Q^2)} = \frac{\alpha}{2\pi} [P_{\bar{e}\bar{e}}^0 \otimes \Gamma_{\bar{e}i} + P_{\bar{e}\gamma}^0 \otimes \Gamma_{\gamma i}](x, Q^2) \quad (4.24)$$

$$\frac{\partial \Gamma_{ei}(x, Q^2)}{\partial (\log Q^2)} = \frac{\alpha}{2\pi} [P_{ee}^0 \otimes \Gamma_{ei} + P_{e\gamma}^0 \otimes \Gamma_{\gamma i}](x, Q^2) \quad (4.25)$$

$$\frac{\partial \Gamma_{\gamma i}(x, Q^2)}{\partial (\log Q^2)} = \frac{\alpha}{2\pi} [P_{\gamma e}^0 \otimes (\Gamma_{\bar{e}i} + \Gamma_{ei}) + P_{\gamma\gamma}^0 \otimes \Gamma_{\gamma i}](x, Q^2) \quad (4.26)$$

With a set of input parameters, a solution for this system can be calculated. In the case of an electron (in the definition of a cloud of partons: electrons, positrons and photons) we naturally assume that at zero momentum, i.e.  $Q^2 = m_e^2$ , it consists only of an electron parton without positrons or photons. This results in the boundary conditions

$$\Gamma_{ee}(x, m_e^2) = \delta(1-x), \quad \Gamma_{\bar{e}e}(x, m_e^2) = \Gamma_{\gamma e}(x, m_e^2) = 0. \quad (4.27)$$

Looking at the kernel functions we see that only the diagonal ones give large contributions for the soft-photon limit  $x \rightarrow 1$ . So we make an approximation and put the others to zero. For the electron structure function, this is equal to the boundary value  $\Gamma_{\gamma e}(x, Q^2) = 0$ , in the language of QCD the so-called non-singlet (NS) case. The three equations (4.13)-(4.15) decouple and we can concentrate on the electron density function  $\Gamma_{ee}^{\text{NS}}$ . Setting  $\Gamma_{\gamma e}(x, Q^2) = 0$  for all values of  $Q^2$  means that we neglect electrons or positrons in loops and also the corresponding real corrections where electron-positron pairs are emitted. In other words, we take only corrections with virtual or real photons into account

$$\frac{\partial \Gamma_{ee}^{\text{NS}}(x, Q^2)}{\partial (\log Q^2)} = \frac{\alpha(Q^2)}{2\pi} [P_{ee} \otimes \Gamma_{ee}^{\text{NS}}](x, Q^2), \quad (4.28)$$

$$\Gamma_{ee}^{\text{NS}}(x, Q^2) = \delta(1-x) + \int_{m_e^2}^{Q^2} \frac{dk^2}{k^2} \frac{\alpha(k^2)}{2\pi} [P_{ee} \otimes \Gamma_{ee}^{\text{NS}}](x, k^2). \quad (4.29)$$

Neglecting the running of  $\alpha$ , a solution for this equation can be obtained by an iteration in the following form

$$\begin{aligned} \Gamma_{ee}^{\text{NS}, \log}(x, Q^2) = & \delta(1-x) + \frac{\alpha}{2\pi} \int_{m_e^2}^{Q^2} \frac{dk^2}{k^2} P_{ee}(x_1) \otimes \left[ \delta(1-x_2) + \right. \\ & \left. \frac{\alpha}{2\pi} \int_{m_e^2}^{k^2} \frac{d\bar{k}^2}{\bar{k}^2} P_{ee}(x_2) \otimes (\delta(1-x_3) + \dots) \right]. \end{aligned} \quad (4.30)$$

Using the relation

$$\underbrace{\int \frac{1}{x} \left( \int \frac{1}{x} \left( \int \frac{1}{x} \left( \int \dots \right) dx \right) dx \right) dx}_{n \text{ nested integrals}} = \frac{\log^n(x)}{n!} \quad (4.31)$$

we get

$$\Gamma_{ee}^{\text{NS}, \log}(x, Q^2) = \delta(1-x) + \sum_{n=1}^{\infty} \left( \frac{\alpha}{2\pi} \right)^n \frac{1}{n!} \mathcal{P}_n(x) L_e^n(Q^2), \quad (4.32)$$

with

$$\begin{aligned} \mathcal{P}_n(x) &= \underbrace{[P_{ee} \otimes P_{ee} \otimes \dots \otimes P_{ee}]}_{n \text{ kernels in convolution}}(x), \\ &= \int_0^1 \prod_{i=1}^n dx_i P_{ee}(x_1) \dots P_{ee}(x_n) \delta \left( x - \prod_{i=1}^n x_i \right). \end{aligned} \quad (4.33)$$

Expanding the kernel function in a series in  $\alpha$

$$P_{ee}(x) = P_{ee}^0(x) + \alpha P_{ee}^1 + O(\alpha^2) \quad (4.34)$$

leads to sub-leading log terms. The leading-log result for the electron structure function has the form

$$\begin{aligned} \Gamma_{ee}^{\text{NS,LL}}(x, Q^2) &= \delta(1-x) + \sum_{n=1}^{\infty} \left(\frac{\alpha}{2\pi}\right)^n \frac{1}{n!} \mathcal{P}_n^0(x) L_e^n(Q^2) \\ &= \delta(1-x) + \frac{\alpha}{2\pi} P_{ee}^0(x) L_e + \frac{1}{2} \left(\frac{\alpha}{2\pi}\right)^2 [(P_{ee}^0 \otimes P_{ee}^0) L_e^2] + O(\alpha^3), \end{aligned} \quad (4.35)$$

with the leading-log terms

$$\begin{aligned} P_{ee}^0 &= \lim_{\varepsilon \rightarrow 0} \left[ \delta(1-x) \left( \frac{3}{2} + 2 \log \varepsilon \right) + \theta(1-\varepsilon-x) \frac{1+x^2}{1-x} \right], \quad (4.36) \\ \frac{1}{2} (P_{ee}^0 \otimes P_{ee}^0) &= \lim_{\varepsilon \rightarrow 0} \left( \delta(1-x) \left[ 2 \log^2 \varepsilon + 3 \log \varepsilon + \frac{9}{8} - \frac{\pi^2}{3} \right] + \theta(1-\varepsilon-x) \times \right. \\ &\quad \left. \left[ \frac{1+x^2}{1-x} (2 \log(1-x) - \log(x) + \frac{3}{2}) + \frac{1}{2} (1+x) \log(x) - (1-x) \right] \right). \end{aligned} \quad (4.37)$$

The correction term  $-\frac{\pi^2}{3}$  in the soft part of  $\frac{1}{2}(P_{ee}^0 \otimes P_{ee}^0)$  is due to the fact that the energies of the two soft-photons are not independent, but must obey  $\epsilon_1 + \epsilon_2 < \varepsilon$ . The non-logarithmic (constant) part  $\Gamma_{ee}^{\text{non-log}}$  cannot be obtained in the structure function formalism, but it is possible to derive it in an explicit way, calculating the required Feynman diagrams.

A convenient way to deal with evolution equations and in particular with the non-singlet equation eq. (4.28) is to apply the Mellin transformation. The Mellin transformation is defined by

$$\tilde{f}(z) = \int_0^{\infty} dx x^{z-1} f(x), \quad (4.38)$$

$$f(x) = \frac{1}{2\pi i} \int_{c-i\infty}^{c+i\infty} dz x^{-z} \tilde{f}(z). \quad (4.39)$$

The transform  $\tilde{f}(z)$  exists, if the integral

$$\int_0^{\infty} dx |f(x)| x^{k-1} \quad (4.40)$$

is bounded for some  $k > 0$ . Then the inverse  $f(x)$  exists for any  $c > k$ . So the multiplicative convolution eq. (4.16) can be written as ordinary product

$$h(x) = f(x) \otimes g(x) \leftrightarrow \tilde{h}(z) = \tilde{f}(z) \cdot \tilde{g}(z). \quad (4.41)$$

The evolution equations can then be transformed to linear equations of the Mellin transformed structure functions. In the non-singlet case we obtain

$$\frac{\partial \tilde{\Gamma}_{ee}^{\text{NS}}(z, Q^2)}{\partial (\log Q^2)} = \frac{\alpha(Q^2)}{2\pi} \tilde{P}_{ee}(z) \cdot \tilde{\Gamma}_{ee}^{\text{NS}}(z, Q^2). \quad (4.42)$$

The leading-log result can then be simply written in the form

$$\tilde{\Gamma}_{ee}^{\text{NS,LL}}(z, Q^2) = \exp\left(\frac{\alpha}{2\pi}L_e(Q^2)\tilde{P}_{ee}^0(z)\right), \quad (4.43)$$

$$\Gamma_{ee}^{\text{NS,LL}}(x, Q^2) = \frac{1}{2\pi} \int_{-\infty}^{+\infty} dt x^{-it-c} \exp\left(\frac{\alpha}{2\pi}L_e(Q^2)\tilde{P}_{ee}^0(it+c)\right), \quad (4.44)$$

with

$$\tilde{P}_{ee}^0(z) = \frac{3}{2} - 2\gamma_E - \psi(z) - \psi(z+2), \quad \psi(z) = \Gamma'(z)/\Gamma(z), \quad (4.45)$$

whereas  $\Gamma(z)$  and  $\Gamma'(z)$  are the ordinary gamma function and its derivative. The problem has then be shifted from expanding expressions in  $\otimes$  products to the evaluation of inverse Mellin transformations.

## 4.4 Soft photon resummation

In the famous paper of Yennie, Frautschi and Suura [43], they discussed the infrared divergence problem in a very general way. Summing up the contributions of virtual and real photons leads to a finite result, order by order in perturbation theory. Furthermore they have shown that the soft-photon contributions can be summed up to all orders. For  $e^+e^-$  processes the cross-section is then proportional to  $\exp(\beta(\log \varepsilon - \gamma_E))/\Gamma(1 + \beta(s))$  with  $\beta(Q^2) = \frac{2\alpha}{\pi}(L_e(Q^2) - 1)$  and  $\varepsilon = \frac{\Delta E}{E}$  the soft-photon cut-off.

Let us now compare this result with our previous leading-log result eq. (4.35). We see indeed from the expressions proportional to  $\delta(1-x)$  in  $P_{ee}^0$  and  $P_{ee}^0 \otimes P_{ee}^0$  that there are terms that seem to exponentiate up to all orders (besides the correction term  $-\frac{\pi^2}{3}$ ). Our Question is now: Can we resum the soft-photon part also in the structure function formalism, but without introducing an  $\varepsilon$  cut-off dependence? We define a soft part of the structure function kernel  $P_{ee}^{0,\text{soft}}$  in the following way

$$\begin{aligned} P_{ee}^{0,\text{soft}} &= \left(\frac{2}{1-x}\right)_+ \\ &= \lim_{\varepsilon \rightarrow 0} \left[ \delta(1-x)(2 \log \varepsilon) + \theta(1-\varepsilon-x) \frac{2}{1-x} \right] \end{aligned} \quad (4.46)$$

We insert this into eq. (4.35) and extract only the leading terms in the soft-photon limit  $x \rightarrow 1$ . This provides the possibility to resum a soft ( $\propto \log \varepsilon$ ) and a hard ( $\propto \log(1-x)$ ) part in the following way:

$$\begin{aligned} \Gamma_{ee}^{\text{soft}}(x, Q^2) &= \delta(1-x) + \lim_{\varepsilon \rightarrow 0} \sum_{n=1}^{\infty} \left(\frac{\alpha}{\pi}L_e\right)^n \left[ \delta(1-x) \frac{(\log \varepsilon)^n}{n!} \right. \\ &\quad \left. + \theta(1-x-\varepsilon) \frac{1}{(n-1)!} \frac{\log^{n-1}(1-x)}{1-x} \right] \\ &= \lim_{\varepsilon \rightarrow 0} \left[ \delta(1-x) \exp\left(\frac{\alpha}{\pi}L_e \log \varepsilon\right) \right. \\ &\quad \left. + \theta(1-x-\varepsilon) \frac{\alpha}{\pi}L_e \frac{1}{1-x} \exp\left(\frac{\alpha}{\pi}L_e \log(1-x)\right) \right] \\ &= \frac{\alpha}{\pi}L_e (1-x)^{\frac{\alpha}{\pi}L_e - 1} \end{aligned} \quad (4.47)$$

Due to the resummation of a soft and also a hard part, it is possible to avoid an  $\varepsilon$  dependence. Unfortunately, we have not included the complete soft-photon contribution, but only that part where the  $n$  photons can be considered as independent.

Another analytical solution to eq. (4.28) in the soft-photon limit  $x \rightarrow 1$  was found by Gribov and Lipatov [44]. In the asymptotic limit for large  $z$  the digamma function  $\psi(z)$  behaves like a regular logarithm

$$\lim_{z \rightarrow \infty} \psi(z) \sim \log(z). \quad (4.48)$$

By taking again only the leading part of the kernel function, but allowing  $\alpha$  to be running, one obtains

$$\tilde{\Gamma}_{ee}^{\text{GL}}(z, Q^2) = \exp\left(\frac{\eta}{4}\left(\frac{3}{2} - 2\gamma_E\right)\right) z^{-\frac{\eta}{2}}, \quad (4.49)$$

$$\Gamma_{ee}^{\text{GL}}(x, Q^2) = \frac{\exp\left(\frac{\eta}{4}\left(\frac{3}{2} - 2\gamma_E\right)\right)}{\Gamma\left(\frac{\eta}{2}\right)} (-\log x)^{\frac{\eta}{2}-1}, \quad (4.50)$$

with

$$\alpha(Q^2) = \alpha / \left(1 - \frac{\alpha}{3\pi} \log \frac{Q^2}{m_e^2}\right) + O(\alpha^3), \quad (4.51)$$

$$\eta(Q^2) = \int_{m_e^2}^{Q^2} \frac{dk^2}{k^2} \frac{\alpha(k^2)}{\pi} = \frac{2\alpha}{\pi} L_e \left(1 + \frac{\alpha}{6\pi} L_e\right) + O(\alpha^3). \quad (4.52)$$

This is indeed a good approximation for the soft-photon area, as can be checked against the full result. Now it is possible to combine these two soft-photon results, to have the complete soft part resummed, but also the leading hard contribution. In the soft-photon limit  $x \sim 1$ , where the Gribov-Lipatov solution is applicable, the  $-\log(x)$  term can be replaced by its first element in the Taylor expansion  $(1-x)$ . Furthermore, we obtain the  $(1-x)$  behaviour of eq. (4.47) and thus the leading hard terms for  $x \sim 1$  are correctly included. This solution, found by Kuraev and Fadin [45] in the context of an  $O(\alpha^2)$  discussion, has finally the form

$$\Gamma_{ee}^{\text{KF}}(x, Q^2) = \frac{\exp\left(-\frac{1}{2}\eta\gamma_E + \frac{3}{8}\eta\right)}{\Gamma\left(1 + \frac{\eta}{2}\right)} \frac{\eta}{2} (1-x)^{\frac{\eta}{2}-1}. \quad (4.53)$$

Expanding the soft-photon results in  $\alpha$  one can see that the Kuraev-Fadin solution  $\Gamma_{ee}^{\text{KF}}$  contains  $\Gamma_{ee}^{\text{soft}}$  but has additional terms resummed at  $O(\alpha^2)$ . Furthermore, the Kuraev-Fadin solution shows in the soft limit a very similar form to the YFS term, if we choose  $\alpha = \text{const}$ . But there is a big difference to notice. The Kuraev-Fadin solution contains only the leading-log term  $\eta$  proportional to  $L_e$ , whereas the YFS term contains the term  $\beta$  with an additional non-leading log term. For the cancellation of the infrared divergence it is absolutely necessary to have the factor  $\beta$  instead of  $\eta$  in the soft-photon range. From this point of view it is mandatory to improve the leading-log result in the soft-photon limit with this non-leading contribution. So we have to replace  $\eta$  with  $\beta$  just “by hand”.

In principle, the structure functions can be splitted up in a resummed part and a so-called hard part, e.g.

$$\Gamma_{ee}^{\text{NS,LL}}(x, Q^2) = \frac{\beta_S}{2} (1-x)^{\frac{\beta_S}{2}-1} \delta^{\text{V+S}} + \delta^{\text{H}}(\beta_H). \quad (4.54)$$

Since there is no unique way which parts should be resummed ( $\delta^{V+S}$ ) and which not ( $\delta^H$ ), there are different procedures known in the literature and they all differ at a certain order of  $\alpha$ . For a review, see e.g.[46]. Which values should we now choose for  $\beta_S$  and  $\beta_H$ ? Due to the discussion above,  $\beta_S$  must have the value  $\beta$  to cancel the infrared divergence. For the hard part, there is no reason to include also a non-leading contribution in our leading-log approximation. However, for simplicity we also choose  $\beta_H = \beta$ . In principle, the running of  $\alpha$  can be considered by replacing  $\alpha$  with  $\alpha(1 + \frac{\alpha}{6\pi}L_e)$ , see eq. (4.52). These additional terms regard the leading effects of collinear electron-positron pairs.

## 4.5 Leading-Log result

We finally present two formulas for the non-singlet leading-log structure function, exact at  $O(\alpha^3)$  and differing at  $O(\alpha^4)$ , taken from [47]

$$\begin{aligned} \Gamma_{ee}^{\text{NS,KF}} &= \frac{\exp(-\frac{1}{2}\beta\gamma_E + \frac{3}{8}\beta)\beta}{\Gamma(1 + \frac{\beta}{2})} \frac{\beta}{2} (1-x)^{\frac{\beta}{2}-1} \\ &\quad - \frac{\beta}{4}(1+x) + \frac{\beta^2}{16} \left( -2(1+x)\log(1-x) - \frac{2\log x}{1-x} + \frac{3}{2}(1+x)\log x - \frac{x}{2} - \frac{5}{2} \right) \\ &\quad + \left(\frac{\beta}{2}\right)^3 \left[ -\frac{1}{2}(1+x) \left( \frac{9}{32} - \frac{\pi^2}{12} + \frac{3}{4}\log(1-x) + \frac{1}{2}\log^2(1-x) - \frac{1}{4}\log x \log(1-x) \right. \right. \\ &\quad \left. \left. + \frac{1}{16}\log^2 x - \frac{1}{4}\text{Li}_2(1-x) \right) + \frac{1}{2} \frac{1+x^2}{1-x} \left( -\frac{3}{8}\log x + \frac{1}{12}\log^2 x - \frac{1}{2}\log x \log(1-x) \right) \right. \\ &\quad \left. - \frac{1}{4}(1-x) \left( \log(1-x) + \frac{1}{4} \right) + \frac{1}{32}(5-3x)\log x \right] + O(\alpha^4), \end{aligned} \quad (4.55)$$

and

$$\begin{aligned} \Gamma_{ee}^{\text{NS,YFS}} &= \frac{\exp(-\frac{1}{2}\beta\gamma_E + \frac{3}{8}\beta)\beta}{\Gamma(1 + \frac{\beta}{2})} \frac{\beta}{2} (1-x)^{\frac{\beta}{2}-1} \left[ \frac{1}{2}(1+x^2) + \frac{\beta}{8} \left( -\frac{1}{2}(1+3x^2)\log x - (1-x)^2 \right) \right. \\ &\quad \left. + \frac{1}{8} \left(\frac{\beta}{2}\right)^2 \left( (1-x)^2 + \frac{1}{2}(3x^2 - 4x + 1)\log x + \frac{1}{12}(1+7x^2)\log^2 x + (1-x^2)\text{Li}_2(1-x) \right) \right] \\ &\quad + O(\alpha^4). \end{aligned} \quad (4.56)$$

Formula one includes a Kuraev-Fadin type resummation of the soft part and all other terms are hard. The second one resums the complete result and no hard part ( $\delta^H$ ) is left. Since there is no justification why the complete hard part should be resummed, the first formula seems to be more reasonable from the theoretical point of view. On the other hand, the second formula is much shorter and more elegant.

We checked the correctness of these two results in the following way. The two structure functions are expanded in orders of  $\alpha$ . One has to keep in mind that the correct expansion has the structure

$$\Gamma_{ee}^{\text{NS,LL}}(x) = \delta(1-x) + \sum_n \alpha^n (\Gamma_{ee}^{O(\alpha^n)}(x))_+, \quad (4.57)$$

which follows from the initial condition eq. (4.27) and the normalization condition

$$\int_0^1 \Gamma_{ee}^{\text{NS,LL}}(x) dx = 1. \quad (4.58)$$

Then we applied the Mellin transformation and compared this with the exact result of the Mellin transformed non-singlet equation eq. (4.43) expanded up to  $O(\alpha^3)$ . As expected, we found perfect agreement.

# Chapter 5

## Pair Production of Charginos and Neutralinos in $e^+e^-$ collisions

### 5.1 Tree-Level

The tree-level pair production processes for charginos Fig. 5.1, and neutralinos Fig. 5.2, within the Minimal Supersymmetric Standard Model,

$$\begin{aligned} e^-(p_1) e^+(p_2) &\rightarrow \tilde{\chi}_i^-(k_1) \tilde{\chi}_j^+(k_2) & (i, j = 1, 2), \\ e^-(p_1) e^+(p_2) &\rightarrow \tilde{\chi}_i^0(k_1) \tilde{\chi}_j^0(k_2) & (i, j = 1, 2, 3, 4), \end{aligned}$$

have been already extensively discussed in the literature [48, 49]. The chargino pair production is characterized by the s-channel diagrams with photon and Z-boson exchange and the t-channel contribution by a virtual electron-sneutrino  $\tilde{\nu}_e$  exchange.

In the case of neutralino pair production, there is only one s-channel diagram with Z-boson

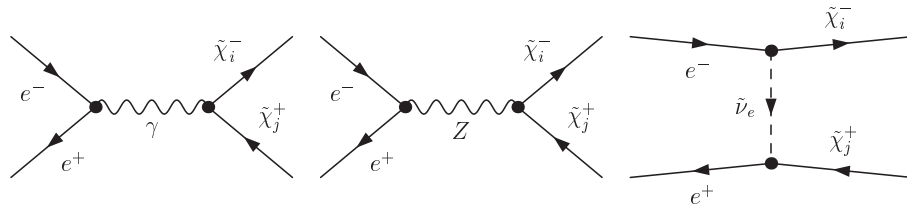


Figure 5.1: Tree-level chargino production

exchange, since neutralinos do not couple with photons at leading order. In addition, there are four diagrams with selectron  $\tilde{e}_{L,R}$  exchange. Both left and right-handed selectrons are exchanged via a t-channel and, due to the Majorana nature of the neutralinos, also via a u-channel diagram. For both production processes we neglect the Feynman-diagrams with s-channel Higgs-exchange. The  $e^-e^+$ -Higgs couplings are proportional to the electron mass  $m_e$  and thus negligible.

Furthermore we neglect two terms in the fermion-sfermion-neutralino/chargino couplings that are also proportional to the electron mass: The Yukawa parts and the selectron L-R

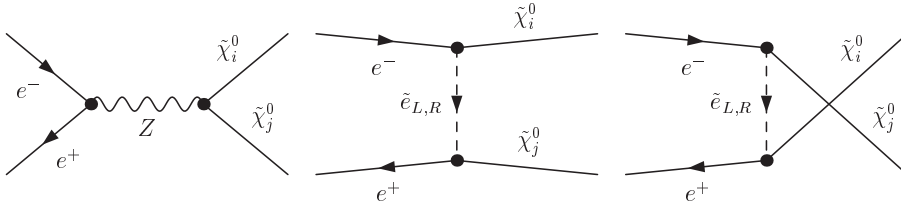


Figure 5.2: Tree-level neutralino production

mixing. In this limit the couplings conserve chirality, i.e.: left-handed electrons  $e_L$  couple only on left-handed selectrons  $\tilde{e}_L$  or electron-sneutrinos  $\tilde{\nu}_e$  and right-handed electrons  $e_R$  only on right-handed selectrons  $\tilde{e}_R$ . In this chiral limit it is possible to write the t-/u-channel Feynman-diagrams in the same Dirac structure as the s-channel diagrams, by applying the Fierz identity

$$(1 \otimes 1)_{\alpha\beta, \alpha'\beta'} = \frac{1}{4} \left( 1 \times 1 + \gamma_\mu \times \gamma^\mu + \frac{1}{2} \sigma_{\mu\nu} \times \sigma^{\mu\nu} - \gamma_\mu \gamma_5 \times \gamma^\mu \gamma^5 + \gamma^5 \times \gamma^5 \right)_{\alpha\beta', \alpha'\beta}. \quad (5.1)$$

After this Fierz transformation the tree-level matrix-elements can be expressed in terms of four independent helicity amplitudes

$$\mathcal{M}_{\alpha\beta} = i \frac{e^2}{s} Q_{\alpha\beta} [\bar{v}(p_2) \gamma_\mu P_\alpha u(p_1)] [\bar{u}(k_1) \gamma^\mu P_\beta v(k_2)], \quad \{\alpha, \beta\} \in \{L, R\}. \quad (5.2)$$

The bilinear charges  $Q_{\alpha\beta}^\pm$  for charginos and  $Q_{\alpha\beta}^0$  for neutralinos are

$$\begin{aligned} Q_{LL}^\pm &= \delta_{ij} + D_Z C_L \mathcal{U}_{ij}, & Q_{LR}^\pm &= \delta_{ij} + D_Z C_L \mathcal{V}_{ij} + D_{\tilde{\nu}} \tilde{\mathcal{V}}_{ij}, \\ Q_{RL}^\pm &= \delta_{ij} + D_Z C_R \mathcal{U}_{ij}, & Q_{RR}^\pm &= \delta_{ij} + D_Z C_R \mathcal{V}_{ij}, \\ Q_{LL}^0 &= D_Z C_L \mathcal{N}_{ij} - D_{u,L} \mathcal{L}_{ij}, & Q_{LR}^0 &= -D_Z C_L \mathcal{N}_{ij}^* + D_{t,L} \mathcal{L}_{ij}^*, \\ Q_{RL}^0 &= D_Z C_R \mathcal{N}_{ij} + D_{t,R} \mathcal{R}_{ij}, & Q_{RR}^0 &= -D_Z C_R \mathcal{N}_{ij}^* - D_{u,R} \mathcal{R}_{ij}^*. \end{aligned}$$

The first index denotes the chirality of the  $e^\pm$  current, the second one of the  $\tilde{\chi}_{i,j}^{0,\pm}$  current. We have introduced the projection operators  $P_{L/R} = P_{-/+} = \frac{1}{2}(1 \mp \gamma_5)$ , the kinematical variables

$$s = (p_1 + p_2)^2, \quad t = (p_1 - k_1)^2 \quad \text{and} \quad u = (p_1 - k_2)^2, \quad (5.3)$$

the normalized propagators

$$D_Z = \frac{s}{s - m_Z^2}, \quad D_{\tilde{\nu}} = \frac{s}{t - m_{\tilde{\nu}^2}}, \quad D_{t,L/R} = \frac{s}{t - m_{\tilde{e}_{L/R}}^2}, \quad D_{u,L/R} = \frac{s}{u - m_{\tilde{e}_{L/R}}^2}, \quad (5.4)$$

and the coupling matrices

$$\begin{aligned} C_L &= (s_W^2 - \frac{1}{2}) / (s_W^2 c_W^2), \quad C_R = 1/c_W^2, \\ \mathcal{U}_{ij} &= (s_W^2 \delta_{ij} - U_{i1} U_{j1}^* - \frac{1}{2} U_{i2} U_{j2}^*), \quad \mathcal{V}_{ij} = \mathcal{U}_{ij}(U \rightarrow V), \\ \tilde{\mathcal{V}}_{ij} &= V_{i1}^* V_{j1} / (2 s_W^2), \quad \mathcal{N}_{ij} = (N_{i3} N_{j3}^* - N_{i4} N_{j4}^*) / 2, \\ \mathcal{L}_{ij} &= (N_{i2} c_W + N_{i1} s_W)(N_{j2}^* c_W + N_{j1}^* s_W) / (4 s_W^2 c_W^2), \quad \mathcal{R}_{ij} = N_{i1} N_{j1}^* / c_W^2. \end{aligned} \quad (5.5)$$

Summing up the final state helicities  $\mathcal{M}_\alpha = \sum_{\beta=\pm} \mathcal{M}_{\alpha\beta}$ , the differential tree-level cross-section for polarized beams reads

$$d\sigma^{\text{tree}} = \frac{\mathcal{S}_{ij}}{\varphi} \sum_{\alpha=\pm} \frac{1}{4} (1 + \alpha \xi_-)(1 - \alpha \xi_+) |\mathcal{M}_\alpha|^2 d\Phi_2, \quad (5.6)$$

with  $\xi_\pm$  the degrees of polarization of the  $e^\pm$  beams,  $\varphi$  the flux factor, and  $d\Phi_2$  the 2-particle phase-space element

$$d\Phi_2 = \frac{d\vec{k}_1}{(2\pi)^3 2k_1^0} \frac{d\vec{k}_2}{(2\pi)^3 2k_2^0} (2\pi)^4 \delta^{(4)}(p_1 + p_2 - k_1 - k_2). \quad (5.7)$$

The symmetry-factor  $\mathcal{S}_{ij}$  respects the Majorana nature of the neutralinos and has the value  $\mathcal{S}_{ij} = 1/2$  if two identical neutralinos are produced and  $\mathcal{S}_{ij} = 1$  otherwise. For the particle kinematics, we naturally choose the CM system

$$\text{CMS :} \quad \vec{p}_1 + \vec{p}_2 = 0 = \vec{k}_1 + \vec{k}_2.$$

The momenta of the incoming particles can thus be parameterized as

$$\vec{p}_1 = (p_1^0, 0, 0, p_{\text{in}}), \quad \vec{p}_2 = (p_2^0, 0, 0, -p_{\text{in}}), \quad (5.8)$$

with

$$(p_1^0)^2 = p_{\text{in}}^2 + m_1^2, \quad (p_2^0)^2 = p_{\text{in}}^2 + m_2^2, \quad (5.9)$$

$$p_{\text{in}}^2 = \frac{(s + m_2^2 - m_1^2)^2}{4s} - m_2^2. \quad (5.10)$$

The flux factor  $\varphi$  is then given by

$$\varphi = 2\sqrt{\lambda(s, m_1^2, m_2^2)} = 4p_{\text{in}}\sqrt{s}, \quad \lambda(x, y, z) := (x - y - z)^2 - 4yz. \quad (5.11)$$

In the limit for incoming massless electrons and positrons  $m_e \rightarrow 0$ , we obtain

$$p_1 = \frac{\sqrt{s}}{2}(1, 0, 0, 1), \quad p_2 = \frac{\sqrt{s}}{2}(1, 0, 0, -1), \quad \varphi = 2s. \quad (5.12)$$

The outgoing momenta can be parameterized by the angle  $\theta = \angle(\vec{p}_1, \vec{k}_1)$

$$k_1 = (k_1^0, p_{\text{out}} \sin \theta, 0, p_{\text{out}} \cos \theta), \quad k_2 = (k_2^0, -p_{\text{out}} \sin \theta, 0, -p_{\text{out}} \cos \theta), \quad (5.13)$$

with

$$(k_1^0)^2 = p_{\text{out}}^2 + m_{\tilde{\chi}_i}^2, \quad (k_2^0)^2 = p_{\text{out}}^2 + m_{\tilde{\chi}_j}^2, \quad (5.14)$$

$$p_{\text{out}}^2 = \frac{(s + m_{\tilde{\chi}_j}^2 - m_{\tilde{\chi}_i}^2)^2}{4s} - m_{\tilde{\chi}_j}^2. \quad (5.15)$$

The total cross-section can then be obtained by

$$\sigma_{\text{tot}}^{\text{tree}} = \frac{\mathcal{S}_{ij} p_{\text{out}}}{16\pi s^{3/2}} \int_{-1}^1 \sum_{\alpha=\pm} \frac{1}{4} (1 + \alpha \xi_-)(1 - \alpha \xi_+) |\mathcal{M}_\alpha|^2 d\cos \theta. \quad (5.16)$$

Although calculated in the CM system,  $\sigma_{\text{tot}}$  is obviously a lorentz-invariant quantity. The forward-backward asymmetry is determined by the expression

$$A_{\text{FB}} = \frac{N(\theta < \frac{\pi}{2}) - N(\theta > \frac{\pi}{2})}{N(\theta < \frac{\pi}{2}) + N(\theta > \frac{\pi}{2})}, \quad (5.17)$$

where  $N(\theta < \frac{\pi}{2})/N(\theta > \frac{\pi}{2})$  are the numbers of events with the  $\tilde{\chi}_i^{0,-}$  with momentum  $k_1$  propagating in the forward/backward hemisphere. Since  $\theta = \angle(\vec{p}_1, \vec{k}_1)$  is not lorentz-invariant, also the forward-backward asymmetry depends on the system where the angle  $\theta$  is defined. In our case this is naturally the CM system. So for the  $2 \rightarrow 2$  process,  $A_{\text{FB}}$  for unpolarized beams can be written in terms of different cross-sections

$$A_{\text{FB}} = \frac{\sigma_{\text{F}} - \sigma_{\text{B}}}{\sigma_{\text{F}} + \sigma_{\text{B}}} = \frac{2\sigma_{\text{F}} - \sigma_{\text{tot}}}{\sigma_{\text{tot}}}, \quad (5.18)$$

with

$$\sigma_{\text{F}}^{\text{tree}} = \frac{\mathcal{S}_{ij} p_{\text{out}}}{16\pi s^{3/2}} \int_0^1 \sum_{\alpha=\pm} \frac{1}{4} |\mathcal{M}_{\alpha}|^2 d\cos\theta, \quad \sigma_{\text{B}}^{\text{tree}} = \frac{\mathcal{S}_{ij} p_{\text{out}}}{16\pi s^{3/2}} \int_{-1}^0 \sum_{\alpha=\pm} \frac{1}{4} |\mathcal{M}_{\alpha}|^2 d\cos\theta. \quad (5.19)$$

The left-right asymmetry for full polarized electrons and unpolarized positrons is obtained from

$$A_{\text{LR}} = \frac{\sigma_{\text{L}} - \sigma_{\text{R}}}{\sigma_{\text{L}} + \sigma_{\text{R}}} = \frac{\sigma_{\text{L}} - \sigma_{\text{tot}}}{\sigma_{\text{tot}}}, \quad (5.20)$$

with

$$\sigma_{\text{L}}^{\text{tree}} = \frac{\mathcal{S}_{ij} p_{\text{out}}}{16\pi s^{3/2}} \int_0^1 \frac{1}{2} |\mathcal{M}_{\text{L}}|^2 d\cos\theta, \quad \sigma_{\text{R}}^{\text{tree}} = \frac{\mathcal{S}_{ij} p_{\text{out}}}{16\pi s^{3/2}} \int_{-1}^0 \frac{1}{2} |\mathcal{M}_{\text{R}}|^2 d\cos\theta. \quad (5.21)$$

## 5.2 Virtual Corrections

For a high precision analysis of the neutralino and chargino sector, the inclusion of higher order corrections is mandatory. In the following elaborate calculations, a large number of Feynman diagrams is involved. Hence, it is necessary to use an appropriate computer algebra tool. For our calculations, the FeynArts 3.2 [50] package consists of all necessary ingredients to identify all contributing diagrams and to calculate them within the included MSSM model [51]. This is performed in the  $\xi = 1$  Feynman-'t Hooft gauge. The provided MSSM model contains the complete MSSM tree-level interaction Lagrangian. We have extended the model by integrating the renormalization scheme discussed in chapter 3. More details on this topic are given in the appendix.

The FormCalc 4 [52] package is adopted for the further processing of the Feynman amplitudes. Among other things, this tool contracts indices, calculates fermion traces, and includes the tensor reduction. In the latter case this is done in CDR which is identical to  $\overline{\text{DR}}$  at the one-loop level, as discussed in chapter 3.1.3. The output of FormCalc 4 has the appropriate form for a further numerical evaluation. For this purpose the Mathematica output is translated into Fortran code. The computation of the one-loop integrals is based on

the packages LoopTools and FF [53].

The virtual corrections for polarized beams can be written in the form

$$\int d\sigma^{\text{virt}} = \frac{\mathcal{S}_{ij} p_{\text{out}}}{16\pi s^{3/2}} \int \sum_{\alpha=\pm} \frac{1}{4} (1 + \alpha \xi_-)(1 - \alpha \xi_+) 2 \operatorname{Re} \{ (\mathcal{M}_\alpha)^\dagger \mathcal{M}_\alpha^1 \} d\cos\theta. \quad (5.22)$$

The one-loop matrix element  $\mathcal{M}_\alpha^1$ , generically given in Fig. 5.3, consists of all possible vertex corrections (Fig. 5.4), self-energy (Fig. 5.5) and box (Fig. 5.6) diagrams and the corresponding counter-terms. We again neglect the electron mass  $m_e$  wherever possible. The analytic expression for the counter-term Lagrangian is given in the appendix.

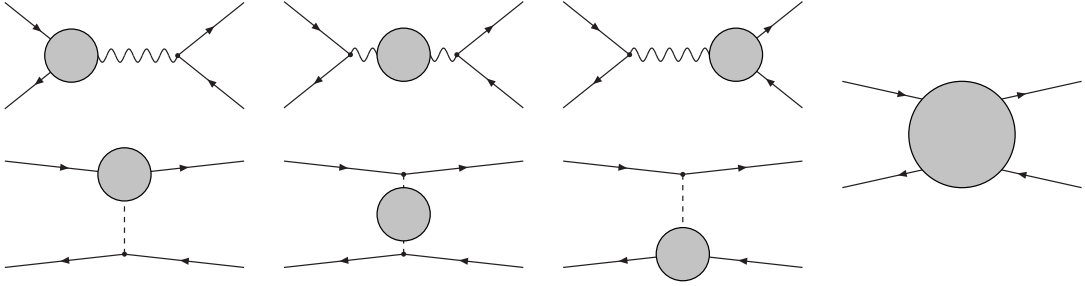


Figure 5.3: Generic virtual diagrams. The virtual corrections are structured into vertex, propagator and box contributions.

### 5.3 QED corrections

The full one-loop corrections include diagrams with virtual photons attached to the tree-level diagrams. These contributions are IR divergent and regularized by an infinitesimal photon mass  $\lambda$ . Concerning chargino and neutralino production, these diagrams cannot be separated from the residual weak corrections in a gauge invariant and UV finite way. This can be traced back to the tree-level selectron and sneutrino t-channel diagrams, which introduce the charged current coupling  $g \equiv e/s_w$ . The same effect can be observed in the SM, e.g. for  $W$  pair production [54]. For pure neutral current processes like  $e^+e^-$  annihilation processes into third generation fermions or sfermions [55], the gauge invariant and UV finite separation is possible, due to a Ward identity.

Therefore the cross-sections become IR finite and thus physically meaningful only by inclusion of real photon emission. The fact that IR singularities cancel between virtual and real soft-photon corrections is known as the Bloch-Nordsieck theorem [56]. The bremsstrahlung diagrams for the concerning processes are shown in Fig. 5.7. For both production processes we naturally have to consider the initial-state-radiation (ISR) from the incoming  $e^\pm$  beams. In the case of chargino production we also have to deal with final-state-radiation radiated off the produced chargino pair. For neutralino production the photon radiation of the intermediate selectrons  $\tilde{e}_{L,R}$  has to be considered, but gives a pure IR finite contribution, since the selectrons are off-shell and no resonances can occur in the t-/u- channel.

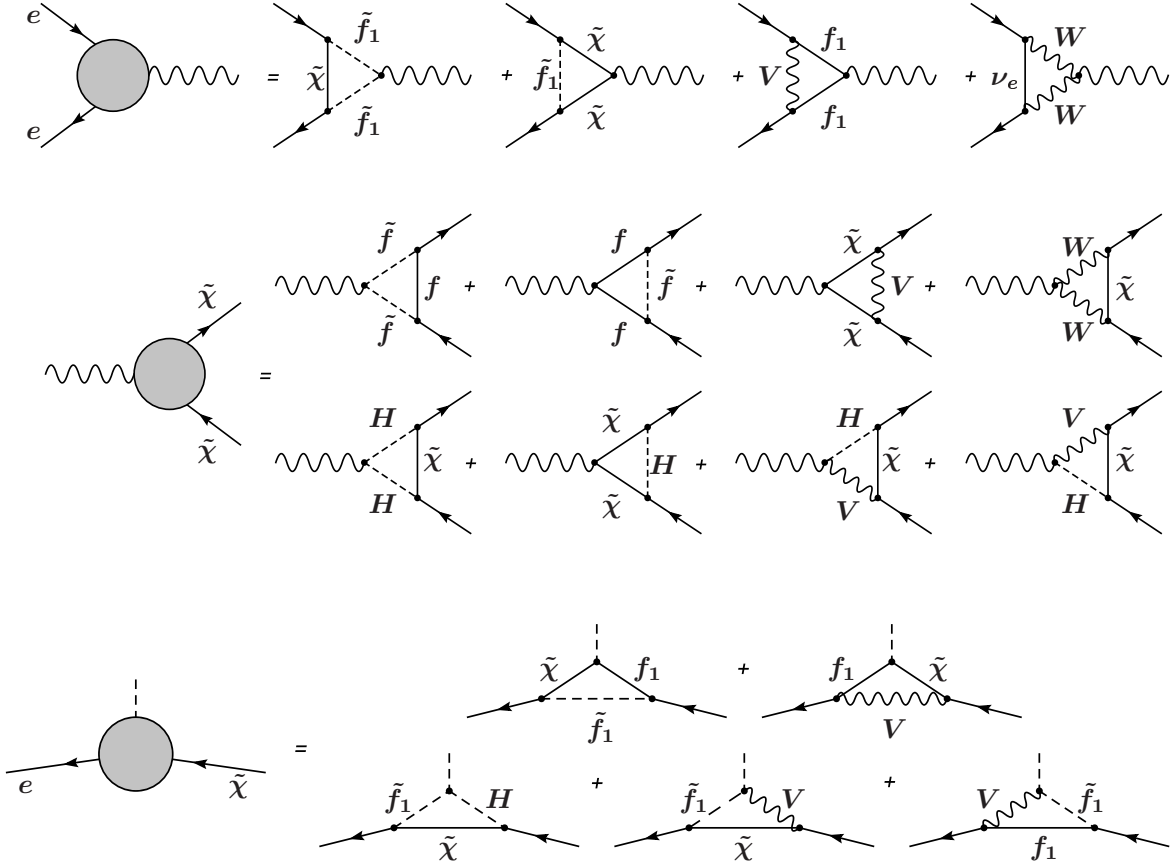


Figure 5.4: Generic diagrams for the different vertex corrections. Seven different classes of particles are introduced:  $f$  for all SM fermions,  $f_1$  for  $e$  and  $\nu_e$  only,  $\tilde{f}$  for all sfermions,  $\tilde{f}_1$  for  $\tilde{e}_{L,R}$  and  $\tilde{\nu}_e$  only,  $\tilde{\chi}$  for neutralinos and charginos,  $V$  for vector bosons, and  $H$  for Higgs and Goldstone bosons.

For the calculation of the real photonic corrections, we use the so-called phase-space slicing method [57]. The singular soft and collinear parts in the bremsstrahlung phase space are separated from the finite region. Both contributions can be written proportional to the tree-level cross-section, up to small terms of  $O(\Delta E_\gamma/\sqrt{s})$  and  $O(\Delta\theta_\gamma)$ , and performed analytically. The collinear (soft) singularities are regularized by the electron (infinitesimal photon) mass and cancel the corresponding terms in the virtual corrections.

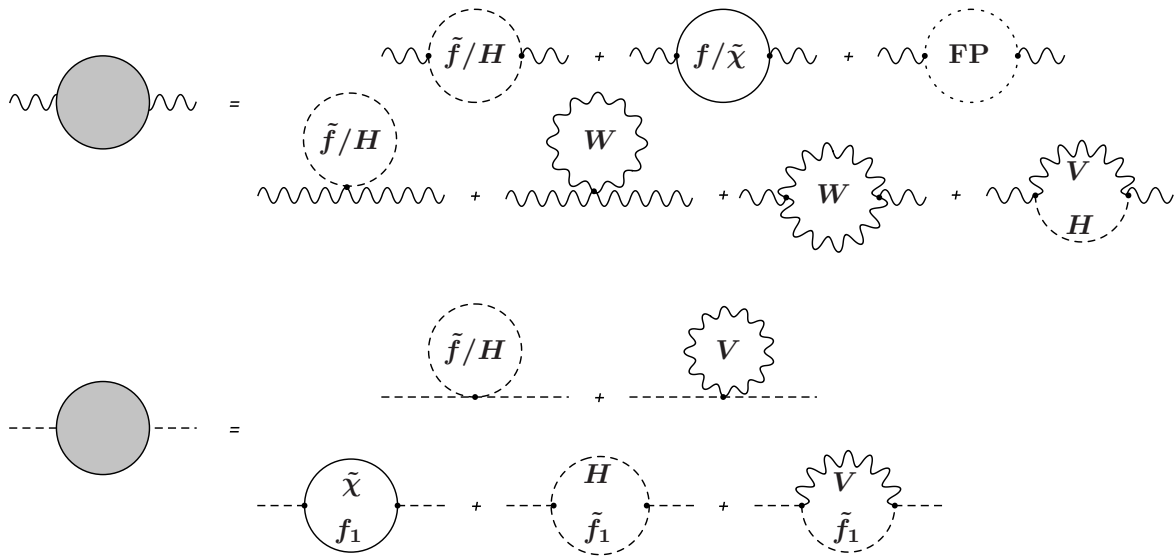


Figure 5.5: Generic self-energy diagrams for the s-channel vector and the t/u channel slepton propagators. FP denotes the class of Faddeev-Popov ghosts. All other particle classes are the same as in Fig. 5.4.

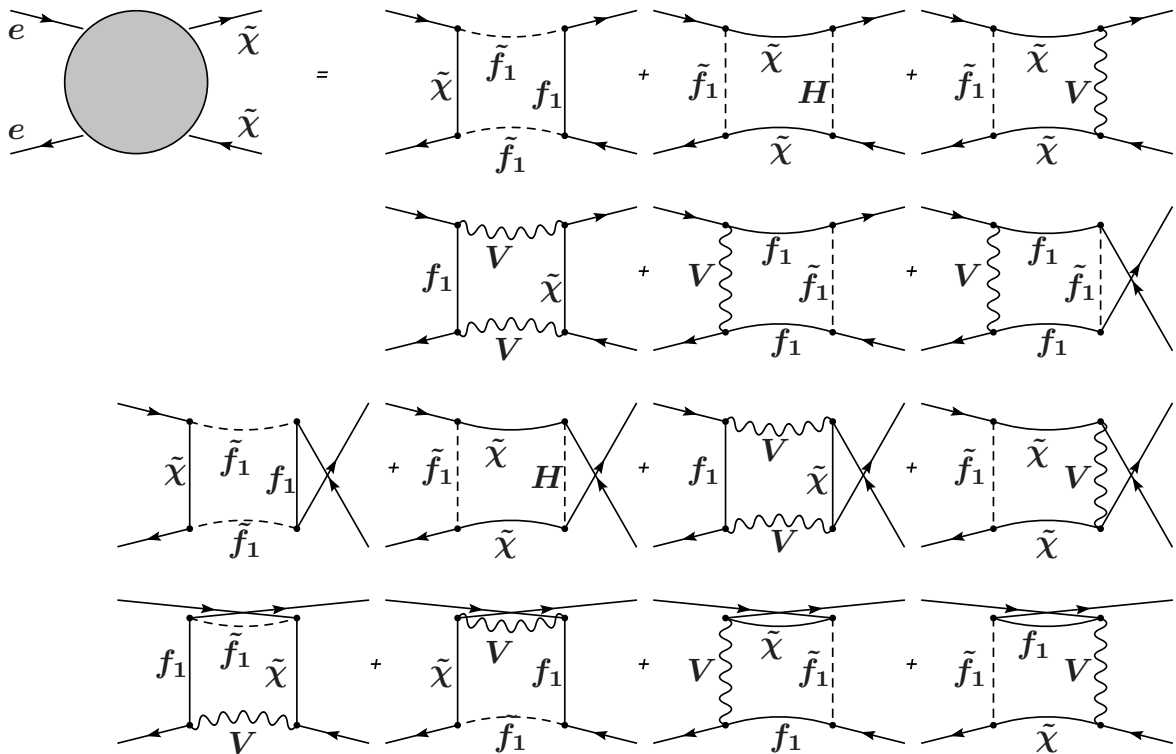


Figure 5.6: Generic box diagrams. The notation is taken over from Fig. 5.4.

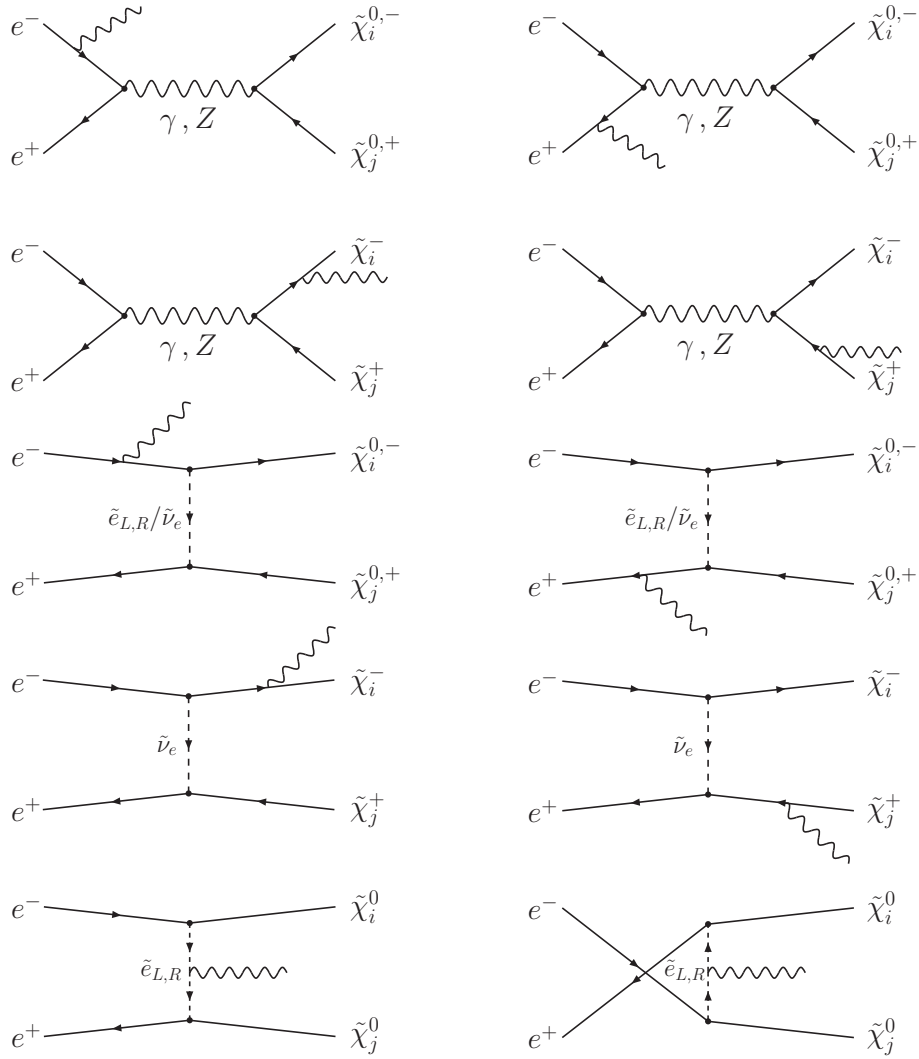


Figure 5.7: Bremsstrahlung Feynman diagrams.

### 5.3.1 Soft-photon region

In the soft-photon area only photons up to a CM (center-of-mass) energy  $\Delta E_\gamma$  are considered

$$d\sigma^{\text{soft}} = -d\sigma^{\text{tree}} \frac{\alpha}{4\pi^2} \int_{k_\gamma^0 \leq \Delta E_\gamma} \frac{d^3\vec{k}_\gamma}{k_\gamma^0} \left( \frac{p_1^\mu}{p_1 k_\gamma} - \frac{p_2^\mu}{p_2 k_\gamma} + Q_{\tilde{\chi}} \frac{k_1^\mu}{k_1 k_\gamma} - Q_{\tilde{\chi}} \frac{k_2^\mu}{k_2 k_\gamma} \right)^2, \quad (5.23)$$

whereas  $Q_{\tilde{\chi}} = 0/-1$  stands for the electric charge of the neutralino/chargino respectively. The three-particle phase space can be gladly separated into the usual two particle phase-space and the photon phase-space. Both can be integrated independently. The result is expressed in terms of the soft-photon integrals according to ref. [16]

$$I_{ab} = \int_{|\vec{k}_\gamma| \leq \Delta E_\gamma} \frac{d^3\vec{k}_\gamma}{k_\gamma^0} \frac{a \cdot b}{a \cdot k_\gamma b \cdot k_\gamma}, \quad (5.24)$$

for arbitrary momenta  $a$  and  $b$ , resulting in

$$d\sigma^{\text{soft}} = -d\sigma^{\text{tree}} \frac{\alpha}{4\pi^2} (\delta_{\text{soft}}^{\text{ISR}} + \delta_{\text{soft}}^{\text{FSR}} + \delta_{\text{soft}}^{\text{ISR-FSR}}), \quad (5.25)$$

$$\delta_{\text{soft}}^{\text{ISR}} = I_{p_1 p_1} + I_{p_2 p_2} - 2I_{p_1 p_2}, \quad \delta_{\text{soft}}^{\text{FSR}} = Q_{\tilde{\chi}}^2 (I_{k_1 k_1} + I_{k_2 k_2} - 2I_{k_1 k_2}), \quad (5.26)$$

$$\delta_{\text{soft}}^{\text{ISR-FSR}} = 2Q_{\tilde{\chi}} (I_{p_1 k_1} + I_{p_2 k_2} - I_{p_1 k_2} - I_{p_2 k_1}). \quad (5.27)$$

The integration over the photon phase-space can be performed analytically and the general solution is given by

$$I_{ab} = 4\pi \frac{\alpha a \cdot b}{(\alpha a)^2 - b^2} \left\{ \frac{1}{2} \log \frac{(\alpha a)^2}{b^2} \log \frac{4\Delta E_\gamma^2}{\lambda^2} \left[ \frac{1}{4} \log^2 \frac{u_0 - |\vec{u}|}{u_0 + |\vec{u}|} + \text{Li}_2 \left( 1 - \frac{u_0 + |\vec{u}|}{v} \right) + \text{Li}_2 \left( 1 - \frac{u_0 - |\vec{u}|}{v} \right) \right]_b^{u=\alpha a} \right\}, \quad (5.28)$$

where  $v$  and  $\alpha$  are defined by the relations

$$v = \frac{(\alpha a)^2 - b^2}{2(\alpha a_0 - b_0)} \quad (5.29)$$

$$\alpha^2 a^2 - 2\alpha a \cdot b + b^2 = 0, \quad \frac{\alpha a_0 - b_0}{b_0} \geq 0. \quad (5.30)$$

However, for our purpose we are able to use various simplifications. For the integrals  $I_{k_1 k_1}$ ,  $I_{k_2 k_2}$ , where the two momenta are identical we obtain

$$I_{aa} = 2\pi \left\{ \log \frac{4\Delta E_\gamma^2}{\lambda^2} + \frac{a_0}{|\vec{a}|} \log \frac{a_0 - |\vec{a}|}{a_0 + |\vec{a}|} \right\}. \quad (5.31)$$

A further simplification can be done for  $I_{p_1 p_1}$ ,  $I_{p_2 p_2}$ , where the electron mass is neglected whenever possible. Exceptions are the logarithmic terms, which reflect the collinear singularity

$$I_{p_i p_i} = 2\pi \left\{ \log \frac{4\Delta E_\gamma^2}{\lambda^2} - \log \frac{s}{m_e^2} \right\}. \quad (5.32)$$

In the next step we consider the integral  $I_{k_1 k_2}$ , where we use in the CMS frame the relation  $\vec{k}_1 = -\vec{k}_2 \equiv \vec{q}$

$$I_{ab} = \frac{2\pi (a_0 b_0 + |\vec{q}|^2)}{(a_0 + b_0) |\vec{q}|} \left\{ \frac{1}{2} \log \frac{a_0 + |\vec{q}|}{a_0 - |\vec{q}|} \log \frac{4\Delta E_\gamma^2}{\lambda^2} - \text{Li}_2 \left( \frac{2|\vec{q}|}{a_0 + |\vec{q}|} \right) - \frac{1}{4} \log^2 \frac{a_0 + |\vec{q}|}{a_0 - |\vec{q}|} + \frac{1}{2} \log \frac{b_0 + |\vec{q}|}{b_0 - |\vec{q}|} \log \frac{4\Delta E_\gamma^2}{\lambda^2} - \text{Li}_2 \left( \frac{2|\vec{q}|}{b_0 + |\vec{q}|} \right) - \frac{1}{4} \log^2 \frac{b_0 + |\vec{q}|}{b_0 - |\vec{q}|} \right\} \quad (5.33)$$

This result can be also applied for the integral  $I_{p_1 p_2}$  and furthermore the limit  $m_e \rightarrow 0$  is performed

$$I_{p_1 p_2} = 2\pi \left\{ \log \frac{4\Delta E_\gamma^2}{\lambda^2} \log \frac{s}{m_e^2} - \frac{1}{2} \log^2 \frac{s}{m_e^2} - \frac{\pi^2}{3} \right\}. \quad (5.34)$$

Considering the integrals  $I_{p_1 k_2}$ ,  $I_{p_2 k_1}$ , there is no relation between the two momenta, but we take again the limit for vanishing electron mass

$$I_{p_i k_j} = 2\pi \left\{ \log \frac{4\Delta E_\gamma^2}{\lambda^2} \log \frac{2 p_i \cdot k_j}{m_e^2 m_j^2} - \frac{1}{4} \log^2 \frac{m_j^2}{(k_j^0 + |\vec{k}_j|)^2} - \frac{1}{4} \log^2 \frac{s}{m_e^2} - \frac{\pi^2}{6} \right. \\ \left. - \text{Li}_2 \left( 1 - \frac{\sqrt{s} m_j^2}{2(k_j^0 + |\vec{k}_j|) p_i k_j} \right) - \text{Li}_2 \left( 1 - \frac{\sqrt{s}(k_j^0 + |\vec{k}_j|)}{2 p_i k_j} \right) \right\}. \quad (5.35)$$

### 5.3.2 Collinear region

In the collinear region, we consider hard photons ( $p_\gamma^0 > \Delta E_\gamma$ ) radiated off the incoming  $e^\pm$  beams in a small angle  $\Delta\theta_\gamma$  around the beam axis. The photons emit an energy  $\sum_i (1-x_i) p_i^0$  and as a consequence reduce the beam momenta

$$\{p_1, p_2\} \rightarrow \{\hat{p}_1 = x_1 p_1, \hat{p}_2 = x_2 p_2\}. \quad (5.36)$$

The beam energy is thus lowered

$$\sqrt{s} \rightarrow \sqrt{\hat{s}} = \sqrt{x_1 x_2 s}. \quad (5.37)$$

First, we consider the general reduced cross-section

$$\hat{\sigma}^{\text{tree}}(x_1, x_2, s) = \int d\sigma^{\text{tree}}(x_1 p_1, x_2 p_2) \quad (5.38)$$

that has to be calculated in the two-particle sub-phase-space. Afterwards the photon phase-space is considered by multiplication with a kernel function and a subsequent integration over the energy fractions  $x_i$ .

The reduction of the incoming momenta leads to the problem, that we are no longer in the CM system, since  $\hat{p}_1 + \hat{p}_2 \neq 0$ , and we have to perform a Lorentz-transformation. Demanding that the new momenta fulfill the relations

$$\hat{p}_1^{\text{CMS}} + \hat{p}_2^{\text{CMS}} = 0, \quad (\hat{p}_1^{\text{CMS}} + \hat{p}_2^{\text{CMS}})^2 = (\hat{p}_1 + \hat{p}_2)^2 = \hat{s} \quad (5.39)$$

the velocity  $v$  (in units of the speed-of-light)

$$v = \frac{x_2 - x_1}{x_1 + x_2} \quad (5.40)$$

for the Lorentz-boost (from the original in the new CMS frame) is obtained. Thus the incoming momenta in the new CMS are

$$\hat{p}_{1,2}^{\text{CMS}} = \sqrt{x_1 x_2} p_{1,2}. \quad (5.41)$$

Due to its Lorentz-invariance the reduced total cross-section is just given by

$$\hat{\sigma}_{\text{tot}}^{\text{tree}}(x_1, x_2, s) = \sigma_{\text{tot}}^{\text{tree}}(\hat{s}). \quad (5.42)$$

Attention is necessary, if cuts on the integration angle  $\theta$  are applied. To obtain the correct cross-sections  $\hat{\sigma}_{\text{F,B}}$ , the cut on  $\theta$  has to be transformed in the new CM system. The reduced forward cross-section for unpolarized beams then reads

$$\hat{\sigma}_{\text{F}}^{\text{tree}}(x_1, x_2, s) = \frac{\mathcal{S}_{ij} \hat{p}_{\text{out}}}{16\pi \hat{s}^{3/2}} \int_c^1 \sum_{\alpha=\pm} \frac{1}{4} |\mathcal{M}_\alpha|^2 d\cos \hat{\theta}^{\text{CMS}}, \quad (5.43)$$

with

$$c = v \frac{\sqrt{\hat{p}_{\text{out}}^2 + m_{\chi_i}^2}}{\hat{p}_{\text{out}}}, \quad \hat{p}_{\text{out}}^2 = \frac{(\hat{s} + m_{\chi_j}^2 - m_{\chi_i}^2)^2}{4\hat{s}} - m_{\chi_j}^2. \quad (5.44)$$

The collinear cross-section in the general form reads

$$\int d\sigma^{\text{coll}}(p_1, p_2, \xi_-, \xi_+) = \frac{\alpha}{2\pi} \int_0^{1-2\Delta E_\gamma/\sqrt{s}} dx \sum_{\alpha=\pm} G_\alpha(s, x, \Delta\theta_\gamma) \cdot \left[ \int d\sigma^{\text{tree}}(xp_1, p_2, \alpha\xi_-, \xi_+) + \int d\sigma^{\text{tree}}(p_1, xp_2, \xi_-, \alpha\xi_+) \right], \quad (5.45)$$

with

$$G_+(s, x, \Delta\theta_\gamma) = \frac{1+x^2}{1-x} \left[ \log \left( \frac{s\Delta\theta_\gamma^2}{4m_e^2} \right) - 1 \right], \quad G_-(s, x, \Delta\theta_\gamma) = 1-x. \quad (5.46)$$

The kernel function  $G_+$  reveals the collinear divergence for  $\Delta\theta_\gamma \rightarrow 0$  and the IR divergence for  $x \rightarrow 1$ .

The total, the forward and the left-handed collinear cross-sections thus are

$$\sigma_{\text{tot}}^{\text{coll}}(s) = \frac{\alpha}{2\pi} \int_0^{1-2\Delta E_\gamma/\sqrt{s}} dx 2\sigma_{\text{tot}}^{\text{tree}}(xs) [G_+ + G_-](s, x, \Delta\theta_\gamma), \quad (5.47)$$

$$\sigma_{\text{F}}^{\text{coll}}(s) = \frac{\alpha}{2\pi} \int_0^{1-2\Delta E_\gamma/\sqrt{s}} dx (\hat{\sigma}_{\text{F}}^{\text{tree}}(x, 1, s) + \hat{\sigma}_{\text{F}}^{\text{tree}}(1, x, s)) [G_+ + G_-](s, x, \Delta\theta_\gamma), \quad (5.48)$$

$$\sigma_{\text{L}}^{\text{coll}}(s) = \frac{\alpha}{2\pi} \int_0^{1-2\Delta E_\gamma/\sqrt{s}} dx 2 [\sigma_{\text{L}}^{\text{tree}}(xs)G_+ + \sigma_{\text{tot}}^{\text{tree}}(xs)G_-](s, x, \Delta\theta_\gamma). \quad (5.49)$$

In the numerical evaluation, the terms proportional to  $G_-$  are due to the absence of a collinear singularity in general negligible compared to those proportional to  $G_+$ .

### 5.3.3 Finite region

The finite hard bremsstrahlung has to be calculated by integration of the squared tree-level matrix-element for  $e^+e^- \rightarrow \tilde{\chi}_i \tilde{\chi}_j \gamma$  over the three-particle final-state phase-space

$$\int d\sigma^{\text{finite}} = \frac{\mathcal{S}_{ij}}{2s} \int d\Phi_\gamma |\mathcal{M}^\gamma|^2, \quad (5.50)$$

with the three-particle phase-space-element

$$d\Phi_\gamma \equiv d\Phi_3 = \frac{d^3\vec{k}_1}{(2\pi)^3 2k_1^0} \frac{d^3\vec{k}_2}{(2\pi)^3 2k_2^0} \frac{d^3\vec{k}_\gamma}{(2\pi)^3 2k_\gamma^0} (2\pi)^4 \delta^{(4)}(p_1 + p_2 - k_1 - k_2 - k_\gamma). \quad (5.51)$$

For the hard bremsstrahlung process in the finite region, the separation into a two-particle phase-space and a photon part is no longer valid, and the full three-particle phase space has to be considered. The parameterization has to be done in such a way, that cuts on the photon scattering angle  $\theta_\gamma$  and on the photon energy  $k_\gamma^0$  can be easily applied. We therefore choose as parameter input

$$\theta_\gamma, \quad \eta, \quad k_1^0, \quad \text{and} \quad k_\gamma^0.$$

The angles are defined in Fig. 5.8. The plane  $\sigma$  is spanned by the momenta  $\vec{p}_1$  and  $\vec{k}_\gamma$ , the

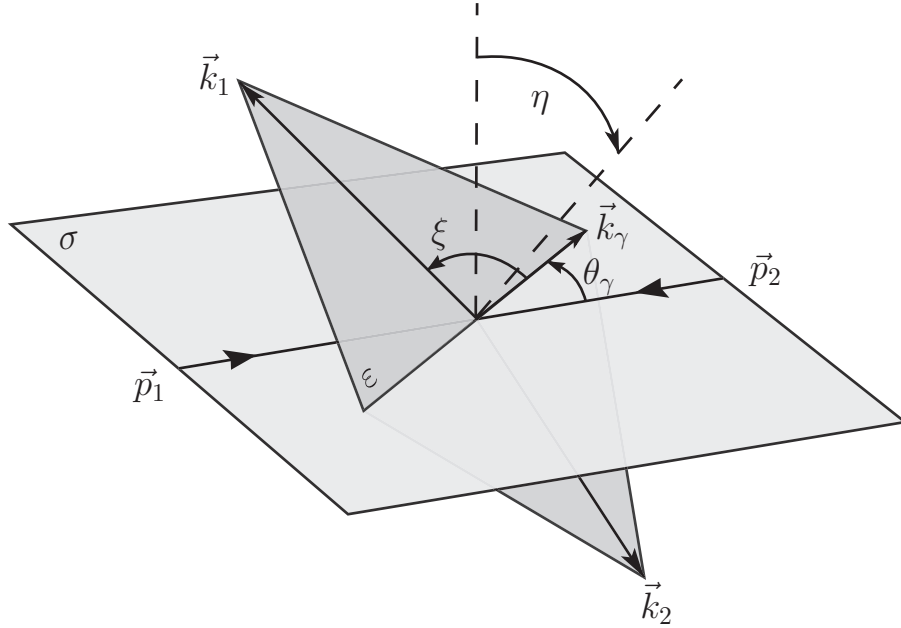


Figure 5.8: Parameterization of the three-particle final-state phase-space.

plane  $\varepsilon$  by  $\vec{k}_1$  and  $\vec{k}_2$ . Due to momentum conservation in the CMS the cut line of these two planes is  $\vec{k}_\gamma$ . The three shown angles are

$$\eta = \sphericalangle(\sigma, \varepsilon), \quad \theta_\gamma = \sphericalangle(\vec{p}_1, \vec{k}_\gamma), \quad \xi = \sphericalangle(\vec{k}_1, \vec{k}_\gamma).$$

The explicit representation of the outgoing momenta is

$$k_i = (k_i^0, |\vec{k}_i| \vec{e}_i), \quad \text{with} \quad |\vec{k}_i| = \sqrt{(k_i^0)^2 - m_{\chi_i}^2},$$

and the unit vectors

$$\vec{e}_\gamma = (\sin \theta_\gamma, 0, \cos \theta_\gamma), \quad (5.52)$$

$$\vec{e}_1 = (\cos \theta_\gamma \cos \eta \sin \xi + \sin \theta_\gamma \cos \xi, \sin \eta \sin \xi, \cos \theta_\gamma \cos \xi - \sin \theta_\gamma \cos \eta \sin \xi). \quad (5.53)$$

Momentum  $k_2$  is given by four-momentum conservation. In the CMS frame this is

$$k_1^0 + k_2^0 + k_\gamma^0 = \sqrt{s} \quad \text{and} \quad \vec{k}_1 + \vec{k}_2 + \vec{k}_\gamma = 0.$$

The auxiliary angle  $\xi$  is likewise determined by momentum conservation

$$\cos \xi = \frac{|\vec{k}_2|^2 - |\vec{k}_1|^2 - |\vec{k}_\gamma|^2}{2|\vec{k}_1||\vec{k}_\gamma|}. \quad (5.54)$$

The (cut-dependent) cross-section can then be written as

$$\sigma^{\text{finite}}(\Delta E_\gamma, \Delta\theta_\gamma) = \frac{\mathcal{S}_{ij}}{(4\pi)^4 s} \int_{\Delta E_\gamma}^{(k_\gamma^0)^{\text{max}}} dk_\gamma^0 \int_{(k_1^0)^{\text{min}}}^{(k_1^0)^{\text{max}}} dk_1^0 \int_{-\cos \Delta\theta_\gamma}^{\cos \Delta\theta_\gamma} d \cos \theta_\gamma \int_0^{2\pi} d\eta |\mathcal{M}^\gamma|^2, \quad (5.55)$$

with

$$(k_\gamma^0)^{\text{max}} = \frac{\sqrt{s}}{2} - \frac{(m_{\chi_i} + m_{\chi_j})^2 - m_\gamma^2}{2\sqrt{s}}, \quad (5.56)$$

and

$$(k_1^0)^{\text{max,min}} = \frac{1}{2\tau} \left[ \sigma(\tau + m_+ m_-) \pm |\vec{k}_\gamma| \sqrt{(\tau - m_+^2)(\tau - m_-^2)} \right], \quad (5.57)$$

$$\sigma = \sqrt{s} - k_\gamma^0, \quad \tau = \sigma^2 - |\vec{k}_\gamma|^2, \quad m_\pm = m_{\chi_i} \pm m_{\chi_j}. \quad (5.58)$$

From the discussion above, we know that only small cuts  $\Delta E_\gamma$  and  $\Delta\theta_\gamma$  on the photon energy and scattering angle are allowed to obtain a numerical result of high precision. Thus, we are already in a range, where the integrand notices the divergent soft and collinear behaviour according to

$$\mathcal{M}_{\gamma,\text{soft}} \sim \frac{1}{E_\gamma}, \quad \mathcal{M}_{\gamma,\text{coll}} \sim \frac{1}{p_1 \cdot k_\gamma} \sim \frac{1}{1 - \cos \theta_\gamma}.$$

The integrand is flattened by transforming  $E_\gamma$  and  $\cos \theta_\gamma$  to the new variables [58]

$$\widehat{E}_\gamma = \log \frac{E_\gamma}{\sqrt{s}}, \quad \widehat{\cos \theta_\gamma} = \log \frac{E_\gamma}{2\sqrt{s}} \left( 1 + \sqrt{1 - \frac{4m_e^2}{s} \cos \theta_\gamma} \right). \quad (5.59)$$

Note, that the corresponding Jacobian determinant mimics the correct behaviour of the integrand near the two poles. For the numerical evaluation, we used the multi-dimensional integration routines of the CUBA library [59]. This package consists of four algorithms which use different approaches for the numerical integration. The above discussed integrand flattening made it possible to obtain a result at a certain precision in less CPU time. We evaluated the hard bremsstrahlung cross-section with all four routines and found perfect agreement within the aimed accuracy. This is a good check for the reliability of the numerical result.

The complete  $O(\alpha)$  corrections can then be written as a sum of virtual, soft, collinear, and finite contributions, all depending on unphysical auxiliary parameters

$$\Delta\sigma_{O(\alpha)} = \int (d\sigma^{\text{virt}}(\lambda) + d\sigma^{\text{soft}}(\lambda, \Delta E_\gamma)) + \int d\sigma^{\text{coll}}(\Delta E_\gamma, \Delta\theta_\gamma) + \int d\sigma^{\text{finite}}(\Delta E_\gamma, \Delta\theta_\gamma). \quad (5.60)$$

Summing up the contributions in  $\Delta\sigma_{O(\alpha)}$ , we obtain a cut-off independent result. This has been checked analytically for  $\lambda$  and numerically for  $\Delta E_\gamma$  and  $\Delta\theta_\gamma$  in the intervals  $10^{-5} \leq \Delta E_\gamma / \sqrt{s} \leq 10^{-2}$  and  $10^{-3} \leq \Delta\theta_\gamma \leq 10^{-2}$ .

### 5.3.4 The structure function approach

For precise predictions of chargino and neutralino pair production higher orders beyond  $O(\alpha)$  have to be taken into account. The structure function formalism provides the possibility of defining process-independent logarithmic QED corrections, which originate from collinear virtual and real photons radiated off the incoming electron-positron beams, as discussed in chapter 4

$$\int d\sigma^{\text{tree}} + \int d\sigma^{\text{univ}} = \int_0^1 dx_1 \int_0^1 dx_2 \Gamma_{ee}^{\text{LL}}(x_1, Q^2) \Gamma_{ee}^{\text{LL}}(x_2, Q^2) \int d\sigma^{\text{tree}}(x_1 p_1, x_2 p_2). \quad (5.61)$$

We use the leading-log structure function of the Kuraev-Fadin type up to  $O(\alpha^3)$ , eq. (4.55)

$$\Gamma_{ee}^{\text{LL}}(x, Q^2) \equiv \Gamma_{ee}^{\text{NS,KF}}(x, Q^2). \quad (5.62)$$

In this approach only a subset (the collinear QED corrections) of the complete  $O(\alpha^n)$  corrections are taken into account. Therefore, the factorization scale  $Q$  does not vanish (as it does in a complete on-shell calculation), but is a free parameter. Although the variation of  $Q$  in  $d\sigma^{\text{univ}}$  can be considered as a higher order effect, an appropriate choice for this scale should be physically motivated to avoid unnatural terms. Near the threshold, where soft-photons are dominant, a satisfying choice is  $Q^2 = s$ , which we use for simplicity also for higher CM energies. A discussion about this topic can be found e.g. in [54].

The above calculated correction  $\Delta\sigma_{O(\alpha)}$  already contains the universal terms of  $O(\alpha)$

$$\int d\sigma^{\text{univ},1} = \int_0^1 dx_1 \int_0^1 dx_2 \Gamma_{ee}^{\text{LL},1}(x_1, Q^2) \Gamma_{ee}^{\text{LL},1}(x_2, Q^2) \int d\sigma^{\text{tree}}(x_1 p_1, x_2 p_2), \quad (5.63)$$

with

$$\Gamma_{ee}^{\text{LL},1}(x, Q^2) = \frac{\beta}{4} \lim_{\varepsilon \rightarrow 0} \left\{ \delta(1-x) \left[ \frac{3}{2} + 2 \log(\varepsilon) \right] + \theta(1-x-\varepsilon) \frac{1+x^2}{1-x} \right\}. \quad (5.64)$$

So we have to subtract them from the complete corrections to avoid double counting.

The final result, where all considered corrections are included is given by

$$\int d\sigma^{\text{complete}} = \int d\sigma^{\text{tree}} + \Delta\sigma_{O(\alpha)} + \int (d\sigma^{\text{univ}} - d\sigma^{\text{univ},1}). \quad (5.65)$$

Within the structure formalism the collinear part of the ISR is taken into account by the integral of the structure functions for both the electron and the positron beam over the reduced tree-level cross-section, eqs. (5.61) and (5.63). Due to the expansion of the logarithmic part of the structure functions, we can write for the total cross-section including ISR in terms of the total tree-level cross-section  $\sigma_{\text{tree}}$  and the structure functions  $\Gamma_{ee}^{\text{LL}}$  up to  $O(\alpha^n)$

$$\begin{aligned} \sigma_{\text{tot}}^{\text{tree+univ}}(s) &= \int_0^1 dx_1 \int_0^1 dx_2 \Gamma_{ee}^{\text{LL}}(x_1, Q^2) \Gamma_{ee}^{\text{LL}}(x_2, Q^2) \hat{\sigma}_{\text{tot}}^{\text{tree}}(x_1, x_2, s) \\ &= \int_0^1 dx \int_0^1 dx_1 \int_0^1 dx_2 \delta(x - x_1 x_2) \Gamma_{ee}^{\text{LL}}(x_1, Q^2) \Gamma_{ee}^{\text{LL}}(x_2, Q^2) \sigma_{\text{tot}}^{\text{tree}}(xs) \\ &= \int_0^1 dx \Phi(x) \sigma_{\text{tot}}^{\text{tree}}(xs) \end{aligned} \quad (5.66)$$

with

$$\begin{aligned}
\Phi(x) &= [\Gamma_{\bar{e}e}^{\text{LL}}(Q^2) \otimes \Gamma_{ee}^{\text{LL}}(Q^2)](x) \\
&= \frac{1}{2\pi} \int_{-\infty}^{+\infty} dt x^{-it-c} \left[ \exp\left(\frac{\alpha}{2\pi} L_e(Q^2) \tilde{P}_{ee}^0(it+c)\right) \right]^2 + O(\alpha^{n+1}), \\
&= \Gamma_{\bar{e}e}^{\text{LL}}(x, Q^2)(\alpha \rightarrow 2\alpha) + O(\alpha^{n+1})
\end{aligned} \tag{5.67}$$

The rule  $(\alpha \rightarrow 2\alpha)$  means that  $\alpha$  has to be replaced by  $2\alpha$ . Note, that we have inserted in the intermediate step the Mellin transformed exact NS leading-log solution, which differs from an analytical solution up to  $O(\alpha^n)$  at  $O(\alpha^{n+1})$ . Therefore, this simplification is only applicable if the error of  $O(\alpha^{n+1})$  is negligible. As a consequence, it can be used for eq. (5.61) but is not valid for eq. (5.63). For the forward-backward asymmetry, this simplification cannot be used in both cases, since we have used the lorentz-invariance of the total cross-section in the derivation. Further we again have to take care of the correct transformation of the angle cut.

$$\sigma_F^{\text{tree+univ}}(s) = \int_0^1 dx_1 \int_0^1 dx_2 \Gamma_{\bar{e}e}^{\text{LL}}(x_1, Q^2) \Gamma_{ee}^{\text{LL}}(x_2, Q^2) \int_c^1 \frac{d\sigma^{\text{tree}}}{d\cos\theta}(x_1 x_2 s) d\cos\theta, \tag{5.68}$$

where  $c$  is again the cut defined in eq. (5.44).

## 5.4 Definition of weak and QED corrections

In spite of the impossibility to disentangle the different contributions to the  $O(\alpha)$  corrections, it is of special interest to distinguish the genuine weak corrections from the large and on experimental cuts dependent photon part. In fact, there is no unique way of doing this. A naive treatment would be to take the pure virtual corrections and set the photon mass equal to a typical scale of the corresponding process  $\lambda \equiv Q$ . However, this leaves us with enhanced Sudakov double-logarithms  $\log^2 \frac{s}{m_e^2}$  from virtual soft-photons attached to the incoming beams, which are cancelled anyway by the corresponding real, soft part (see eqs. (5.34, 5.35)). Therefore, we take the sum of virtual and soft corrections and extract the  $\Delta E_\gamma$  dependent terms as well as the contributions proportional to  $L_e \equiv \log \frac{s}{m_e^2}$ , stemming from the collinear virtual+soft photons, eq. (5.63)

$$d\sigma^{\text{weak}} = d\sigma^{\text{virt+soft}}(\Delta E_\gamma) - \frac{\alpha}{\pi} d\sigma^{\text{tree}} \left[ \log \frac{4\Delta E_\gamma^2}{s} (L_e - 1 + \Delta_\gamma) + \frac{3}{2} L_e \right]. \tag{5.69}$$

The term  $\Delta_\gamma$  takes the cut-off dependent terms from final state radiation (FSR) and ISR-FSR interference of eq. (5.25) into account. The sum  $d\sigma^{\text{tree}} + d\sigma^{\text{weak}}$  is identical to the “reduced genuine SUSY cross-section” within the SPA convention [60]. The full corrected cross-section can now be obtained by the sum

$$\int d\sigma^{\text{complete}} = \int (d\sigma^{\text{tree}} + d\sigma^{\text{weak}}) + \int d\sigma^{\text{non-univ}} + \int d\sigma^{\text{univ}}, \tag{5.70}$$

with the non-universal QED corrections

$$\int d\sigma^{\text{non-univ}} = \int d\sigma^{\text{coll+finite}}(\Delta E_\gamma) - \int d\sigma^{\text{univ},1} + \frac{\alpha}{\pi} \int d\sigma^{\text{tree}} \left[ \log \frac{4\Delta E_\gamma^2}{s} (L_e - 1 + \Delta_\gamma) + \frac{3}{2} L_e \right]. \quad (5.71)$$

A second way to highlight weak corrections is to compare the complete corrected cross-section (including the hard photon radiation) with an improved tree-level  $d\sigma^{\text{tree+univ}}$  that already contains the universal QED corrections.

$$\int d\sigma^{\text{complete}} = \int d\sigma^{\text{tree+univ}} + \int d\sigma^{\text{residual}}, \quad (5.72)$$

$$\int d\sigma^{\text{residual}} = \int d\sigma^{\text{weak}} + \int d\sigma^{\text{non-univ}}. \quad (5.73)$$

The advantage of such a definition is that it does not require a more or less superficial splitting of virtual and real corrections. On the other hand, the “residual” corrections include the non-universal QED corrections. They are in general small, but can be comparable to the loop corrections, especially the ISR-FSR terms. Furthermore, it can be inconvenient for technical reasons to include the hard bremsstrahlung process in the definition of a “weak” correction.

# Chapter 6

## Numerical Results

With the tools developed in the last chapters, we are able to calculate observables for neutralino and chargino pair production and give precise predictions for experiments at a future linear  $e^+e^-$  collider (FLC) for a certain set of parameter input. Certainly, if SUSY is realized in nature and is found at the FLC it will go the other way round, measuring observables as masses and cross-sections and later on identifying the fundamental SUSY parameters by comparison of measured and calculated results. However, beyond tree-level the definition of the SUSY Lagrangian parameters is not unique but depends on the chosen renormalization scheme. Therefore, the SPA project [60] was established to provide a well defined theoretical framework, including a consistent set of definitions and input parameters. Furthermore, a certain SUSY scenario, the CP and R-parity conserving reference point SPS1a' was proposed to test computer programs in practice. In our numerical analysis, we therefore concentrate especially on the SPS1a' scenario. It is close to the original Snowmass SPS1a benchmark point but with slight changes to be compatible with all available precision data and actual mass and cosmological bounds. More details, like the complete list of parameters and how they are adopted to serve as input for the applied renormalization scheme can be found in the appendix.

Since we use an on-shell renormalization, the appropriate tree-level for the one-loop calculation is given in terms of on-shell parameters. On the other hand, our original input is the SPS1a' scenario, defined in terms of  $\overline{\text{DR}}$  parameters fixed at the scale  $\tilde{M} = 1$  TeV. We therefore show the corrections relative to the tree-level in the SPA convention, i.e. calculated in terms of on-shell masses and  $\overline{\text{DR}}$  values for all couplings. Using this tree-level definition, the relative corrections are the same compared with those calculated in other renormalization schemes, up to terms of higher order. For this purpose the used  $\overline{\text{DR}}$  value at  $\tilde{M}=1$  TeV of the fine structure constant is  $\alpha = 1/124.997$ .

In the presented numerical results, we use for the charge renormalization the  $\alpha^{\text{eff}}(m_Z)|_{\overline{\text{MS}}}$  scheme for neutralino production and the  $G_F$  scheme for chargino production, as discussed in section 3.3. In our numerics,  $\Delta r$  contains the full MSSM one-loop corrections [61] and the leading two-loop QCD corrections [62]. By calculating the same cross-section in both schemes, we find good agreement within a few per-mill in the final results.

## 6.1 Chargino Production

Fig. 6.1 shows the total cross-section for all three channels of chargino pair production in the SPS1a' scenario. The dotted curve depicts the tree-level in the SPA convention. The dashed and solid lines show the tree-level result together with weak and accordingly with full corrections.

Due to the large difference between the parameters  $M$  and  $\mu$ , the  $\tilde{\chi}_1^\pm$  is mainly a wino and the  $\tilde{\chi}_2^\pm$  nearly a pure higgsino. The tree-level diagram with photon-exchange only contributes for diagonal chargino production channels. To a large extent this is also valid for the  $Z$ -exchange, since the wino and the higgsino mix only slightly. In the  $t$ -channel sneutrino diagram, only the Wino component of the charginos contributes. Thus we see the typical behaviour of the three production channels. Large cross-sections for the diagonal pair production and a suppressed off-diagonal  $\tilde{\chi}_1^- \tilde{\chi}_2^+$ . Due to the CP-invariance of the SPS1a' scenario, the cross-section of the production processes  $e^-e^+ \rightarrow \tilde{\chi}_1^- \tilde{\chi}_2^+$  and  $e^-e^+ \rightarrow \tilde{\chi}_1^+ \tilde{\chi}_2^-$  are identical, therefore only the former ones is shown.

In Fig. 6.2 the complete corrections relative to the improved tree-level, where ISR is already

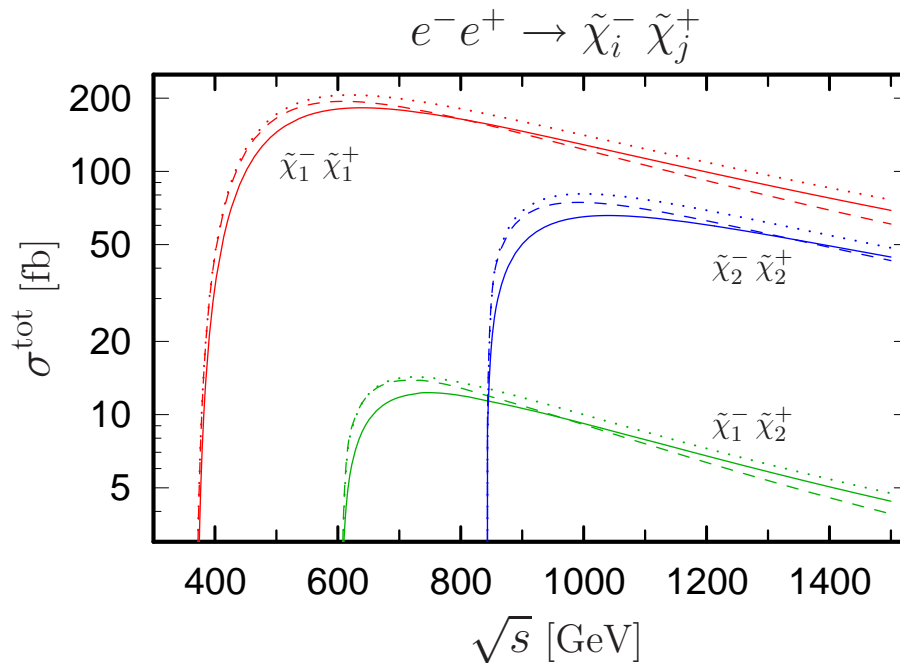


Figure 6.1: Total cross-sections for chargino pair production at tree-level {dotted}, with weak {dashed}, and with complete corrections {solid}.

included, are plotted. Since the soft-photon pole is already absorbed into the tree-level, we observe moderate corrections even near the threshold. Comparing the various corrections to the total tree-level cross-section for the different production channels Figs. 6.3 and 6.4 some common characteristics can be recognized. Near the threshold the negative soft-photon contributions dominate. Far away from the threshold, the positive universal QED corrections partially cancel the large and negative weak contributions. The almost constant non-universal QED corrections are small and in comparison with other corrections often

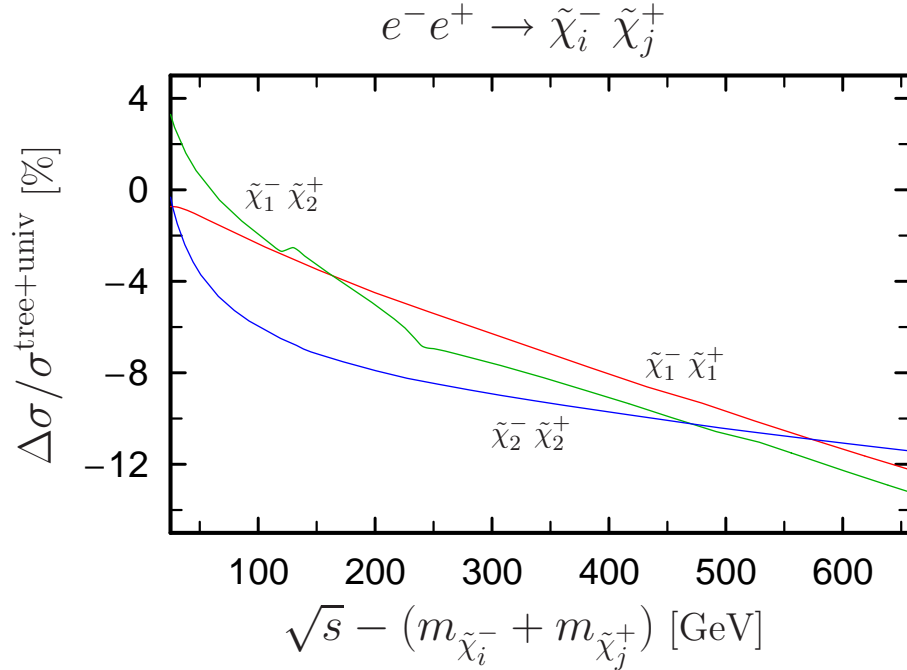


Figure 6.2: Complete corrections relative to the improved tree-level above the particular production threshold.

negligible. Due to the marginal non-universal QED corrections, the differences between the two proposed ways to highlight “genuine weak” corrections are quite small. However, this does not have to be true any longer if cuts on the phase space are applied or distributions in particle energies or scattering angles are discussed.

Moreover, we present results for the left-right asymmetry  $A_{\text{LR}}$  of chargino production in Fig. 6.5. The kinks in the lines can be traced back to so-called normal and anomalous thresholds. They occur for special combinations of masses in the propagators of a Passarino-Veltman integral.

In Fig. 6.6 the forward-backward asymmetry at tree-level, and with weak and complete corrections included, is shown. Furthermore, the relative corrections to the tree-level in SPA convention are depicted. Both asymmetries obtain sizeable corrections for all three production channels. At last, Fig. 6.7 provides an interesting view on the hard bremsstrahlung process

$$e^-e^+ \rightarrow \tilde{\chi}_1^- \tilde{\chi}_1^+ \gamma. \quad (6.1)$$

The differential cross-sections  $\frac{d\sigma^{\text{finite}}}{dE_\gamma}(\Delta E_\gamma, \Delta\theta_\gamma, E_\gamma)$  and  $\frac{d\sigma^{\text{finite}}}{d\cos\theta_\gamma}(\Delta E_\gamma, \Delta\theta_\gamma, \cos\theta_\gamma)$  are presented. To avoid mass singularities the angular and energy cuts of  $\theta_\gamma > 5^\circ$  and  $E_\gamma > 5$  GeV have to be imposed. The two figures impressively demonstrate the singular behaviour in the soft-photon limit  $E_\gamma \rightarrow 0$  and near the collinear region  $\cos\theta_\gamma \rightarrow \pm 1$ .

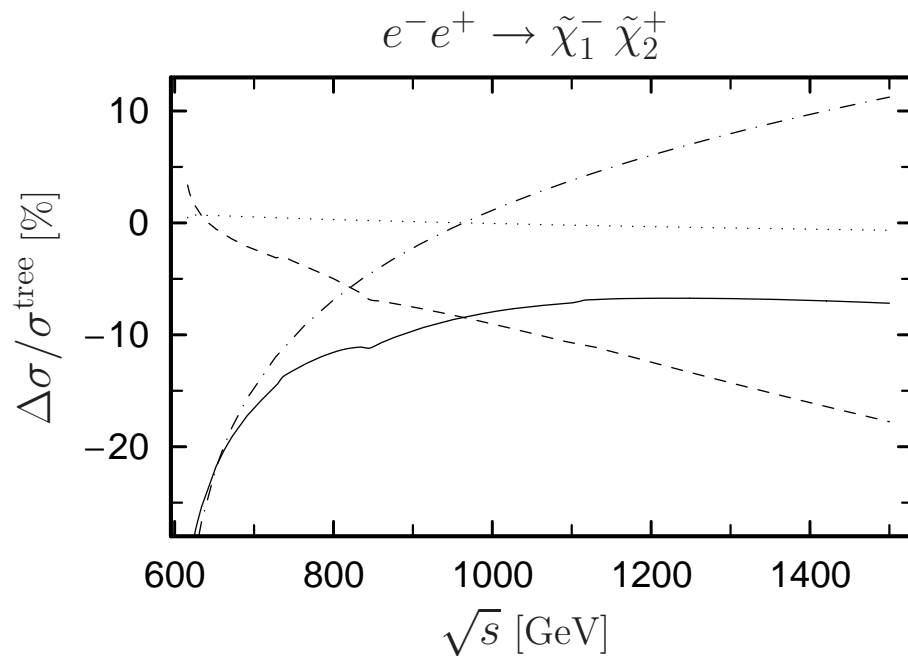
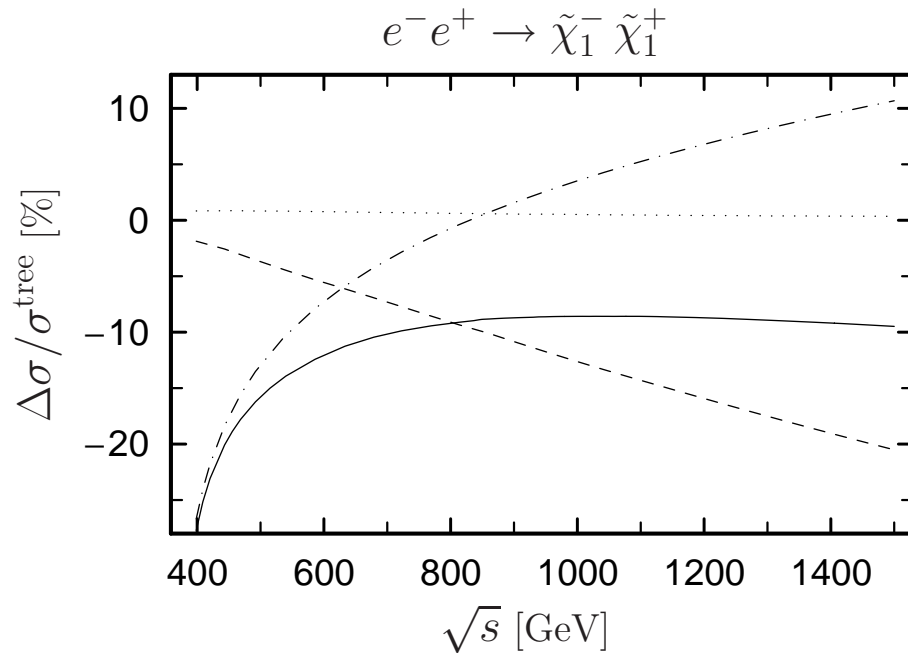


Figure 6.3: Radiative corrections for chargino pair production. The {full, dashed, dotted, dash-dotted} line corresponds to the {complete, weak, non-universal QED, universal QED} corrections to the total tree-level cross-section.

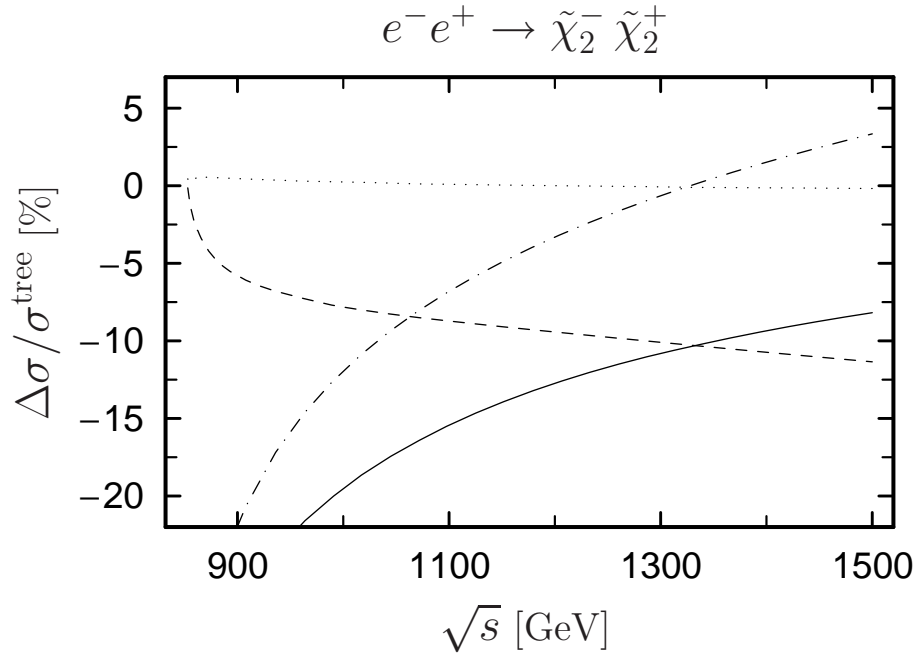


Figure 6.4: Radiative corrections for chargino pair production. The {full, dashed, dotted, dash-dotted} line corresponds to the {complete, weak, non-universal QED, universal QED} corrections to the total tree-level cross-section.

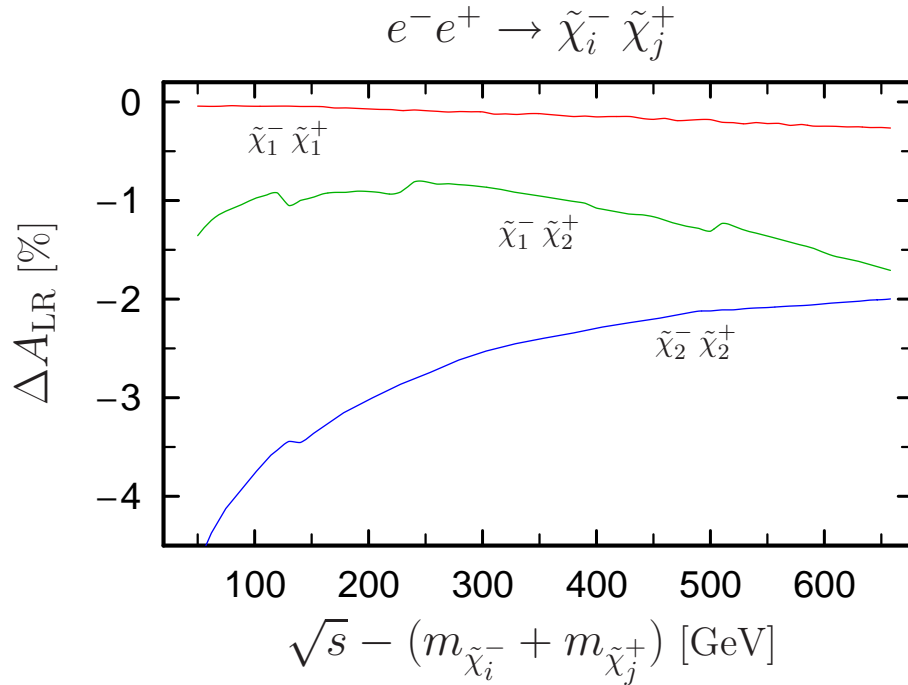


Figure 6.5: Radiative corrections for chargino pair production. Complete corrections to  $A_{\text{LR}}$  for all three chargino pair production channels.

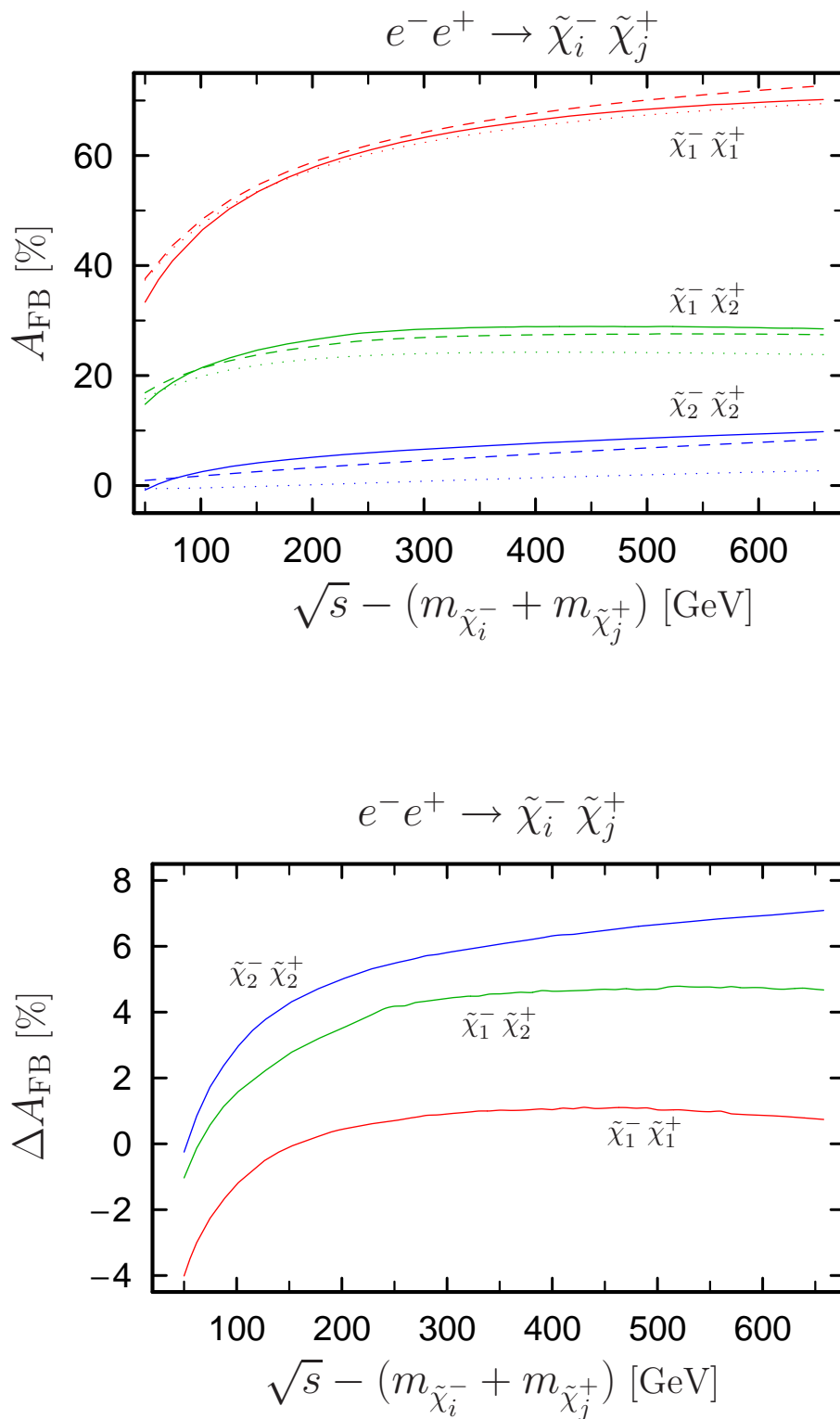


Figure 6.6: Top: Forward-backward asymmetry for chargino pair production at tree-level {dotted}, with weak {dashed}, and with complete corrections {solid}. Bottom: Complete corrections to  $A_{\text{FB}}$ .

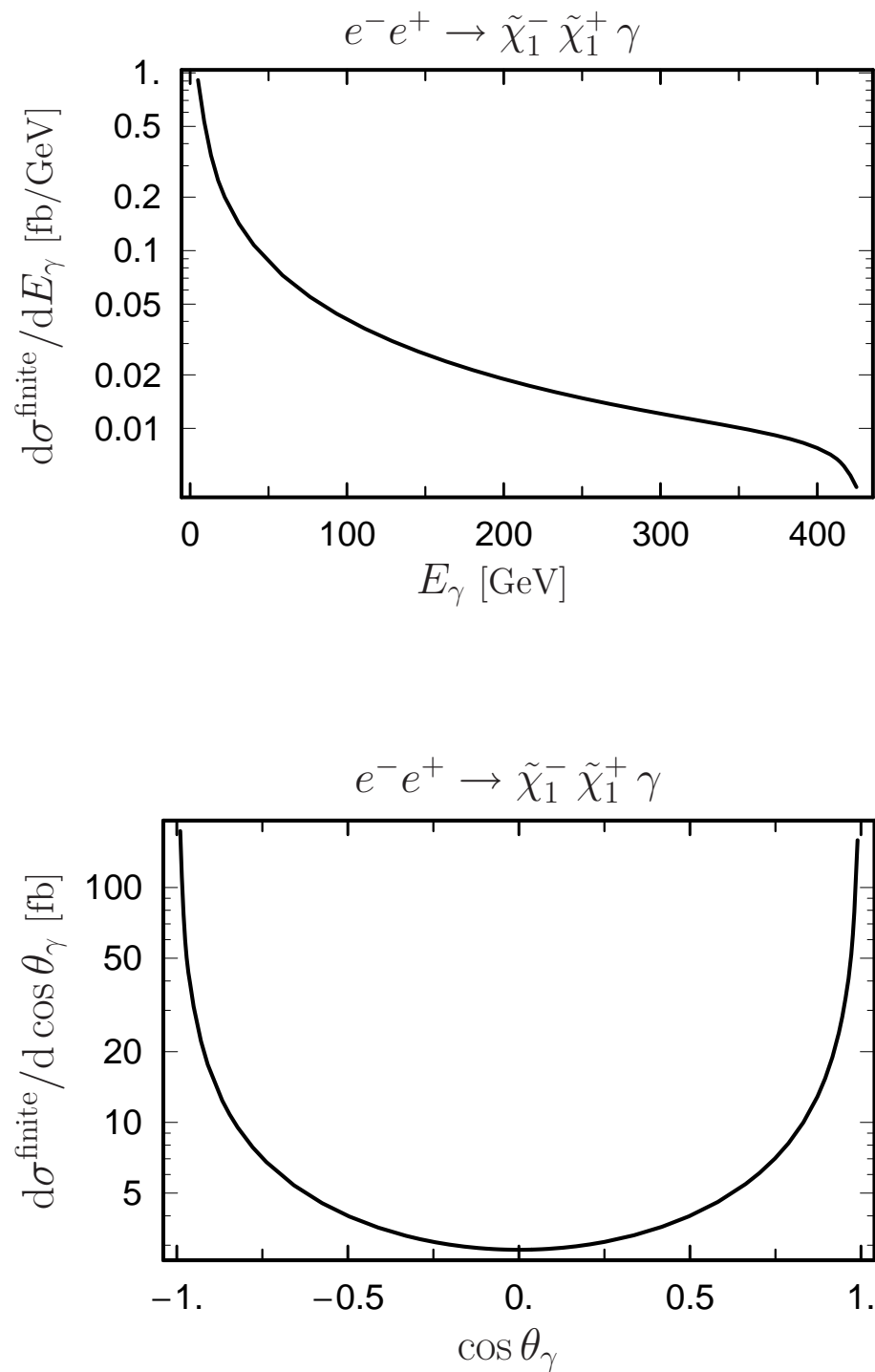


Figure 6.7: Distribution in the photon energy  $E_\gamma$  and in the photon angle  $\cos \theta_\gamma$  for  $e^-e^+ \rightarrow \tilde{\chi}_1^- \tilde{\chi}_1^+$  at  $\sqrt{s} = 1$  TeV. We have imposed angular and energy cuts of  $\theta_\gamma > 5^\circ$  and  $E_\gamma > 5$  GeV.

## 6.2 Neutralino Production

The gaugino and higgsino characters of the four neutralino mass eigenstates within the SPS1a' scenario are

$$\begin{aligned}\tilde{\chi}_1^0 &: 98\% \text{ bino}, & \tilde{\chi}_2^0 &: 92\% \text{ wino and } 7\% \text{ higgsino}, \\ \tilde{\chi}_3^0 &: 99\% \text{ higgsino}, & \tilde{\chi}_4^0 &: 92\% \text{ higgsino and } 7\% \text{ wino},\end{aligned}$$

calculated from the corresponding absolute-squared of the neutralino rotation matrix entries  $|N_{ij}|^2$ . Please note, that the entries of  $N_{ij}$  and thus the neutralino characters are renormalization scheme dependent. The given results are the values in the  $\overline{\text{DR}}$  scheme and differ from those in the on-shell scheme at  $O(\alpha)$ . The lightest neutralino is nearly a pure bino, the second one a neutral Wino with a small higgsino component and the two heavier states are higgsino dominated. This is typical for a mSUGRA motivated MSSM scenario.

At tree-level, the s-channel diagram with  $Z$ -exchange couples only on the higgsino components, and the t-channel selectron diagrams are pure gaugino contributions.

Let us consider the higgsino- $Z$  coupling in more detail. The corresponding term in the Lagrangian has in the Weyl fermion gauge-eigenstate basis  $\psi_H = (\psi_{H_1}^1, \psi_{H_2}^2)$  the form

$$\mathcal{L} \propto [\psi_{H_1}^1 \sigma^\mu \bar{\psi}_{H_1}^1 - \psi_{H_2}^2 \sigma^\mu \bar{\psi}_{H_2}^2] Z_\mu. \quad (6.2)$$

As one can see a cancellation between the two higgsino contributions occur. In the pure higgsino limit, where the mixing between gauginos and higgsinos is negligible, the higgsino mass matrix is of the form

$$Y_{\psi_H} = \begin{pmatrix} 0 & -\mu \\ -\mu & 0 \end{pmatrix}, \quad (6.3)$$

and the mass eigenstates denoted as  $\chi_3^0, \chi_4^0$  (both with positive mass eigenvalue  $\mu$ ) are given by the linear combinations

$$\chi_3^0 = \frac{i}{\sqrt{2}}(\psi_{H_1}^1 + \psi_{H_2}^2), \quad \chi_4^0 = \frac{1}{\sqrt{2}}(\psi_{H_2}^2 - \psi_{H_1}^1). \quad (6.4)$$

Inserting the mass eigenstates into the Lagrangian yields, that only the off-diagonal couplings remain and the diagonal ones are cancelled completely

$$\mathcal{L} \propto [\chi_3^0 \sigma^\mu \bar{\chi}_4^0 - \chi_4^0 \sigma^\mu \bar{\chi}_3^0] Z_\mu. \quad (6.5)$$

This implicates that in the higgsino limit, the diagonal higgsino production is a pure loop-induced process.

In our discussed scenario the two heavy neutralinos are not pure higgsinos but slightly mix with the gauginos and thus only a partial cancellation takes place in the diagonal case. Nevertheless, the total cross-sections for the diagonal higgsino production channels  $e^+e^- \rightarrow \tilde{\chi}_i^0 \tilde{\chi}_i^0$ , with  $i = 3, 4$  are below 1 fb and thus neglected in the following numerical analysis. Due to the large cancellation at tree-level, that no longer occurs in higher orders, the one-loop corrections are in the range of 30% or higher even below  $\sqrt{s} = 1$  TeV. Therefore, it would be necessary to include the one-loop squared matrix element  $|\mathcal{M}^1|^2$  in a consistent

way to stabilize the result.

In the R-parity conserving MSSM, the  $\tilde{\chi}_1^0$  is in most scenarios the lightest supersymmetric particle (LSP) and thus stable to serve as a dark matter candidate. Therefore the  $\tilde{\chi}_1^0\tilde{\chi}_1^0$  production is of less phenomenological interest. The LSP's just escape the detector and the only signal is missing energy. So besides the higgsino channels also the  $\tilde{\chi}_1^0\tilde{\chi}_1^0$  production is omitted in the numerics.

Fig. 6.8 shows the total cross-sections for the remaining production processes: The tree-level approximation in the SPA-convention as well as with weak and complete corrections included. The Figs. 6.9 and 6.10 depict the individual contributions to the electroweak corrections for selected production channels. The behaviour is quite similar to the chargino case: The dominating soft-photon corrections near the threshold, partial cancellation of QED and weak corrections for high energies, and the negligible non-universal QED corrections. Conspicuously large are the weak corrections in the  $\tilde{\chi}_2^0\tilde{\chi}_2^0$  case, but this can be also traced back to the significant higgsino component in the  $\tilde{\chi}_2^0$  state. This leads again at tree-level to a suppression of the  $Z$ -exchange diagrams and also a partial cancellation of the  $s$  and  $t$  channel diagrams occurs.

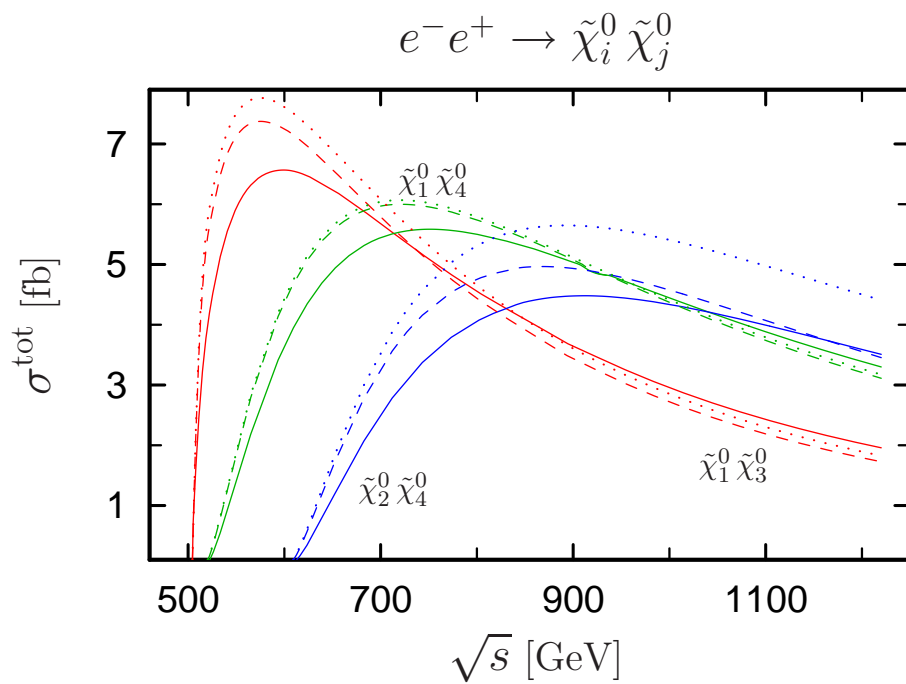
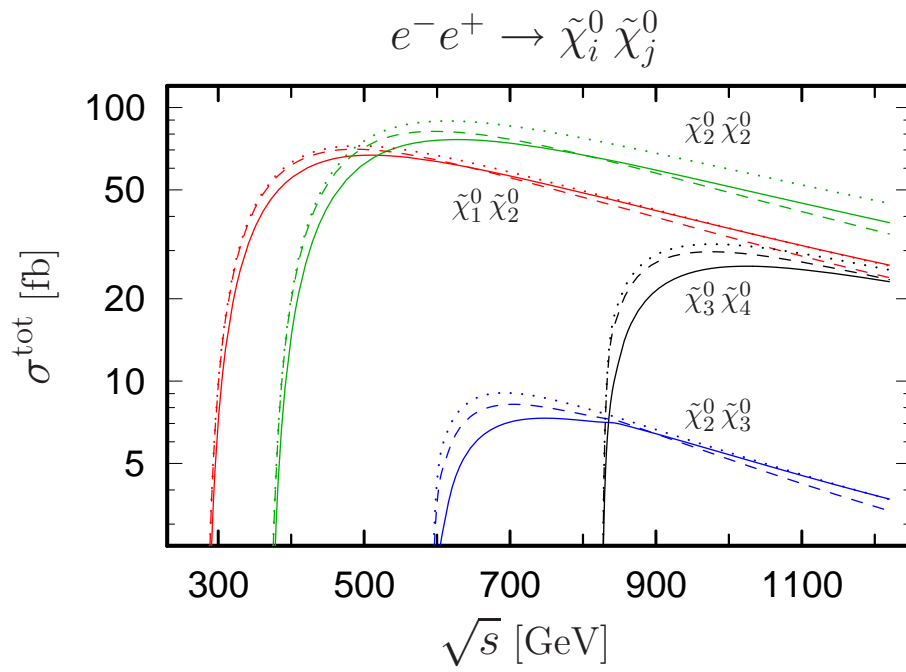


Figure 6.8: Total cross-sections for neutralino pair production at tree-level {dotted}, with weak {dashed}, and with complete corrections {solid}.

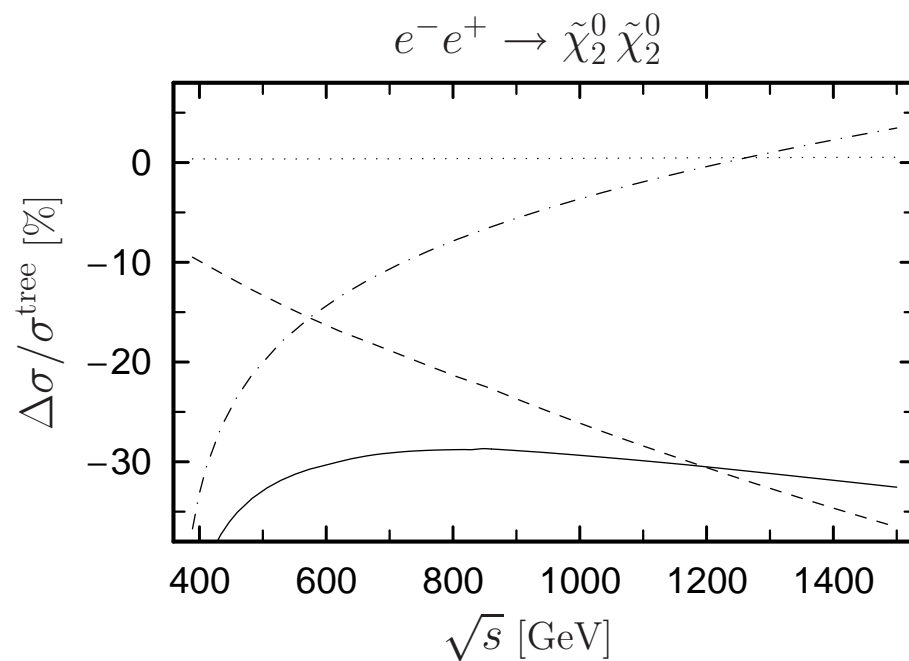
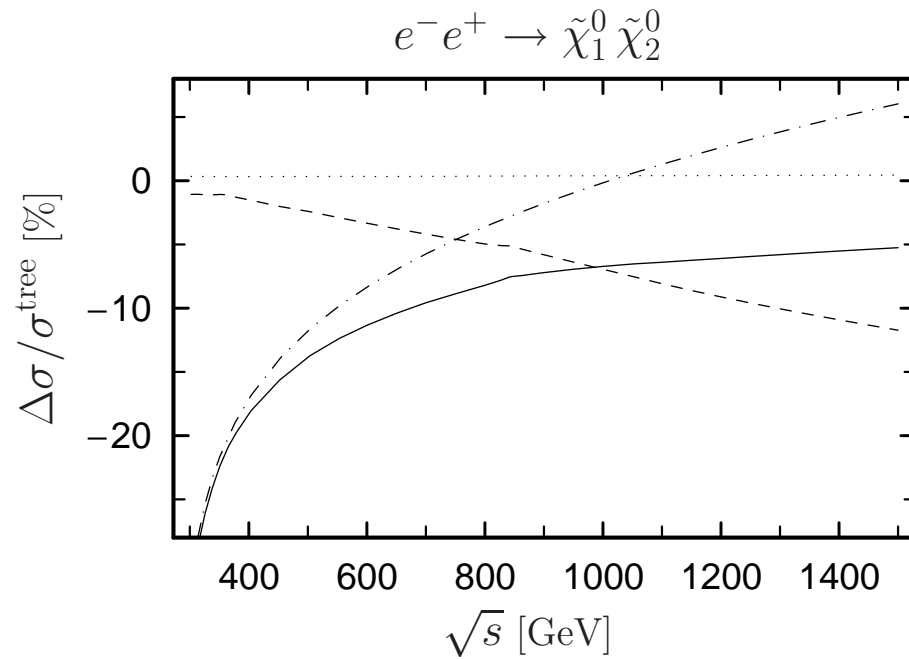


Figure 6.9: Radiative corrections for neutralino pair production. The {full, dashed, dotted, dash-dotted} line corresponds to the {complete, weak, non-universal QED, universal QED} corrections to the total tree-level cross-section.

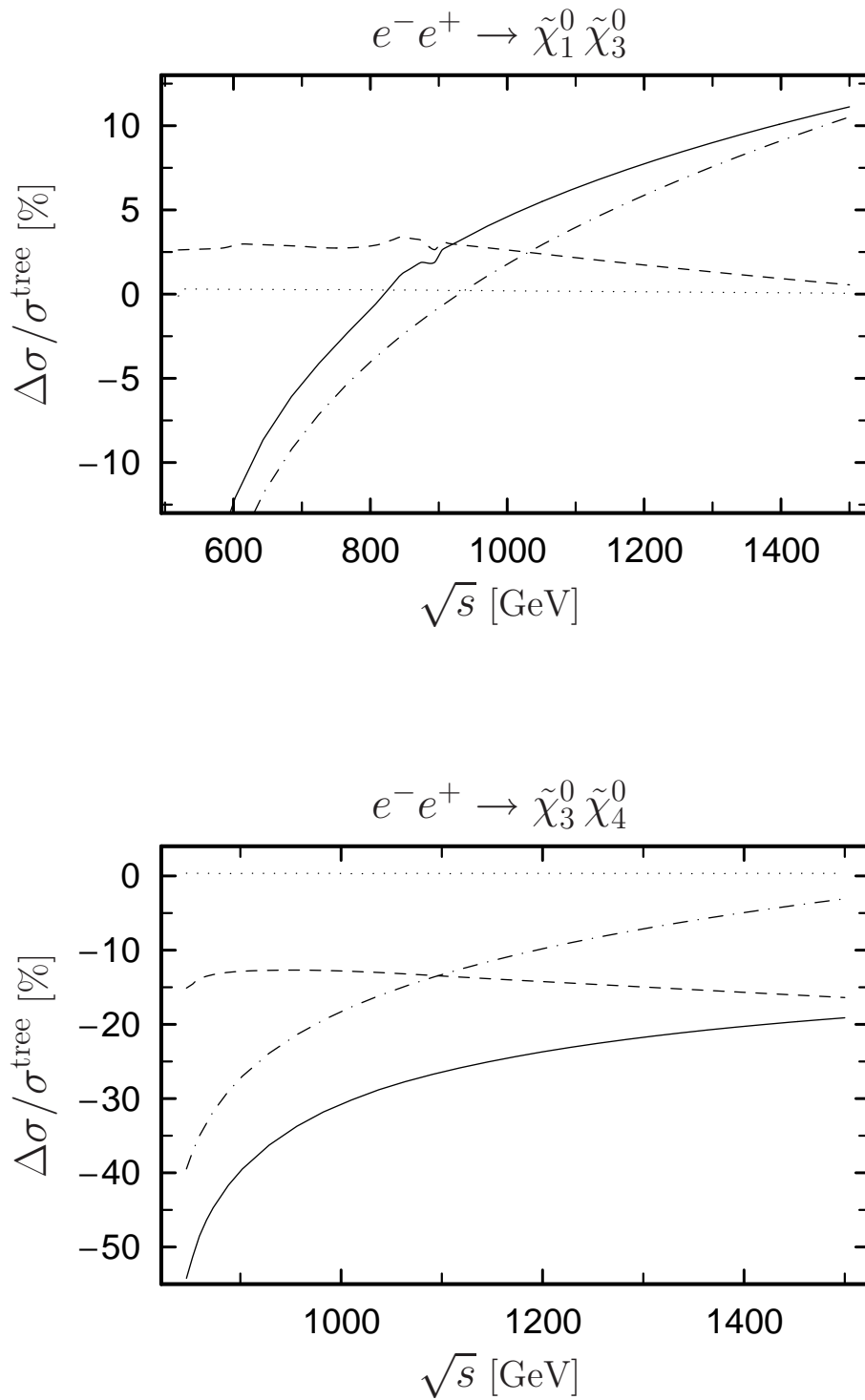


Figure 6.10: Radiative corrections for neutralino pair production. The {full, dashed, dotted, dash-dotted} line corresponds to the {complete, weak, non-universal QED, universal QED} corrections to the total tree-level cross-section.

# Appendix A

## Feynman-rules

### A.1 Definitions

In this appendix we want to discuss the implementation of counter-terms necessary for this thesis into the FeynArts package. The formulation of Feynman-rules within FeynArts can be found in the corresponding program manual and in more detail in [63]. The Lagrangian of a general field theory can be written in the form

$$\mathcal{L} = c \varphi_i(x) v_{ij} \varphi_j(x) + \mathcal{L}_I(\varphi), \quad (\text{A.1})$$

where  $\varphi$  stands for all fields  $\varphi_i$  that appear in the Lagrangian and can be of different type. The pre-factor  $c$  is  $c = \frac{1}{2}$  for real and  $c = 1$  for complex fields. The propagator of a field  $\varphi$  is defined to be the inverse of the matrix operator  $v_{ij}$

$$\Delta_{ij}(k) = i[v(k)]_{ij}^{-1}. \quad (\text{A.2})$$

A general term in the interaction Lagrangian  $\mathcal{L}_I$  can have the form

$$\mathcal{L}_I = \alpha_{i_1 \dots i_n} (\partial_{i_1}, \dots, \partial_{i_n}) \varphi_{i_1}(x) \dots \varphi_{i_n}(x), \quad (\text{A.3})$$

with  $\partial_i = \frac{\partial \varphi_i}{\partial x}$ . The coupling  $\mathbf{C}$  is defined as the Fourier transform of the coefficients in eq. (A.3)

$$\mathbf{C}(\varphi_{i_1} \dots \varphi_{i_n}) = i \sum_{\{1, \dots, n\}} (-1)^P \tilde{\alpha}_{i_1 \dots i_n}(-ik_1, \dots, -ik_n). \quad (\text{A.4})$$

The overall-factor  $(2\pi)^4 \delta^4(k_1 + \dots + k_n)$  that respects the momentum conservation is omitted in this definition. Notice, that all momenta are defined as incoming. The sum runs over all permutations of the indices and  $P$  denotes the sign of a permutation of anti-commuting fields among the  $\varphi_i$ . The coupling  $\mathbf{C}$  is further separated in a momenta-dependent kinematical part  $\vec{\Gamma}$  that contains the Lorentz and Dirac-structure and a coupling “constant”  $\vec{\mathcal{G}}$ . Both are vector-valued quantities. The kinematical part purely depends on the generic structure of the coupling, i.e. on the type of fields that are involved. The coupling  $\mathbf{C}$  can thus be written as

$$\mathbf{C}(\varphi_{i_1} \dots \varphi_{i_n}) = \left( \vec{\mathcal{G}}_{\varphi_{i_1} \dots \varphi_{i_n}} \right)^T \cdot \vec{\Gamma}_{T(\varphi_{i_1}) \dots T(\varphi_{i_n})}(k_1, \dots, k_n), \quad (\text{A.5})$$

where  $T(\varphi)$  is the generic type of the field  $\varphi$ . The kinematic couplings that are of interest in order to introduce the necessary counter-terms are

$$\vec{\Gamma}_{FFV_\mu} = \begin{pmatrix} \gamma_\mu P_L \\ \gamma_\mu P_R \end{pmatrix}, \quad (\text{A.6})$$

$$\vec{\Gamma}_{FFS} = \begin{pmatrix} P_L \\ P_R \end{pmatrix}, \quad (\text{A.7})$$

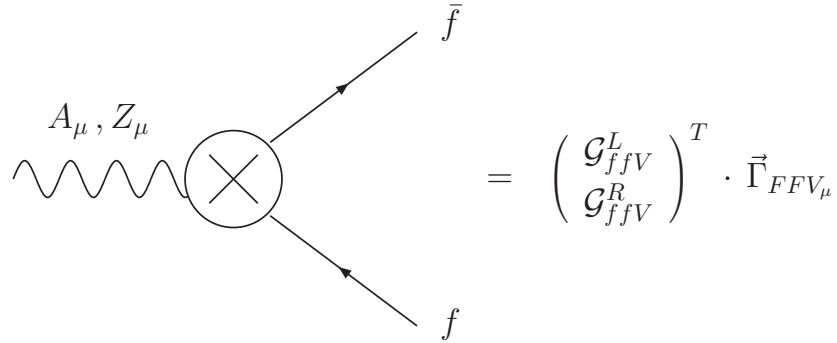
$$\vec{\Gamma}_{SS} = \begin{pmatrix} k_1 \cdot k_2 \\ 1 \end{pmatrix}, \quad (\text{A.8})$$

$$\vec{\Gamma}_{V_\mu V_\nu} = \begin{pmatrix} g_{\mu\nu}(k_1 \cdot k_2) \\ g_{\mu\nu} \\ k_{1\mu} \cdot k_{2\nu} \end{pmatrix}, \quad (\text{A.9})$$

with  $k_{1\mu} = -k_{2\mu}$ . The abbreviations  $F, S, V_\mu$  denote fermions, scalars and vector fields, respectively. A complete list can be found in the FeynArts manual.

## A.2 Counter-term Lagrangian

The counter-term Lagrangian  $\mathcal{L}_{\text{CT}}$  is as usually obtained by splitting the “bare” parameters in the tree-level Lagrangian into renormalized ones and the corresponding renormalization constants, as discussed in chapter 3, and linearly expand the result. The required counter-term Lagrangian for neutralino and chargino pair production is given together with the corresponding tree-level Lagrangian (if existent) as follows. First we consider the SM fermion-neutral gauge boson vertex. The coupling constants are



$$= \begin{pmatrix} \mathcal{G}_{ffV}^L \\ \mathcal{G}_{ffV}^R \end{pmatrix}^T \cdot \vec{\Gamma}_{FFV_\mu}$$

$$\mathcal{G}_{ffA}^{L/R} = -ie Q_f \left[ 1 + \frac{\delta e}{e} + \frac{1}{2} \delta Z_{AA} + \delta Z_f^{L/R} \right] - ie g_f^{L/R} \frac{1}{2} \delta Z_{ZA}, \quad (\text{A.10})$$

$$\mathcal{G}_{ffZ}^{L/R} = -ie g_f^{L/R} \left[ 1 + \frac{\delta e}{e} + \frac{\delta g_f^{L/R}}{g_f^{L/R}} + \frac{1}{2} \delta Z_{ZZ} + \delta Z_f^{L/R} \right] - ie Q_f \frac{1}{2} \delta Z_{AZ}, \quad (\text{A.11})$$

with

$$g_f^L = \frac{I_f^{3L} - Q_f s_W^2}{s_W c_W}, \quad g_f^R = -Q_f \frac{s_W}{c_W}, \quad (\text{A.12})$$

$$\delta g_f^L = -g_f^L \left( \frac{\delta s_W}{s_W} + \frac{\delta c_W}{c_W} \right) - \frac{2Q_f \delta s_W}{c_W}, \quad \delta g_f^R = g_f^R \left( \frac{\delta s_W}{s_W} - \frac{\delta c_W}{c_W} \right). \quad (\text{A.13})$$

The  $\tilde{\chi}_i^- \tilde{\chi}_j^- V$  vertex has similar structure, but the chargino mixing has additionally to be taken into account. The couplings we derived are

$$= \begin{pmatrix} \mathcal{G}_{\tilde{\chi}_i^- \tilde{\chi}_j^- V}^L \\ \mathcal{G}_{\tilde{\chi}_i^- \tilde{\chi}_j^- V}^R \end{pmatrix}^T \cdot \vec{\Gamma}_{FFV\mu}$$

$$\mathcal{G}_{\tilde{\chi}_i^- \tilde{\chi}_j^- A}^L = ie \left[ \delta_{ij} \left( 1 + \frac{\delta e}{e} + \frac{1}{2} \delta Z_{AA} \right) + \frac{1}{2} \delta \tilde{Z}_{ij}^{-,L} + \frac{1}{2} (\delta \tilde{Z}_{ji}^{-,L})^* \right] - ie \frac{\mathcal{U}_{ij}}{s_W c_W} \frac{1}{2} \delta Z_{ZA} \quad (\text{A.14})$$

$$\begin{aligned} \mathcal{G}_{\tilde{\chi}_i^- \tilde{\chi}_j^- Z}^L &= -\frac{ie}{s_W c_W} \left[ \mathcal{U}_{ij} \left( 1 + \frac{\delta e}{e} - \frac{\delta s_W}{s_W} - \frac{\delta c_W}{c_W} + \frac{1}{2} \delta Z_{ZZ} \right) + \delta \mathcal{U}_{ij} \right. \\ &\quad \left. + \sum_{k=1}^2 \frac{1}{2} \left( \delta \tilde{Z}_{kj}^{-,L} \mathcal{U}_{ik} + (\delta \tilde{Z}_{ki}^{-,L})^* \mathcal{U}_{kj} \right) \right] + ie \delta_{ij} \frac{1}{2} \delta Z_{AZ}, \end{aligned} \quad (\text{A.15})$$

$$\mathcal{G}_{\tilde{\chi}_i^- \tilde{\chi}_j^- V}^R = \mathcal{G}_{\tilde{\chi}_i^- \tilde{\chi}_j^- V}^L (L \rightarrow R, \mathcal{U}_{lm} \rightarrow \mathcal{V}_{ml}), \quad (\text{A.16})$$

and

$$\delta \mathcal{U}_{ij} = \delta_{ij} \delta s_W^2 - \delta U_{i1} U_{j1}^* - U_{i1} \delta U_{j1}^* - \frac{1}{2} \delta U_{i2} U_{j2}^* - \frac{1}{2} U_{i2} \delta U_{j2}^*, \quad (\text{A.17})$$

$$\delta \mathcal{V}_{ij} = \delta \mathcal{U}_{ij} (U \rightarrow V). \quad (\text{A.18})$$

Although neutralinos do not couple with photons at tree-level, the photon- $Z$  boson mixing has to be taken into account at one-loop level. Thus we find

$$\mathcal{G}_{\tilde{\chi}_i^0 \tilde{\chi}_j^0 A}^L = -ie \frac{\mathcal{N}_{ij}}{s_W c_W} \frac{1}{2} \delta Z_{ZA}, \quad (\text{A.19})$$

$$\begin{aligned} \mathcal{G}_{\tilde{\chi}_i^0 \tilde{\chi}_j^0 Z}^L &= -\frac{ie}{s_W c_W} \left[ \mathcal{N}_{ij} \left( 1 + \frac{\delta e}{e} - \frac{\delta s_W}{s_W} - \frac{\delta c_W}{c_W} + \frac{1}{2} \delta Z_{ZZ} \right) + \delta \mathcal{N}_{ij} \right. \\ &\quad \left. + \sum_{k=1}^4 \frac{1}{2} \left( \delta \tilde{Z}_{kj}^{0,L} \mathcal{N}_{ik} + \delta \tilde{Z}_{ki}^{0,R} \mathcal{N}_{kj} \right) \right], \end{aligned} \quad (\text{A.20})$$

$$\mathcal{G}_{\tilde{\chi}_i^0 \tilde{\chi}_j^0 V}^R = -\mathcal{G}_{\tilde{\chi}_i^0 \tilde{\chi}_j^0 V}^L (L \rightarrow R, \mathcal{N}_{lm} \rightarrow \mathcal{N}_{ml}), \quad (\text{A.21})$$

The diagram shows a vertex represented by a circle with an 'X' inside. A wavy line labeled  $A_\mu, Z_\mu$  enters from the left. Two straight lines exit to the right, labeled  $\tilde{\chi}_i^0$  (top) and  $\tilde{\chi}_j^0$  (bottom). The vertex is equated to the product of a vector of coupling constants and a matrix  $\vec{\Gamma}_{FFV_\mu}$ .

$$= \begin{pmatrix} \mathcal{G}_{\tilde{\chi}_i^0 \tilde{\chi}_j^0 V}^L \\ \mathcal{G}_{\tilde{\chi}_i^0 \tilde{\chi}_j^0 V}^R \end{pmatrix}^T \cdot \vec{\Gamma}_{FFV_\mu}$$

with

$$\delta \mathcal{N}_{ij} = \frac{1}{2} (\delta N_{i3} N_{j3}^* + N_{i3} \delta N_{j3}^* - \delta N_{i4} N_{j4}^* - N_{i4} \delta N_{j4}^*) . \quad (\text{A.22})$$

$$(\text{A.23})$$

The fermion-sfermion-chargino/neutralino couplings are more involved, and therefore we give here only the results for those vertices with leptons. For charginos this is the  $\tilde{\chi}_i^- l \tilde{\nu}_l$  vertex. The coupling constants are given by

The diagram shows a vertex represented by a circle with an 'X' inside. A dashed line labeled  $\tilde{\nu}_l$  enters from the left. Two straight lines exit to the right, labeled  $\tilde{\chi}_i^-$  (top) and  $\bar{l}$  (bottom). The vertex is equated to the product of a vector of coupling constants and a matrix  $\vec{\Gamma}_{FFS}$ .

$$= \begin{pmatrix} \mathcal{G}_{\tilde{\chi}_i^- l \tilde{\nu}_l}^L \\ \mathcal{G}_{\tilde{\chi}_i^- l \tilde{\nu}_l}^R \end{pmatrix}^T \cdot \vec{\Gamma}_{FFS}$$

$$\mathcal{G}_{\tilde{\chi}_i^- l \tilde{\nu}_l}^L = iY_l \left[ U_{i2}^* \left( 1 + \frac{\delta Y_l}{Y_l} + \frac{1}{2} \delta Z_l^R + \frac{1}{2} \delta Z^{\tilde{\nu}_l} \right) + \delta U_{i2}^* + \frac{1}{2} \sum_{k=1}^2 \delta \tilde{Z}_{ki}^{-,L} U_{k2}^* \right] \quad (\text{A.24})$$

$$\mathcal{G}_{\tilde{\chi}_i^- l \tilde{\nu}_l}^R = -i \frac{e}{s_W} \left[ V_{i1} \left( 1 + \frac{\delta e}{e} - \frac{\delta s_W}{s_W} + \frac{1}{2} \delta Z_l^L + \frac{1}{2} \delta Z^{\tilde{\nu}_l} \right) + \delta V_{i1} + \frac{1}{2} \sum_{k=1}^2 \delta \tilde{Z}_{ki}^{-,R} V_{k1} \right] , \quad (\text{A.25})$$

whereas  $Y_l$  is the leptonic Yukawa coupling

$$Y_l = \frac{e m_l}{\sqrt{2} m_W s_W \cos \beta} , \quad (\text{A.26})$$

with the variation

$$\delta Y_l = Y_l \left( \frac{\delta e}{e} + \frac{\delta m_l}{m_l} - \frac{\delta s_W}{s_W} - \frac{\delta m_W}{m_W} - \frac{\delta \cos \beta}{\cos \beta} \right). \quad (\text{A.27})$$

In case of the first generation the Yukawa part can be safely neglected, due to the vanishing electron mass. The conjugate coupling with an incoming lepton and an outgoing chargino is obtained by the interchange

$$i\mathcal{G}_{\tilde{\chi}_i^- \tilde{\nu}_l}^L \leftrightarrow (i\mathcal{G}_{\tilde{\chi}_i^- \tilde{\nu}_l}^R)^*. \quad (\text{A.28})$$

The  $\tilde{\chi}_i^- \tilde{\nu}_l$  vertex has a much richer structure, due to the selectron LR-mixing and the neutralino Majorana-nature

$$= \begin{pmatrix} \mathcal{G}_{\tilde{\chi}_i^0 \tilde{l}_j}^L \\ \mathcal{G}_{\tilde{\chi}_i^0 \tilde{l}_j}^R \end{pmatrix}^T \cdot \vec{\Gamma}_{FFS}$$

$$\begin{aligned} \mathcal{G}_{\tilde{\chi}_i^0 \tilde{l}_j}^L &= -i \left[ \left( Y_l N_{i3}^* R_{j1}^{\tilde{l}*} + \sqrt{2} \frac{e}{c_W} N_{i1}^* R_{j2}^{\tilde{l}*} \right) \left( 1 + \frac{1}{2} \delta Z_l^R \right) + \right. \\ & Y_l N_{i3}^* R_{j1}^{\tilde{l}*} \left( \frac{\delta Y_l}{Y_l} + \frac{\delta N_{i3}^*}{N_{i3}^*} + \frac{\delta R_{j1}^{\tilde{l}*}}{R_{j1}^{\tilde{l}*}} \right) + \sqrt{2} \frac{e}{c_W} N_{i1}^* R_{j2}^{\tilde{l}*} \left( \frac{\delta e}{e} - \frac{\delta c_W}{c_W} + \frac{\delta N_{i1}^*}{N_{i1}^*} + \frac{\delta R_{j2}^{\tilde{l}*}}{R_{j2}^{\tilde{l}*}} \right) + \\ & \left. \frac{1}{2} \sum_{k=1}^4 \delta \tilde{Z}_{ki}^{0,L} \left( Y_l N_{k3}^* R_{j1}^{\tilde{l}*} + \frac{\sqrt{2}e}{c_W} N_{k1}^* R_{j2}^{\tilde{l}*} \right) + \frac{1}{2} \sum_{k=1}^2 \delta Z_{kj}^{\tilde{f}} \left( Y_l N_{i3}^* R_{k1}^{\tilde{l}*} + \frac{\sqrt{2}e}{c_W} N_{i1}^* R_{k2}^{\tilde{l}*} \right) \right], \end{aligned} \quad (\text{A.29})$$

$$\begin{aligned} \mathcal{G}_{\tilde{\chi}_i^0 \tilde{l}_j}^R &= -i \left[ \left( Y_l N_{i3} R_{j2}^{\tilde{l}*} - \frac{e \bar{N}_i R_{j1}^{\tilde{l}*}}{\sqrt{2} s_W c_W} \right) \left( 1 + \frac{1}{2} \delta Z_l^L \right) + \right. \\ & Y_l N_{i3} R_{j2}^{\tilde{l}*} \left( \frac{\delta Y_l}{Y_l} + \frac{\delta N_{i3}}{N_{i3}} + \frac{\delta R_{j2}^{\tilde{l}*}}{R_{j2}^{\tilde{l}*}} \right) - \frac{e \bar{N}_i R_{j1}^{\tilde{l}*}}{\sqrt{2} s_W c_W} \left( \frac{\delta e}{e} - \frac{\delta s_W}{s_W} - \frac{\delta c_W}{c_W} + \frac{\delta \bar{N}_i}{\bar{N}_i} + \frac{\delta R_{j1}^{\tilde{l}*}}{R_{j1}^{\tilde{l}*}} \right) + \\ & \left. \frac{1}{2} \sum_{k=1}^4 \delta \tilde{Z}_{ki}^{0,R} \left( Y_l N_{k3} R_{j2}^{\tilde{l}*} - \frac{e \bar{N}_k R_{j1}^{\tilde{l}*}}{\sqrt{2} s_W c_W} \right) + \frac{1}{2} \sum_{k=1}^2 \delta Z_{kj}^{\tilde{f}} \left( Y_l N_{i3} R_{k2}^{\tilde{l}*} - \frac{e \bar{N}_i R_{k1}^{\tilde{l}*}}{\sqrt{2} s_W c_W} \right) \right], \end{aligned} \quad (\text{A.30})$$

with

$$\bar{N}_i = N_{i1} s_W + N_{i2} c_W, \quad \delta \bar{N}_i = \delta N_{i1} s_W + N_{i1} \delta s_W + \delta N_{i2} c_W + N_{i2} \delta c_W. \quad (\text{A.31})$$



# Appendix B

## Reference Point SPS1a'

The SPA convention defines a clear theoretical framework for precision calculations within supersymmetric extensions of the SM, in particular the MSSM. It will serve to extract the fundamental supersymmetric Lagrangian parameters including the SUSY-breaking parameters from future data.

The SM input is fixed by the values given in table B.1. The reference point SPS1a' is proposed within the SPA project as a benchmark point to test the currently available and future tools for a supersymmetry parameter analysis. It is defined by a full set of  $\overline{\text{DR}}$  parameters of the CP and R-parity conserving MSSM fixed at the scale  $\tilde{M}=1$  TeV, shown in Tab. B.2. The two vacuum expectation values  $v_1, v_2$  can be deduced from

$$\tan \beta = \frac{v_2}{v_1}, \quad v^2 = v_1^2 + v_2^2. \quad (\text{B.1})$$

The  $\overline{\text{DR}}$  masses of the gauge bosons and the third generation SM fermions are determined by

$$m_W^2 = \frac{1}{4}g^2v^2, \quad m_Z^2 = \frac{1}{4}(g^2 + g'^2)v^2, \quad (\text{B.2})$$

and

$$m_t = \frac{1}{\sqrt{2}}Y_tv_2, \quad m_b = \frac{1}{\sqrt{2}}Y_bv_1, \quad m_\tau = \frac{1}{\sqrt{2}}Y_\tau v_1. \quad (\text{B.3})$$

The SPS1a' reference point was originally calculated from the following mSUGRA parameters:

$M_{1/2}$	=	250 GeV	$\text{sign}(\mu)$	=	+1
$M_0$	=	70 GeV	$\tan \beta(\tilde{M})$	=	10
$A_0$	=	-300 GeV			

(B.4)

They have been chosen in such a way, that the SPS1a' scenario is compatible with all high-energy mass bounds and with the low-energy precision data, as well as with the available cosmological data. With the help of RGE's the mSUGRA parameters are evolved from the unification scale down to 1 TeV using W. Porod's Spheno 2.2.2 [64]. One reason, why the extensive MSSM parameter set serves as SPS1a' definition instead of the small mSUGRA one is quite simple. The current deviations between different available computer codes, calculating the low-scale parameters from the GUT parameters are not acceptable for precision

$m_e$	$5.110 \cdot 10^{-4}$	$m_t$	178.0
$m_\mu$	0.1057	$m_b(m_b^2)$	4.2
$m_\tau$	1.777	$m_Z$	91.1876
$m_u(Q^2)$	$3 \cdot 10^{-3}$	$G_F$	$1.1664 \cdot 10^{-5}$
$m_d(Q^2)$	$7 \cdot 10^{-3}$	$1/\alpha$	137.036
$m_s(Q^2)$	0.12	$\Delta\alpha_{\text{had}}^{(5)}(m_Z^2)$	0.02769
$m_c(m_c^2)$	1.2	$\alpha_s^{\overline{\text{MS}}}(m_Z^2)$	0.119

Table B.1: Numerical values of the SM input according to the SPA convention. Masses are given in GeV, for the leptons and the  $t$  quark the pole masses, for the lighter quarks the  $\overline{\text{MS}}$  masses either at the mass scale itself, for  $c$ ,  $b$ , or, for  $u$ ,  $d$ ,  $s$ , at the scale  $Q = 2$  GeV.

$\mathcal{P}$	$\overline{\text{DR}}$	$\mathcal{P}$	$\overline{\text{DR}}$
$g'$	0.36355	$M'$	103.22
$g$	0.64809	$M$	193.31
$g_s$	1.08419	$M_3$	572.33
$Y_\tau$	0.10368	$A_\tau$	-445.5
$Y_t$	0.89828	$A_t$	-535.4
$Y_b$	0.13575	$A_b$	-938.5
$M_{H_1}^2$	$2.5586 \cdot 10^4$	$M_{H_2}^2$	$-1.4820 \cdot 10^5$
$\mu$	402.87	$\tan\beta$	10.0
$v$	242.86	$m_{A^0}$	377.13

$\mathcal{P}$	$\overline{\text{DR}}$	$\mathcal{P}$	$\overline{\text{DR}}$
$M_{L_1}^2$	$3.2853 \cdot 10^4$	$M_{L_3}^2$	$3.2215 \cdot 10^4$
$M_{E_1}^2$	$1.3360 \cdot 10^4$	$M_{E_3}^2$	$1.2066 \cdot 10^4$
$M_{Q_1}^2$	$27.758 \cdot 10^4$	$M_{Q_3}^2$	$22.208 \cdot 10^4$
$M_{U_1}^2$	$25.774 \cdot 10^4$	$M_{U_3}^2$	$14.791 \cdot 10^4$
$M_{D_1}^2$	$25.550 \cdot 10^4$	$M_{D_3}^2$	$25.134 \cdot 10^4$

Table B.2: The SPS1a'  $\overline{\text{DR}}$  Lagrangian parameters at the scale  $\tilde{M} = 1$  TeV (mass units in GeV). In addition, the Higgs mass  $m_{A^0}$  and the vacuum expectation value  $v$  are given in the  $\overline{\text{DR}}$  scheme.

studies. For such a comparison of different programs, we refer to [65].

The SPS1a' input needs to be adjusted to be compatible with the on-shell renormalization scheme used in this thesis. First of all, a translation from the SUSY  $\overline{\text{DR}}$  parameters  $\mathcal{P}(\tilde{M})$  to our on-shell definition  $\mathcal{P}^{\text{OS}}$  has to be performed by subtraction of the finite parts of the corresponding on-shell counter-terms  $\delta_1\mathcal{P}(\tilde{M})$

$$\mathcal{P}^{\text{OS}} = \mathcal{P}(\tilde{M}) - \delta_1\mathcal{P}(\tilde{M}). \quad (\text{B.5})$$

The used values in this work can be seen in table B.3. For all other parameters that are free of renormalization conditions, the  $\overline{\text{DR}}$  or on-shell values can be used. The difference is of higher order for the current processes. These on-shell parameters now serve as input of our used renormalization procedure. For example to calculate the on-shell masses of the SUSY partners, as depicted in the “lower way” of Fig. B.1. Please note, that before the diagonalization of the on-shell mass matrix the finite mass-shifts  $\Delta M$  have to be taken into

$\mathcal{P}$	OS	$\mathcal{M}$	$\overline{\text{DR}}$	OS	$\mathcal{M}$	$\overline{\text{DR}}$	OS
$M'$	100.32	$m_{\tilde{\chi}_1^\pm}$	181.0	184.2	$m_{\tilde{\chi}_1^0}$	100.7	97.75
$M$	197.03	$m_{\tilde{\chi}_2^\pm}$	423.4	421.1	$m_{\tilde{\chi}_2^0}$	181.4	184.4
$\mu$	399.94	$m_{\tilde{e}_L}$	186.9	190.1	$m_{\tilde{\chi}_3^0}$	408.6	406.9
$\tan\beta$	10.31	$m_{\tilde{e}_R}$	123.6	125.2	$m_{\tilde{\chi}_4^0}$	423.0	419.6
$M_{\tilde{E}_1}$	117.71	$m_{\tilde{\nu}_e}$	169.9	172.8			
$M_{\tilde{L}_1}$	183.98						

Table B.3: Parameters of the SPS1a' scenario in the on-shell scheme and the corresponding  $\overline{\text{DR}}$  and on-shell particle masses.

$$\begin{array}{ccc}
\text{SPA input} = \begin{pmatrix} m_{11} & m_{12} \\ m_{21} & m_{22} \end{pmatrix}_{\overline{\text{DR}}} & \xrightarrow{\text{diag}} & \begin{pmatrix} m_1 & 0 \\ 0 & m_2 \end{pmatrix}_{\overline{\text{DR}}} = \overline{\text{DR}} \text{ masses} \\
\delta_1 \downarrow & & \delta_2 \downarrow \\
\text{On-shell input} = \begin{pmatrix} M_{11} & M_{12} \\ M_{21} & M_{22} \end{pmatrix}_{\text{OS}} & \xrightarrow[\Delta M]{\text{diag}} & \begin{pmatrix} M_1 & 0 \\ 0 & M_2 \end{pmatrix}_{\text{OS}} = \text{Pole masses}
\end{array}$$

Figure B.1: Two different ways from  $\overline{\text{DR}}$  parameters to on-shell masses.

account, as discussed in chapter 3. An independent check can be done by following the “upper way” of Fig. B.1. After diagonalization of the  $\overline{\text{DR}}$  mass matrix the on-shell masses can be obtained by subtracting the finite parts of the on-shell mass counter-terms  $\delta_2 m_i(\tilde{M})$  from the  $\overline{\text{DR}}$  masses. Both ways lead to the same mass eigenstates, certainly up to terms of higher order. This non-trivial check has been performed for all SUSY particles.

Our effective charge renormalization procedures, discussed in chapter 3.3, need as input the fine-structure constant  $\alpha$  in the Thomson limit, the vacuum polarization  $\Delta\alpha_{\text{had}}^{(5)}$  and the Fermi constant  $G_F$ , which is consistent with the SM input, table B.1.

We use both gauge boson on-shell masses  $m_Z$  and  $m_W$  as input in contrast to the SPA convention, where only  $m_Z$  is given on-shell and the  $W$ -mass is calculated from  $G_F$  and the other parameters of the MSSM. For consistency with the SPA convention we thus use for the numerical value of the  $W$ -mass not the measured quantity but the one derived within the  $G_F$ -scheme with Sphenon 2.2.2 at the SPS1a' benchmark point

$$m_W = 80.4214 \text{ GeV}. \quad (\text{B.6})$$

# Bibliography

- [1] S. Glashow, Nucl. Phys. **22** (1961) 579; S. Weinberg, Phys. Rev. Lett. **19** (1967) 1264; A. Salam, in “*Elementary Particle Theory*”, ed. N. Svartholm, Almqvist and Wiksells, Stockholm (1969), p. 367.
- [2] M. Gell-Mann, Phys. Lett. **8** (1964) 214; G. Zweig, CERN-Report 8182/TH401 (1964); H. Fritzsch, M. Gell-Mann and H. Leutwyler, Phys. Lett. B **47** (1973) 365; D. Gross and F. Wilczek, Phys. Rev. Lett. **30** (1973) 1343; H.D. Politzer, Phys. Rev. Lett. **30** (1973) 1346.
- [3] J. Ellis, S. Kelley and D.V. Nanopoulos, Phys. Lett. B **260** (1991) 131; U. Amaldi, W. de Boer and H. Fürstenau, Phys. Lett. B **260** (1991) 447; P. Langacker and M. Luo, Phys. Rev. D **44** (1991) 817; C. Giunti, C.W. Kim and U.W. Lee, Mod. Phys. Lett. A **6** (1991) 1745.
- [4] E.W. Kolb and M.S. Turner, “*The Early Universe*”, Addison–Wesley, New York, 1990.
- [5] D.N. Spergel *et al.* (WMAP Collaboration), Astrophys. J. Suppl. **148** (2003) 175.
- [6] J. Wess and B. Zumino, Nucl. Phys. B **70** (1974) 39; J. Wess and B. Zumino, Nucl. Phys. B **78** (1974) 1.
- [7] J. Wess and J. Bagger, “*Supersymmetry and Supergravity*”, Princeton Series in Physics, New Jersey, 1992.
- [8] D. Bailin and A. Love, “*Supersymmetric Gauge Field Theory and String Theory*”, Adam Hilger imprint, Bristol 1996.
- [9] S. Martin, in “*Perspectives on Supersymmetry*”, Ed. G.L. Kane, World Scientific, Singapore, 1998 [arXiv:hep-ph/9709356].
- [10] R. Haag, J.T. Lopuszanski and M. Sohnius, Nucl. Phys. B **88** (1975) 257.
- [11] L. Girardello and M. Grisaru, Nucl. Phys. B **194** (1982) 65.
- [12] H. E. Haber and G. L. Kane, Phys. Rep. **117** (1985) 75.
- [13] G. ’t Hooft and M. J. G. Veltman, Nucl. Phys. B **44** (1972) 189.
- [14] G. ’t Hooft and M. J. G. Veltman, Nucl. Phys. B **153** (1979) 365.

- [15] G. Passarino and M. J. G. Veltman, Nucl. Phys. B **160** (1979) 151.
- [16] A. Denner, Fortschr. Phys. **41** (1993) 307.
- [17] H. Eberl, PhD Thesis (in german) (1998).
- [18] W. Siegel, Phys. Lett. B **84** (1979) 193.
- [19] F. del Aguila and M. Perez-Victoria, Acta Phys. Polon. B **28** (1997) 2279 [arXiv:hep-ph/9710442]; F. del Aguila, A. Culatti, R. Munoz Tapia and M. Perez-Victoria, Nucl. Phys. B **537** (1999) 561 [arXiv:hep-ph/9806451]; F. del Aguila, A. Culatti, R. Munoz-Tapia and M. Perez-Victoria, Phys. Lett. B **419** (1998) 263 [arXiv:hep-th/9709067].
- [20] F. del Aguila and M. Perez-Victoria, arXiv:hep-ph/9901291.
- [21] T. Hahn and M. Perez-Victoria, Comput. Phys. Commun. **118** (1999) 153 [arXiv:hep-ph/9807565].
- [22] H. Burkhardt and B. Pietrzyk, Phys. Lett. B **513** (2001) 46.
- [23] F. Jegerlehner, Nucl. Phys. Proc. Suppl. **131** (2004) 213 [arXiv:hep-ph/0312372].
- [24] K. Hagiwara, A. Martin, D. Nomura and T. Teubner, Phys. Rev. D **69** (2004) 093003, hep-ph/0312250.
- [25] F. Jegerlehner, contribution to the “*2nd Joint ECFA/DESY Study on Physics and Detectors for a Linear Electron-Positron Collider*”, arXiv:hep-ph/0105283.
- [26] G. Degrassi, S. Fanchiotti and A. Sirlin, Nucl. Phys. B **351** (1991) 49-69.
- [27] W. Hollik, “*Predictions for  $e^+e^-$  Processes*” in “*Precision Tests of the Standard Electroweak Model*”, ed. P. Langacker (1995) p.37.
- [28] H. Eberl, M. Kincel, W. Majerotto and Y. Yamada, Nucl. Phys. B **625** (2002) 372 [arXiv:hep-ph/0111303]; C. Weber, H. Eberl, W. Majerotto Phys. Lett. B **572** (2003) 56 [arXiv:hep-ph/0305250]; C. Weber, H. Eberl, W. Majerotto Phys. Rev. D **68** (2003) 093011 [arXiv:hep-ph/0308146].
- [29] M. Consoli, W. Hollik and F. Jegerlehner, Phys. Lett. B **227** (1989) 167.
- [30] P. H. Chankowski, S. Pokorski, and J. Rosiek, Phys. Lett. B **274** (1992) 191; Nucl. Phys. B **423** (1994) 437; 497.
- [31] A. Dabelstein, Z. Phys. C **67** (1995) 495 ; Nucl. Phys. B **456** (1995) 25.
- [32] A. Freitas and D. Stöckinger, Phys. Rev. D **66** (2002) 095014.
- [33] D. Pierce and A. Papadopoulos, Phys. Rev. D **50** (1994) 565; Nucl. Phys. B **430** (1994) 278; A. B. Lahanas, K. Tamvakis, and N. D. Tracas, Phys. Lett. B **324** (1994) 387; M. A. Díaz, S. F. King, and D. A. Ross, Nucl. Phys. B **529** (1998) 23; [arXiv:hep-ph/0008117].

- [34] A. Denner and T. Sack, Nucl. Phys. B **347** (1990) 203.
- [35] T. Fritzsche, W. Hollik, Eur. Phys. J. C **24** (2002) 619 [arXiv:hep-ph/0203159];
- [36] H. Eberl, M. Kincel, W. Majerotto, Y. Yamada, Phys. Rev. D **64** (2001) 115013 [arXiv:hep-ph/0104109]; W. Öller, H. Eberl, W. Majerotto, C. Weber, Eur. Phys. J. C **29** (2003) 563 [arXiv:hep-ph/0304006].
- [37] T. Blank, Dissertation (in german), TH Karlsruhe (2000).
- [38] Y. Yamada, Phys. Rev. D **64** (2001) 036008;
- [39] G. Altarelli and G. Martinelli, in “*Physics at LEP*”, eds. J. Ellis and R. Peccei, (CERN 86-02, Geneva, 1986), Vol. 1, p.47; F. A. Berends, W. L. van Neerven and G. J. H. Burgers, Nucl. Phys. B **297** (1988) 429 [Erratum-ibid. B **304** (1988) 921].
- [40] W. Beenakker, F.A. Berends and W.L. van Neerven, “*Application of Renormalization Group Methods to Radiative Corrections*” in “*Radiative Corrections for  $e^+e^-$  Collisions*”, ed. J.H. Kühn (1989) p.3.
- [41] G. Altarelli and G. Parisi, Nucl. Phys. B **126** (1977) 298.
- [42] L.N. Lipatov, Sov. J. Nucl. Phys. **20** (1975) 95.
- [43] D.R. Yennie, S.C. Frautschi and H. Suura, Ann. Phys. **13** (1961) 379.
- [44] V.N. Gribov and L.N. Lipatov, Sov. J. Nucl. Phys. **15** (1972) 438 and 675.
- [45] E. A. Kuraev and V. S. Fadin, Sov. J. Nucl. Phys. **41** (1985) 466 [Yad. Fiz. **41** (1985) 733];
- [46] F.A. Berends et al., “*Z Line Shape*” in “*Z Physics at LEP 1*”, Cern 89-08, eds. G. Altarelli, R. Kleiss and C. Verzegnassi (Geneva, 1989) p.89.
- [47] M. Skrzypek and S. Jadach, Z. Phys. C **49** (1991) 577-584.
- [48] S. Y. Choi, J. Kalinowski, G. Moortgat-Pick and P. M. Zerwas, Eur. Phys. J. C **22** (2001) 563 [Addendum-ibid. C **23** (2002) 769] [arXiv:hep-ph/0108117].
- [49] S. Y. Choi, A. Djouadi, M. Guchait, J. Kalinowski, H. S. Song and P. M. Zerwas, Eur. Phys. J. C **14** (2000) 535 [arXiv:hep-ph/0002033]; S. Y. Choi, M. Guchait, J. Kalinowski and P. M. Zerwas, Phys. Lett. B **479** (2000) 235 [arXiv:hep-ph/0001175].
- [50] J. Küblbeck, M. Böhm, A. Denner, Comput. Phys. Commun. **60** (1990) 165; T. Hahn, Comput. Phys. Commun. **140** (2001) 418 [hep-ph/0012260].
- [51] T. Hahn and C. Schappacher, Comput. Phys. Commun. **143** (2002) 54 [arXiv:hep-ph/0105349].

- [52] T. Hahn, M. Perez-Victoria, *Comput. Phys. Commun.* **118** (1999) 153 [hep-ph/9807565]; T. Hahn, *Nucl. Phys. Proc. Suppl.* **135** (2004) 333 [arXiv:hep-ph/0406288].
- [53] G. J. Oldenborgh, *Comput. Phys. Commun.* **66** (1991) 1; T. Hahn, *Acta Phys. Polon. B* **30** (1999) 3469.
- [54] W. Beenakker and A. Denner, *Int. J. Mod. Phys. A* **9** (1994) 4837.
- [55] K. Kovařík, C. Weber, H. Eberl and W. Majerotto, *Phys. Lett. B* **591** (2004) 242 [arXiv:hep-ph/0401092]; K. Kovařík, C. Weber, H. Eberl and W. Majerotto, *Phys. Rev. D* **72** (2005) 053010 [arXiv:hep-ph/0506021].
- [56] F. Bloch and A. Nordsieck, *Phys. Rev.* **52** (1937) 54.
- [57] M. Böhm and S. Dittmaier, *Nucl. Phys. B* **409** (1993) 3 and **412** (1994) 39; A. Denner, S. Dittmaier, M. Roth and M. M. Weber, *Nucl. Phys. B* **660** (2003) 289 [arXiv:hep-ph/0302198].
- [58] A. Freitas, DESY-THESIS-2002-023 (2002).
- [59] T. Hahn, *Comput. Phys. Commun.* **168** (2005) 78 [arXiv:hep-ph/0404043].
- [60] Supersymmetry Parameter Analysis (SPA) project, SPA website <http://spa.desy.de/spa/>
- [61] J. A. Grifols and J. Solà, *Nucl. Phys. B* **253** (1985) 47; P. H. Chankowski *et. al.*, *Nucl. Phys. B* **417** (1994) 101; K. Hagiwara, S. Matsumoto, and Y. Yamada, *Phys. Rev. Lett.* **75** (1995) 3605.
- [62] S. Fanchiotti, B. Kniehl, and A. Sirlin, *Phys. Rev. D* **48** (1993) 307. D. M. Pierce, J. A. Bagger, K. T. Matchev, and R.-J. Zhang, *Nucl. Phys. B* **491** (1997) 3.
- [63] H. Eck, “*FeynArts 2.0 - Development of a generic Feynman diagram generator*”, Phd Thesis 1995.
- [64] W. Porod, *Comput. Phys. Commun.* **153** (2003) 275 [arXiv:hep-ph/0301101].
- [65] G. Belanger, S. Kraml and A. Pukhov, *Phys. Rev. D* **72** (2005) 015003 [arXiv:hep-ph/0502079]; B. C. Allanach, S. Kraml and W. Porod, *JHEP* **0303** (2003) 016 [arXiv:hep-ph/0302102].  
URL: <http://cern.ch/kraml/comparison/>

# Curriculum Vitae

## Persönliche Daten:

**Name:** Dipl.-Ing. Wilhelm Öller

**Geburtsdatum:** 21. Februar 1977

**Geburtsort:** Wien, Österreich

**Staatsangehörigkeit:** österreichisch

**Familienstand:** ledig

**Wohnadresse:** Odoakergasse 10-18/6/17, 1160 Wien

**E-mail:** oeller@hephy.oeaw.ac.at / wil@futuredesign.at

## Ausbildung:

**Sept. 1982 - Juni 1987:** Volksschule in Wien, Neubau

**Sept. 1987 - Mai 1996:** Bundesrealgymnasium in Wien, Josefstadt

**Mai 1996:** AHS-Matura

**Okt. 1996 - Jan. 2003:** Studium “Technische Physik” an der TU-Wien

**Mai 1999:** Abschluss der 1. Diplomprüfung

**Jan. 2003:** Abschluss der 2. Diplomprüfung

Diplomarbeit: “Full one-loop corrections to the chargino and neutralino mass matrices in the on-shell scheme”, unter der Leitung von Univ. Prof. W. Majerotto, Institut für Theoretische Physik, TU-Wien und Institut für Hochenergiephysik der Österreichischen Akademie der Wissenschaften

**seit Feb. 2003:** Dissertation unter der Leitung von Univ. Prof. W. Majerotto, Thema: “Precise Predictions for Neutralino and Chargino Pair Production in Supersymmetry”

## Sonstiges:

**seit Okt. 2003:** Anstellung am Institut für Hochenergiephysik der ÖAW, Nikolsdorfergasse 18, 1050 Wien, Tätigkeitsbereich: Modellrechnungen für LHC und den Linear Collider im Rahmen des Supersymmetrie-Projektes

# List of Publications

- K. Kovařík, W. Öller and C. Weber,  
“*Precise predictions for SUSY processes at the ILC*”,  
arXiv:hep-ph/0506329, to appear in the proceedings of the International Linear Collider Workshop 2005, Stanford, California.
- W. Öller, H. Eberl and W. Majerotto,  
“*Precise predictions for chargino and neutralino pair production in  $e^+e^-$  annihilation*”,  
Phys. Rev. D **71**, 115002 (2005).
- W. Öller, H. Eberl and W. Majerotto,  
“*Full one-loop corrections to neutralino pair production in  $e^+e^-$  annihilation*”,  
Phys. Lett. B **590**, 273 (2004).
- S. Hesselbach, O. Kittel, G. Moortgat-Pick and W. Öller,  
“*New ideas on SUSY searches at future linear colliders*”,  
Eur. Phys. J. C **33**, S746 (2004).
- W. Öller, H. Eberl, W. Majerotto and C. Weber,  
“*Analysis of the chargino and neutralino mass parameters at one-loop level*”,  
Eur. Phys. J. C **29**, 563 (2003).